Targeting Neuroinflammation as a Therapeutic Approach in Alzheimer's Disease Mouse Model

by

Ihab M. Abdallah

A dissertation submitted to the Graduate Faculty of
Auburn University
in partial fulfillment of the
requirements for the Degree of
Doctor of Philosophy

Auburn, Alabama
December 12, 2020

Keywords: Olive leaf extract, Oleuropein, Alzheimer's disease, Neuroinflammation, Amyloid-β, 5xFAD

Approved by

Amal Kaddoumi, Chair, Professor, Department of Drug Discovery and Development
Robert D. Arnold, Professor, Department of Drug Discovery and Development
Jay Ramapuram, Professor, Department of Drug Discovery and Development
Murali Dhanasekaran, Professor, Department of Drug Discovery and Development
Vinicia Biancardi, Assistant Professor, Department of Anatomy, Physiology, and Pharmacology
Mahmoud Mansour, Professor, Department of Anatomy, Physiology, and Pharmacology, (University reader)

Abstract

Alzheimer's disease (AD) is a complex neurodegenerative disorder and the most common form of dementia that affects people in their middle age, in the case of familial cases, and the elderly causing significant losses to the health and economic sectors of countries. Several hallmarks have been associated with AD, including but not limited to extracellular amyloid-beta (Aβ) plaques, neurofibrillary tangle (NFT), compromised blood-brain barrier (BBB) and neuroinflammation. Thus, targeting multiple pathways could be a novel therapeutic approach to prevent and/or treat AD. In the last few decades, olive oil and olive leaf extract (OLE) containing polyphenols have shown a beneficial health effect in experimental and clinical studies. The major bioactive phenol enriched in OLE, named oleuropein, showed a beneficial effect in memory and Aβ accumulation in AD transgenic mice, but the mechanism of these positive effect were not fully elucidated. In the current study, we sought first to test the effect of OLE consumption at advanced disease stage in homozygous 5xFAD mice, starting at the age of 3 months for 3 months treatment. The treatment group was compared to vehicle-treated mice with refined oil. Next, we identified mechanism(s) by which OLE exerts the beneficial effect. Our findings showed that long-term consumption of OLE enhanced the cognitive performance and enhanced the brain function. In addition, OLE shifted the amyloid precursor protein (APP) processing pathway toward the non-amyloidogenic pathway and reduced Aβ-related pathology by reducing neuroinflammation through inhibition of NLRP3 inflammasomes activation. This effect was associated with reduced release of pro-inflammatory cytokines by the inactivation of the NF-κB signaling pathway. In conclusion,

our results suggested diet supplementation with OLE enriched with oleuropein, and a mixture of polyphenols could provide a beneficial effect to slow and/or halt AD progression.

Acknowledgments

All praise is due to Allah, the Lord of the worlds.

First, I want to give a special thanks to my major advisor, Dr. Amal Kaddoumi for providing me priceless instructions to perform this research and develop myself as a researcher. I greatly appreciate her for giving me the opportunity to join her laboratory and to be a part of her research team.

I would also like to express my gratitude to my graduate advisory committee members Dr. Robert D. Arnold, Dr. Jay Ramapuram, Dr. Murali Dhanasekaran, Dr. Vinicia Biancardi, and Dr. Mahmoud Mansour for their invaluable guidance, discussion, ideas, and feedback.

Many thanks to my friends and previous lab colleagues Dr. Yazan Batarseh, Dr. Khalid Elfakhri, Dr. Quoc-Viet Doung, Dr. Sweilem Al-Rihani, Dr. Youssef Mousa, Dr. Andrew Brannen, Dr. Lucy Darakjian, Kamal, Euitaek for their help and encouragement.

Finally, I would like to thank my family, for their continued support, encouragement, and prayers.

Table of Contents

List of Tables

List of Figures

List of Abbreviations

ACN: Acetonitrile

AD: Alzheimer's disease

ADAM-10: A Disintegrin and metalloproteinase domain-containing protein 10

AGEs: Advanced glycated end-products

APLP: Amyloid precursor-like protein

APOE: Apolipoprotein E

APP: Amyloid precursor protein

APS: Ammonium persulfate

Aβ: Amyloid beta

BBB: Blood-brain barrier

BCA: Bicinchoninic acid

BSA: Bovine serum albumin

C/EBP: CCAAT-enhancer-binding proteins

CAA: Cerebral amyloid angiopathy

CDK5: Cyclin-dependent kinase 5

CERAD: Consortium to Establish a Registry for Alzheimer's disease

CNS: Central nervous system

COX-2: Cyclooxygenase-2

CSF: Cerebrospinal fluid

CTE: Chronic traumatic encephalopathy

CVD: Cardiovascular diseases

DAMPs: Damage-associated molecular patterns

DAPI: 4′,6-diamidino-2-phenylindole

DPBS: Dulbecco's phosphate-buffered saline

DS: Down syndrome

ECs: Endothelial cells

EDTA: Ethylenediaminetetraacetic acid

ELISA: Enzyme-linked immunosorbent assay

EOAD: Early-onset Alzheimer’s disease

ETOH: Ethanol

EVOO: Extra-virgin olive oil

GFAP: Glial fibrillary acidic protein

GLUT1: Glucose transporter 1

GWAS: Genome-wide association study

HDL: High-density lipoprotein

HMGb1: High mobility group box 1

HPLC: High-performance liquid chromatography

HT: Hydroxytyrosol

IACUC: Institutional animal care and use committee

Iba 1: Ionized calcium-binding adaptor molecule 1

IDE: Insulin-degrading enzyme

IgG: Immunoglobulin G

IHC: Immunohistochemistry

IL: Interleukin

iNOS: Inducible nitric oxide synthase

IκB-α: inhibitor of NFκB

JAMs: Junctional adhesion molecules

LDL: Low-density lipoprotein

LOAD: Late-onset Alzheimer's disease

LRP1: LDL receptor related protein 1

LTP: Long Term potentiation

MAP: Microtubule-associated protein

MCI: Mild cognitive impairment

MD: Mediterranean diet

MDA: Malondialdehyde

MMSE: Mini-Mental State Examination

MRI: Magnetic resonance imaging

MWM: Morris water maze

nAchR: Nicotine acetylcholine receptor

NHD: Naus-Hakola Disease

NFT: Neurofibrillary tangle

NF-κB: Nuclear factor kappa-light-chain-enhancer of activated B cells

NLRP3: NLR family pyrin domain containing 3

NO: Nitric oxide

NSAIDs: Nonsteroidal anti-inflammatory drugs

OC: Oleocanthal

OCT: Optimal cutting temperature

OLE: Olive leaf extract

OLEA: Oleuropein aglycone

OLEG: Oleuropein glycosylated

PAMPs: Pathogen-associated molecular pattern

PBS: Phosphate buffer saline

PCR: Polymerase chain reaction

PET: Positron emission topography

P-gp: P-glycoprotein

IKK: IκB kinase

PSD-95: Postsynaptic density protein 95

PSEN: Presenilin

PVDF: Polyvinylidene fluoride

RA: Rheumatoid arthritis

RAGE: Receptor of advance glycated end-product

RBCs: Red blood cells

RNS: Reactive nitrogen species

ROS: Reactive oxygen species

sAPP: Soluble amyloid precursor protein

SNAP-25: Synaptosomal-Associated Protein

T2DM: Type 2 diabetes mellitus

TBE: Tris/Borate/EDTA

ThioS: Thioflavin S

TJs: Tight junctions

TLR: Toll-like receptor

TNF-α: Tumor necrosis factors-alpha

TREM2: Triggering receptor on myeloid cells 2

WAIS: Wechsler Adult Intelligence Scale

WT: Wild type

ZO-1: Zona-occludin-1

Chapters

1. Literature Review

1.1. Overview

Alzheimer's disease (AD) is a complex neurodegenerative disorder characterized by memory loss and progressive dementia, affecting the elderly population around the globe (1). First described by a clinical psychiatrist and neuroanatomist, Alois Alzheimer's in Tuebingen, Germany, in 1906, when Augusta D, a 51 years old woman, was admitted to the hospital experiencing problems with language and memory disturbance as well as various physiological problems such as disorientation and hallucinations. Alzheimer presented the case in the 37th Meeting of South-West German Psychiatrists as 'peculiar disease process of the cerebral cortex (2). Her case was known later as AD five years after her death (2). Later, AD has been linked and characterized by memory loss and progressive dementia in advanced stages, impairments in language and behavior (3).

1.2. Epidemiology

In 2019, Alzheimer's disease Association (ADA) considered AD as the 6th leading cause of death in the US and 5th leading cause of death for those aged 65 years or older. AD accounts for an estimated 70% of all dementia cases, with 5.8 million Americans have AD (4), from which an estimated 5.5 million people that are above 65 (5). By 2050, the cases number is expected to reach 13.8 million (5). In addition, the total annual cost of health, long-term and hospice care for people with AD or other dementias are expected to increase from $290 billion in 2019 to more than $1.1 trillion in 2050 in the absence of cure (4).

1.3. AD types

The accumulation of amyloid beta (Aβ) protein causes synapse deterioration and neuronal cell death (6). According to the Alzheimer's disease Association, the prevalence of AD due to autosomal dominant mutations is less than 1% (4). These mutations are encoded in the gene of Aβ producing proteins causes familial AD (7,8), and affects people below 65 years of age. The etiology that triggers the development of sporadic AD is not well known (9).

1.4. Early-onset AD

Early-onset AD (EO-AD) accounts for only less than 5% of all AD cases (10, 11). Most of EO-AD cases develop symptoms between the 40s and 50s. The vast majority of EO-AD cases are attributed to mutations of amyloid precursor protein (APP) (12, 13). Aβ formed by a series of enzymatic cleavage in the processing of APP by β-secretase followed by γ-secretase, resulting in higher production of $A\beta_{42}$ deposition in the brains (13-15).

1.5. Late-onset AD

Late-onset AD (LO-AD) is the most common type of AD, accounts for more than 95% of AD cases (16). LO-AD is also known as sporadic AD and affects people above 65 years of age (17), and do not exhibit autosomal dominant inheritance (18, 19). Patients with LO-AD express different biomarkers, including the presence of Aβ and Tau in the cerebrospinal fluid (CSF), and apolipoprotein E ε4 (APOε4) (20). APOEε4 allele is considered a major risk factor of sporadic AD (8), observed in 50-65% of AD cases (21). On the other hand, APOEε2 allele provides some protection against AD (21).

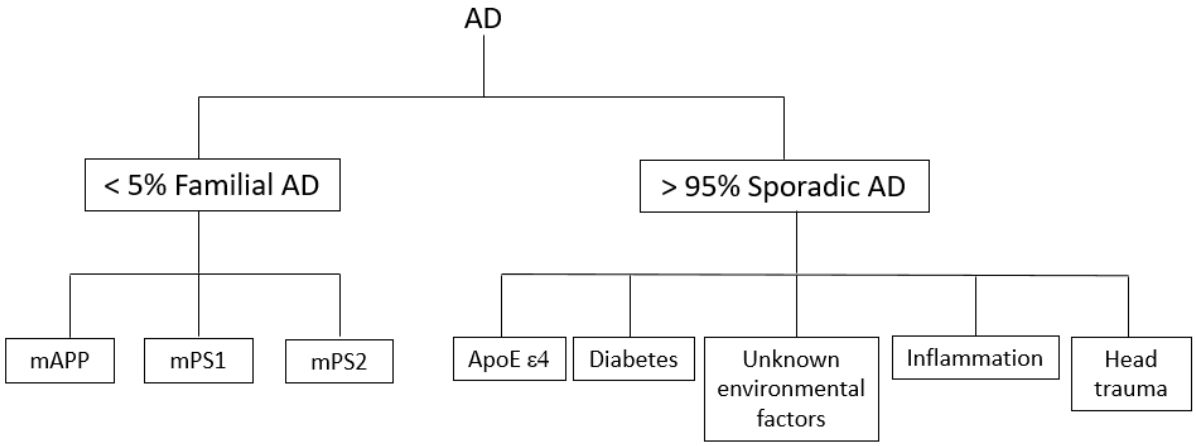

Fig 1. 1: Causes of AD. APP: mutations in the APPβ gene; PS1: mutations in the PSEN1 gene; PS2: mutations in the PSEN2 gene; APOEε4: apolipoprotein E epsilon 4 allele.

1.6. AD diagnosis

AD patients are diagnosed based on their clinical symptoms seen during their life, such as deterioration in cognition, including behavior, memory, speech, and understanding. Doctors utilize several tests to identify the severity, and extent of damage such as screening test named Mini-Mental State Examination (MMSE), complemented by more sophisticated neuropsychological tests, such as Consortium to Establish a Registry for Alzheimer's Disease (CERAD) or Wechsler Adult Intelligence Scale (WAIS) to observe and evaluate the degree of impairment in attention, orientation, constructive abilities, perceptual skills, functional abilities and problem solving (22, 23). These tests are performed in combination with brain imaging techniques, such as positron emission topography (PET), and magnetic resonance imaging (MRI) scans to confirm the AD diagnosis and exclude other types of dementia (24). The PET scan is sensitive and specific enough for AD diagnosis (25). Several studies are trying to find a non-invasive technique for AD Diagnosis (26).

Currently, AD therapies only treat the symptoms and barely slow disease progression. In addition, mono-therapeutic agents are not expected to be enough to rescue the disease damage

over a long period of time. Scientific researchers continue to investigate the multiple mechanisms associated with AD etiology in a wide range of clinical trials (27). Promising drugs to treat and cure AD should attack all symptoms and address the causes of AD.

1.7. Clinical presentation and symptoms

In AD, the overall cognitive impairment is designated by impairment of memory, language, praxis, visuospatial and executive functions (21). However, AD cases with focal cortical symptoms, the memory might be retained for long time (21). In addition, the posterior cortical atrophy symptoms are associated with younger subjects at onset around 60 years (28-30). Non-memory phenotypes in EO-AD is seen roughly in one-fourth of cases in whom language phenotypes and visual or apraxic are most frequent (31).

1.8. Etiology

Causes of AD are not fully understood yet. AD is a complex multi-factorial and multi–mechanism neurological disorder combining genetic, lifestyle and environmental factors that affect human brains and induce progression over time, which leads to structural and functional changes in the brains, and eventually death. Individuals with APP mutations, PSEN1, PSEN2 are at higher risk of developing AD symptoms before age 65, sometimes as early as 30 years (32). In addition, long-term exposure to environmental chemicals and solvents could cause AD (33). Also, it has been reported in several studies that lack of exercise, diet lacking fruits and vegetables, and poor sleep quality might cause memory impairment and cognitive dysfunction (34).

1.9. Neuropathology of AD

AD causes significant structural and functional disruption of a healthy brain. There is a progressive loss of pyramidal cells in the cortex, which mediate higher cognitive functions (35). Moreover, early synaptic dysfunction and impairment of neuronal circuit communication are observed in AD (36). Neurodegeneration starts in the entorhinal cortex and hippocampus (37), triggering early memory impairment and learning shortage in AD (38). Subsequently, the neurodegeneration spread throughout the temporal cortex and parietal areas, then to the frontal cortex, and eventually to the remaining of neocortex (38). Furthermore, AD causes damage to the limbic system (39), including the hippocampus and the fibers that connect the hippocampus to the cerebral cortex, thalamus, amygdala, and cingulate gyrus (38), which result in behavioral changes and cognitive impairment (39). AD patients cannot perform daily life activities, and they experience emotional, personal, and psychiatric disturbances (38).

In AD, the neurological findings are characterized by extracellular disposition of senile plaques and intracellular neurofibrillary tangles (NFT) of hyper-phosphorylated tau protein (40). Disposition of senile plaques starts in the basal region of the temporal, frontal, and occipital lobes and spread to affect the primary sensory areas (40). In contrast, NFT first affects the transentorhinal region and progresses to the limbic system and eventually to the neocortex (41). One study revealed two additional patterns of NFT distribution in AD, the predominant pattern, and the hippocampal spread with less atrophy (41).

1.10. Hallmarks of AD

There are several hallmarks associated with AD, including:

1.10.1. Aβ plaques

Aβ peptide is consists of several soluble monomeric isoforms. The most three common isoforms are ($A\beta_{40}$, $A\beta_{42}$, $A\beta_{38}$) (42). $A\beta_{38}$ is less likely to aggregate compared to other isoforms in the vasculature or the brain (43), while $A\beta_{40}$ is prone to be deposited in the vasculature, as seen in cerebral amyloid angiopathy (CAA), but $A\beta_{42}$ that has two additional amino acids, is more hydrophobic than $A\beta_{40}$ and can form insoluble aggregates (44, 45). Insoluble aggregates of $A\beta_{42}$ form extracellular plaques (46). Aβ plaques consist of spherical and complex protein accumulations with β-sheet structure, which is divided into diffuse and neuritic plaques (47). Aβ cascade hypothesis assumes that Aβ is the primary cause of AD, which triggers other neuropathological changes, including memory loss, neuronal loss, oxidative stress, and neuroinflammation (48, 49).

Several studies have shown that at low concentrations, Aβ has a neurotropic effect by enhancing the synaptic long-term potentiation (LTP), and improving learning (50). However, in AD, increased levels of Aβ aggregation and plaques formation has shown to induce neuroinflammation by activation of astrocytes and microglial cells. The activated astrocytes and microglia have been shown surrounding the Aβ plaques, and mediates the release of pro-inflammatory signals (51, 52). Other studies have shown that Aβ induces neuronal death through ROS release from activated astrocytes and microglia (53-56). In addition, activated astrocytes also release a wide range of cytokines and chemokines, including IL-6, IL-1β, and TNF-α, and promote cell death (57).

1.10.2. Neurofibrillary tangles (NFTs)

Tau protein, a microtubule-associated protein (MAP), is involved in modulating the stability and promotion of microtubules (58); it is localized in the body cells and axons and generated

by the neurons (59). Under normal conditions, nerve growth factors (NGFs) increase the expression of tau protein during neuronal development (60). However, it is also produced by glial cells in some pathological conditions (61). Although the main region of tau expression is the central nervous system (CNS), the gene that encodes for tau protein is also found in peripheral tissues. In the brain, there are six isoforms of tau from a single gene (62). The expression of these isoforms is required for embryonic development, suggesting that regulation of these isoforms is important for brain formation (63). Tau protein undergoes several post-translational modifications, such as non-enzymatic glycosylation, glycosylation, and phosphorylation, which represent the most post-translational modifications among all (64). Fatal tau protein being more phosphorylated and result in NFTs production, neuronal death, which leads to dementia (65). NFTs are composed of p-tau proteins and neurofilaments, which directly associated with neuronal loss (66). The severity degree of dementia in AD brains is associated with the number of NFTs (66). Studies suggested that the deposition of NFT and Aβ occurs in years before the clinical signs and symptoms appearance of AD within the hippocampus, neocortex, and other subcortical structures (67).

1.10.3. Compromised BBB

The BBB is a dynamic barrier that regulates and provides a constant, optimal environment for neuronal function by keeping out harmful components and toxic substances from the CNS (68), and allows nutrients to reach the brain (68). The BBB is also a selective barrier that regulates the movement of molecules entering the brain, thus keeping RBCs, leukocytes, neurotoxic plasma-derived components, and pathogens out of the CNS (69). The BBB is composed of endothelial cells (ECs), astrocytes, pericytes, microglia, and basement membrane (70). In addition to surrounding neurons, these components form the neurovascular unit (NVU) (71).

ECs are connected to each other by tight junction proteins (TJs) supported by junction adhesion molecules (JAMs) (70). The brain endothelium has no fenestrations with few pinocytotic vesicles. Therefore, the BBB physical barrier is a result of the formation of TJs and JAMs between adjacent ECs (71).

There are several endothelial transport systems, receptors that carry energy metabolites and nutrients, and regulate molecules transport across the BBB from blood to brain and vice versa, such as amino acid carriers (LAT1), glucose carrier (GLUT1), insulin receptor, transferrin receptors, lipoprotein receptors, low-density lipoprotein receptor-related protein 1 (LRP1), as well as ATP family of efflux transport proteins such as P-glycoprotein (P-gp) (72-76). The BBB properties undergo significant changes during pathogen attacks, inflammatory conditions, and neurological disorders. These changes affect the BBB integrity and its function, including transport pathways (76). Several studies reported that P-gp expression is reduced significantly in many neurological disorders, including AD (77). These results were supported by the correlation between the expression of P-gp and the deposition of Aβ in AD (78). Several human studies confirmed BBB breakdown in AD-associated disease, with loss of TJs, brain capillary leakiness, degeneration of pericytes and endothelial cells, perivascular accumulation of blood-derived fibrinogen, albumin, thrombin, IgG and hemosiderin (79).

1.10.4. Neuronal loss

The pathogenesis of AD consists of an intense reduction in the number of neurons in different areas of the brain compared to normal aging (80). Neuronal loss starts at an early age in the preclinical stage of AD, when Aβ plaques and NFTs have not yet formed (81), which significantly reduces the number of neurons in the cortex and hippocampus (82). This reduction correlates with the degree and severity of memory impairments (83). The likely reason for this

is a loss of the capacity for rearrangement of the neuronal organization of cerebral structures and the addition of new neurons to them, which are required for normal learning processes to take place (84).

1.10.5. Synaptic loss

Synaptic changes are crucial for AD, where the loss of synapse is considered the best pathological marker correlating with cognitive dysfunction in AD (85). It has been found that synapses loss is most prominent within senile plaques, suggesting that plaques may be a reservoir of synaptotoxic molecules such as Aβ. It has been shown that the severity of synaptic loss correlates with the duration of dementia (86). Since the loss of synaptic function was found to parallel the cognitive state (87), studies showed a significant correlation between synaptic count and the performance in MMSE in AD patients (84). Interestingly, another study evaluated the detrimental effect of NFT, loss of neurons, and synaptic change and found a significant impact on the cognitive decline (88). This finding is supported by the fact that synapses are the main site for long term potentiation (LTP) and neuronal plasticity (87).

1.10.6. Oxidative stress

Oxidative stress is characterized as an imbalance between the production of reactive oxygen/nitrogen species (ROS/RNS) and the ability of cells to neutralize them by the antioxidant defense (89). When the production of (ROS/RNS) increased, it's involved in the production of highly reactive hydroxyl radical ($OH^{\bullet}$), in addition to other oxidant molecules, which leads to tissue damage (89). It has been demonstrated that oxidative stress is increased in aged brains (90). Several mechanisms have been associated with the brain damage via oxidative stress, including but not limited to increases free intracellular Ca^{2+} concentration, neurotoxicity, and release of excitatory amino acids (91).

Besides the well-established pathology of senile plaques and NFT in AD, accumulating evidence has proved that the massive oxidative stress plays a significant role in AD and considered a feature of AD (92). Two studies reported an increment in the level of protein carbonyls and 3-nitrotyrosin which serve as a marker for intermediate of protein oxidation, as well as the expression of as 8-hydroxydeoxyguanosine (8OHdG) and 8- hydroxyguanosine, an indicator for oxidative damage of nucleic acids, in AD brains (93, 94). Also, the lipid peroxidation's products like malondialdehyde (MDA), 4-hydroxynonenal, and F2-isoprostanes are augmented in different regions in the brain as well as the CSF of AD cases (95). Furthermore, the biomolecules were also found to be affected adversely by the level of nitric oxide (NO) and peroxynitrite, which is another sources of oxidative stress. These effects usually result in structural and functional changes of the brain (96).

1.10.7. Neuroinflammation

Brain neuroinflammation plays a key role AD progression. In 1980s, several reports confirmed the presence of immune-related cells and proteins surrounding and in close proximity to Aβ plaques (97, 98). Years later, a number of observational and epidemiological studies were published suggesting the use of anti-inflammatory drugs approved for specific diseases, such as rheumatoid arthritis (RA), could provide protective effects and reduce the risk of AD in the long-term users of nonsteroidal anti-inflammatory drugs (NSAIDs) (99-102). In addition, several studies in transgenic mouse models demonstrated that treatment with NSAIDs can help in reduce AD-related pathology (102). Clinical trials in humans did not show beneficial effect of NSAIDs on cognition and overall disease severity (103).

These various studies serve as a root to support that neuroinflammation is playing an important role in AD development. Unlike other genetic causes and risk factors of AD pathology,

neuroinflammation is not thought to be the cause itself, but rather, a result of other AD-related pathologies, which in association, increase the disease severity by exacerbating Aβ and tau pathologies (104, 105).

Neuroinflammation in the brain has two functions; first, by playing a neuroprotective effect during the acute phase response, while on the long-term, neuroinflammation becomes detrimental when the chronic phase response is mounted (106). Activated microglia release various pro-inflammatory mediators and toxic products, includes reactive oxygen species (ROS), nitric oxide (NO), and cytokines, which could regulate Aβ synthesis. For example, several studies demonstrated an increase in Aβ deposits post-injury in people suffering from head trauma that was simultaneously associated with upregulated levels of interleukin 1 (IL-1) (107, 108). In addition, it has been shown that elevation of IL-1β was associated with increased production of other cytokines, such as IL-6, which in turn stimulates the activation of CDK5, a kinase known to hyperphosphorylate tau (109). In AD brains, neuroinflammation has been observed, which could provide a primary sign for exacerbating Aβ and p-tau pathology.

1.10.7.1. Astrocytes

Astrocytes are a sub-type of glial-cells like in the CNS. They are known as astrocytic glial cells, characterized by star-like shape, highly plastic cells that communicate with each other and other cells including neurons and ECs (110-112). Astrocytes are the most abundant cells in the brain representing about 50% of the CNS. Previously, astrocytes were called the ‘brain glue,’ with the main function to organize the neuronal network in the brain without the ability to communicate with other cells (110). The presence of astrocytes is important for brain homeostasis as well as neuronal functions and survival. They provide several roles as a part of the defense system for BBB maintenance and formation, in addition to transferring the energy

via lactate shuttle system to neurons, and modulating the synaptic activity, formation and remodeling (113,114). Astrocytes are highly organized in the form of 'astrocytic domain' in arrange to sense the encompassing and quickly react to changes within their environment in the brain (41). Like microglia, astrocytes have phagocytic capabilities and also produce several harmful molecules which has been shown to be involved in several neurodegenerative disorders (113,115).

In AD brains, the number of astrocytes surrounding and in close proximity to Aβ plaques increase significantly (115). Additionally, from in-vitro and in-vivo studies, in response to Aβ, spontaneous osclaition of intercellular Ca^{2+} levels have been observed in astrocytes (116, 117). Astrocytes contribute to AD pathogenesis by releasing cytotoxic compounds in response to Aβ, which might lead to microglia activation and other chronic inflammation cycles (52). Furthermore, a study has shown that rat primary astrocytes treated with Aβ induce deleterious neurotoxic effect in co-culture with neurons and induced tau phosphorylation (118). An additional function of astrocytes is to support the neurons, and in case of failure in astrocytes-neurons interaction, this could result in astrocytes neglecting the neurons in a phenomenon called 'neuro-neglect' as revealed by Fuller and his colleagues (119), who collectively demonstrated that Aβ-induced activation of astrocytes neglect the neuroprotective role in AD and expose neurons to toxic insults (119). Whether astrocytes themselves produce Aβ requires more evidence. However, it has been suggested that they directly contribute to the disposition of Aβ plaques. Rossner and colleagues found in Tg2576 mice that BACE1 is synthesized and expressed in astrocytes surrounding and in close proximity to Aβ plaques, suggesting Aβ is produced by astrocytes (120, 121). However, the expression could also be influenced by the production of pro-inflammatory cytokines released by microglia.

1.10.7.2. Microglia

Microglia cells derive from the mesenchymal myeloid precursor cells and migrate to the brain during embryogenesis (122). The microenvironment in the CNS induces mesenchymal myeloid precursor cell maturation to fully developed microglia (122, 123). During the late phase of embryogenesis, the fetal macrophages from the myeloid origin arising from monocytes enter the brain and become a part of mature microglia (124). Microglial cells are plastic, and based on age and different brain regions, they display different phenotypes (125). Microglial cells may be found in two conditions 'resting' or 'activated'. In the resting state, microglial cells morphology are characterized by ramified, long, and dynamic processes, and they move and scan the environment for surveillance. Live imaging of resting microglia from in vivo study, showed the brain undergoes surveillance by microglia multiple times daily (126). In response to a chemical or cell-based stimulus, microglia become activated and undergo phenotypic changes morphologically characterized for an amoeboid shape and short process (127). Microglial activation occurs slowly and gradually from partial to a fully activated state (124). Several activated microglial phenotypes have been proposed to receptor expression in the cell surface and cytokines. Generally, microglia cells are classified into M1 and M2; M1 promotes the expression of pro-inflammatory cytokines via toll-like receptor (TLR), and M2 promotes the expression of anti-inflammatory cytokines, such as IL-4, IL-13, and other molecules (128).

In AD, microglial tend to disrupt the balance between their phenotypes favoring a pro-inflammatory phenotype with less phagocytic abilities (129). Aβ, as a stimulus, cannot be adequately removed. Thus microglial cells act as housekeeping to maintain the brain homeostasis and enhance the clearance of Aβ (130), suggesting microglia has two faces: neuroprotective in the early stage of the disease; and harmful at late stages of AD (131).

Furthermore, one study showed that pro-inflammatory cytokines could inhibit microglial phagocytosis of Aβ *in vitro* (132). The inhibitory effect was achieved by activation of NF-κB and subsequent production of prostaglandins binding to the E prostanoid receptor. Interestingly, ibuprofen was able to rescue Aβ-elicited phagocytosis in a pro-inflammatory milieu (132).

1.10.7.3. Cytokines

Cytokines are small and soluble signaling molecules classified into pro-inflammatory, including IL-1β, IL-6, and TNFα; or anti-inflammatory, such as IL-4, and IL-10. Both are associated with the immune response, and they have an important role and function in normal conditions.

IL-1 is a well-known pro-inflammatory cytokine. In normal conditions, the expression level of IL-1 is low in different types of cells. IL-1 family is consist of three members, IL-1α, IL-1β, and IL-1, these members are encoded by three separate genes, IL-1β is secreted and working intracellularly and converted to the active form by enzymatic cleavage (133) However, the level of IL-1 in the brain of AD patients increases dramatically and is associated with neurotoxic effect (96). It was proven that the overexpression of these cytokines is responsible for Aβ plaques formation and NFTs (134). The microglial cells are the primary cell type that increases the IL-1 expression (96). Interestingly, the up-regulation of IL-1 levels has been associated with AD-related pathologies (96). To support that IL-1 polymorphisms increase the risk of developing LO-AD.

In 1986, Hirano and colleagues discovered that lymphocyte cells within the CNS release an agent which was named IL-6 (135). Later, IL-6 was detected in astrocytes, microglia, and neurons. Signaling pathways such as NF- κB and C/EBP are the most important transcriptional factors (TFs) regulating IL-6 expression. It was also reported that IL-6 stimulates releasing the

cytotoxic and chemotaxis molecules from the astrocytes as well as influence their proliferation. However, in some conditions, IL-6 acts as a neurotrophic factor and enhances neuronal survival, regeneration, and differentiation (136).

In AD progression, IL-6 levels increased significantly in humans and AD-mouse models (137-139), where it servers dual function: neuroprotective at early stages, but harmful when the Aβ plaques increase significantly. Different IL-6 have been associated with AD, but the exact mechanism is debated (140-142), several studies reported that IL-6 influence the APP processing and expression (143, 144), as well as p-tau (145).

1.10.7.4. Nuclear Factor-Kappa B

Nuclear factor-Kappa B (NF-κB) plays a key role in innate immunity, and upregulation of cytokines and chemokines levels. It has been proven that NF-κB was detected in the brains of human AD (146, 147). The activation of NF-κB was significantly increased in response to Aβ in vitro (148, 149). In 1986, NF-κB was first discovered by Sen and Baltimore in mature B-cells (150). The family of NF-κB signaling consists of five members; p65, p50, p52, c-Rel, and RelB. The NF-κB dimers are regulated by the protein of inhibitors of κB (IκB), which are normally in the inactive state. In the cytoplasm, IκB can be rapidly degraded to its phosphorylated form and resynthesized. Upon exposure to stimuli, the level of IκB kinase complex (IKK) increases, and it is responsible for the degradation of IκBα, which increases its phosphorylated level (p- IκBα). Once phosphorylated, IκBα, the NF-κB subunits became free and releasing to the nucleus and activate transcription.

NF-κB is expressed in both astrocytes and microglia (151). Results from pre-treated primary astro-microglial cells with Aβ and IL-1β induced the activation of NF-κB (152). Taken

together, multiple evidences suggest that NF-κB plays a significant role in Aβ plaque formation and even a more critical role in inflammation and cytokine signaling in AD development.

1.10.7.5. High mobility group box 1

High mobility group box 1 (HMGb1), also known as HMG-1 or amphoterin, is a DNA binding protein localized in the nucleus. During cell activation and apoptosis, HMGb1 translocates from the nucleus, and it is released to the extracellular space in the cytoplasm (153). Upon stimulation, HMGb1 undergoes post-translational modification that initiates the production of pro-inflammatory cytokines via TLR4 (153). HMGb1 becomes a double-edged sword during neural development and neurodegeneration when released extracellularly (154, 155).

Recently, several studies indicate that activation of HMGb1 has been observed in hippocampal neuron cultures (156). A study in hippocampal neuronal cells, Aβ used as a marker to induce neuroinflammation, result showed the levels of pro-inflammatory cytokines, such as IL-1β, IL-6 and TNF-α increased and associated with upregulation in HMGb1/RAGE, which activates NF-κB signaling pathway (157), suggesting neuroinflammation plays a significant role in AD pathology through HMGb1 mediated activation of RAGE/ NF-κB signaling pathway (157). In vitro study used N9-mouse microglial cells treated with Aβ (1μM), which significantly increased the level of IL-1β, HMGb1, and NLPR3 inflammasome, suggesting that HMGb1 induced the activation of the microglial cells thus contributing to neuroinflammation (158). The implication of HMGb1 was also shown in transgenic mice of AD, named 5xFAD, TgCRND8, and Tg2576 (159-161).

1.10.7.6. NLR Family Pyrin Domain Containing 3 inflammasome

Inflammasomes are intracellular multi-protein localized in the cytoplasm and regulate the inflammatory signals in the innate immune system in response to pathogens (162). An example

of such inflammasomes is NLR Family Pyrin Domain Containing 3 (NLRP3) inflammasome (162). NLRP3 belongs to the subfamily of NLRP, which induces the production of pro-inflammatory cytokines, such as IL-1β and IL-18, through activation of caspase-1 (162). Activation of NLRP3 inflammasome is divided into two steps, priming, and activation (163). The priming of NLRP3 is provided by a stimulus, which activates the NF-κB pathway. This pathway promotes the transcription and expression of NLRP3, and allow the translocation of pro-IL-1β and pro-IL-18 from the nucleus to the cytoplasm. In addition, the activation step is triggered by pathogen-associated molecular patterns (PAMPs) and damage-associated molecular patterns (DAMPs), which activate caspase-1 and pro-inflammatory cytokines release. NLRP3 inflammasome has been involved in several metabolic and neurological disorders, including AD, T2DM, and multiple sclerosis (164, 165).

In AD, several studies showed that Aβ could initiate the NLRP3 inflammasome signaling pathway, which causes the release of pro-inflammatory cytokines and induces the activation of microglia (166, 167). Another study showed that NLRP3 knockout reduced Aβ accumulation and improved memory dysfunction in AD transgenic mice (168), an effect that was consistent with the use of NLRP3 inhibitor (JC-124) in AD transgenic mice (169).

On the other hand, various studies showed the activation of microglia in response to Aβ plaques phagocytosis induces the expression of IL-1β in mouse models and AD brains through lysosomal destabilization and production of cathepsin B, which make the NLRP3 inflammasome active (170, 171).

1.11. Risk factors of AD

1.11.1. Advanced age

Aging is considered the major risk factor to cause dementia (172). Several cohort studies conducted in Europe and the US showed that the risk of dementia increased exponentially with advanced age (173-176). This association has been observed in all dementia subtypes, including AD (177). A study performed in 1995, showed that the prevalence of AD in a community of 32,000 individuals was 10% among people above 65 years of age, and 47% in people above 85 years of age (178). The majority of AD cases are not able to live independently because they have severe cognitive impairment (178). The incidence rate of AD cases among people above 85 years of age was 14 times higher than people age between 65-69 years. Another study found that the incidence increased by 23% per/year after 65 years of age (179). While age is considered a high and out of control risk factor, lifestyle changes, exercise, and diet could help in reducing the development of AD (180).

1.11.2. Cerebrovascular diseases

Existing evidence suggests that patients with comorbidities are at higher risk of developing AD or dementia. Findings from clinical trials demonstrated that patients with comorbidities have poorer cognitive function compared to healthy subjects (181). Cerebrovascular changes such as small and large ischemic cortical infarcts, and hemorrhage infarcts increase the risk of dementia, but the exact mechanism is unclear (182). Cerebrovascular diseases have been shown to damage the cognitive function regions, thalamus, and thalamo-cortical in the brain. However, they may also increase the disposition of Aβ plaques, and induce the inflammatory response, which leads to cognitive impairment (182). Hypoperfusion, which increases the expression of CDK5, an important serine-kinase for synaptic formation and plasticity plays an important role

in AD (183), and involved in the formation of NFTs and abnormal p-tau (184), which could be a key protein linking NFT to amyloid plaques pathology (184). Data from observational and cross-sectional studies also revealed that hypertension might increase AD risk through disrupting vascular BBB integrity, which leads to cell damage by protein extravasation in brain tissues (185), as well as a reduction in synaptic plasticity, neuronal apoptosis, and increases Aβ accumulation resulting in memory impairment (186).

1.11.3. Type 2 diabetes mellitus

Diabetes mellitus (DM) is one of the most common risk factors associated with memory impairment in AD elderly patients (187). Type 2 diabetes mellitus (T2DM) patients are at higher risk for developing AD compared to healthy subjects (188). T2DM is one of the risk factors that has been associated with multiple CVD-related diseases such as hypertension, stroke, and hyperlipidemia (189). However, other studies reported the non-CVD mechanisms linked to T2DM with AD, such as hyperinsulinemia and the advance glycated end-products (AGEs) (190), but the underlying mechanisms are not fully understood.

Insulin-degrading enzyme (IDE) has been associated with Aβ clearance from the brain; insulin and Aβ are competing substrates of IDE (191). Insulin can increase AD hallmarks in the brain, such as Aβ deposition, and p-tau (192). Interestingly, it has been shown that treatments for T2DM were able to improve memory and cognitive function in AD patients, an effect could be due to the anti-inflammatory properties of anti-diabetic therapies (193).

1.11.4. Traumatic brain injury

The incidence of traumatic brain injury (TBI) is growing rapidly worldwide, affecting the healthcare and socioeconomic of society (194). Patients with TBI suffer from physiological and

neurological morbidities that affect their life quality (195). TBI patients are at higher risk of AD and dementia compared to healthy individuals (196-198). Men with TBI are at higher risk from women according to two meta-analysis studies (199, 200). Existing evidence supporting TBI-AD association increased accumulation of Aβ and tau pathology in brain tissues and CSF of TBI patients (201). TBI is considered as the most significant environmental risk factor associated with AD (202).

1.11.5. Smoking

Existing studies have shown controversial results with regard to smoking as a risk factor for AD. Some indicated that tobacco smoking increases the risk of developing AD (203-205), while others showed no effect (206). Case-controlled studies showed that tobacco smoking could be neuroprotective against AD via nicotine acetylcholine receptor (nAChR) (207, 208). However, other studies linked tobacco smoking with AD risk by increasing free radicals generation, thus leading to high oxidative stress, or by affecting the inflammatory immune system, which activates the phagocytosis and induces oxidative damage (209).

1.11.6. Triggering receptor on myeloid cells 2

Triggering receptor on myeloid cells 2 (TREM2) is a transmembrane receptor of the immunoglobulin superfamily expressed on the plasma membrane of myeloid cells and microglia, and is active in the innate immune response (210). Heterozygous mutation (R47H) of TREM2 causes a rare genetic disorder called Naus-Hakola Disease (NHD) (211). Recently, loss of function of TREM2 has been associated with LO-AD due to its role in inflammation (212). The loss of function of TREM2 showed that the level of Aβ deposits increased significantly in AD (212).

1.11.7. Down syndrome

Down syndrome (DS) is a genetic disorder characterized by a chromosomal abnormality in trisomy 21 (213). The life span of DS patients is between 55-60 years (214), DS has been associated and linked to developing AD. The majority of DS patients suffer from AD, because APP is encoded on the same chromosome as DS, which leads to higher accumulation of Aβ and induces disease progression.

1.11.8. APOE ε4

ApoE is a protein produced in the CNS by astrocytes and located on chromosome 19 (215). Genome-wide association studies (GWAS) identified APOE ε4 as a mutant isoform with the greatest risk of developing AD (216). The presence of APOE ε4 at an early age of life showed a poorer cognitive function and considered as a sign of developing AD (217). Other risk factors, such as head injury, increased the risk of AD ten times for APOE ε4 carriers (218).

1.12. Amyloid precursor protein

APP plays a central role in AD pathology by sequential proteolytic cleavage, results in Aβ peptides formation. APP is a protein localized on the cell membrane or in the intracellular vesicles in a wide variety of cells in the body (219). It is highly expressed in the brain and rapidly metabolized (219). APP belongs to a gene family that includes amyloid precursor-like protein-1 (APLP-1), and amyloid precursor-like protein-2 (APLP-2), which are type-1 transmembrane proteins. APLP-1 and APLP-2 share significant homology sequences in their ectodomains (220). APP gene encodes 3 different isoforms, as shown in Fig 1.2, APP695, APP770, and APP751, highly expressed in both neuronal and non-neuronal cells. APP695 is the most predominant isoform expressed in the neuronal cells in the brain (221). APP isoforms

exist in two forms, the immune form (imAPP) and mature form (mAPP). imAPP traffics through the Golgi to form the mAPP (222). The physiological role of APP is still unclear. However, it has been suggested to be involved in neurodegeneration, and required for neuronal growth (223). Full-length APP can be processed through two different enzymatic pathways, the amyloidogenic and non-amyloidogenic pathways, using three proteases named α, β, and γ secretases, (224).

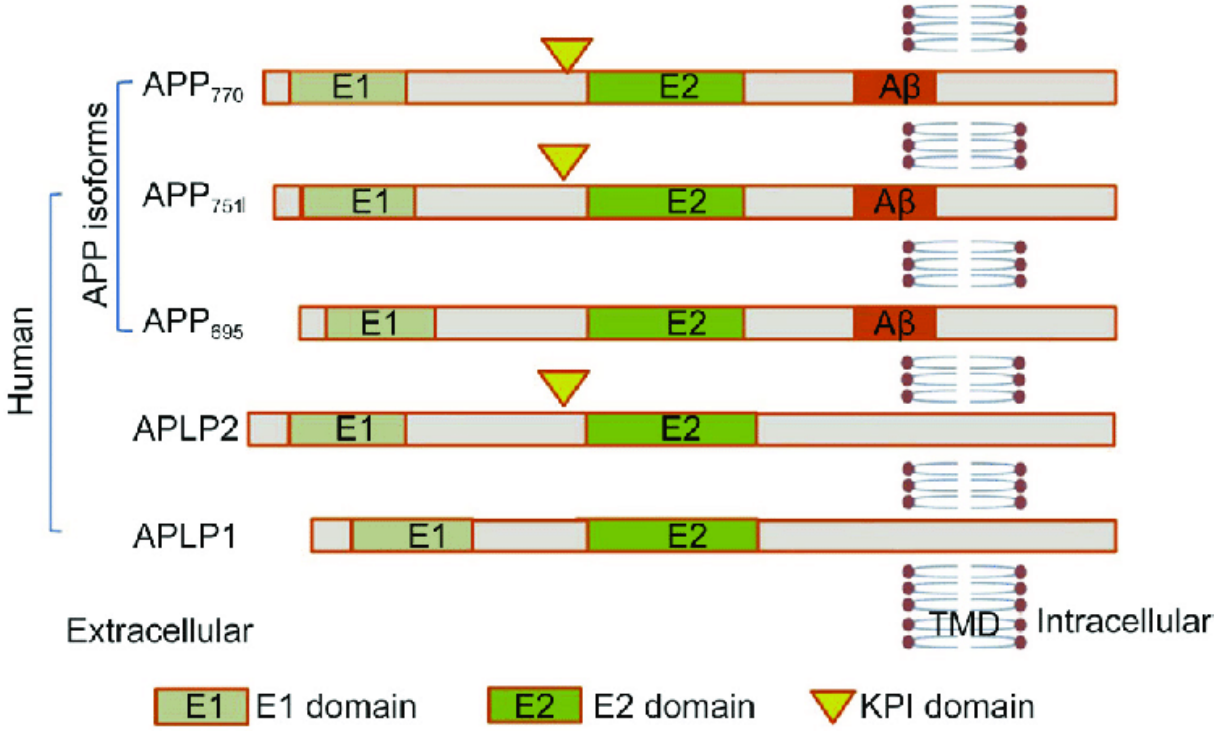

Fig 1. 2: Schematic representation for the structure of 3 APP isoforms and the APP-like proteins (APLP), APLP1, and APLP2. APP isoforms range in size from 695 to 770 amino acids. APP 695 is considered the most abundant isoforms in the brain (285; permission requested). [URL: https://www.nature.com/articles/aps201728]

In the amyloidogenic pathway, as shown in Fig 1.3, APP is proteolyzed by β-secretase and generates a soluble fragment from the N-terminal domain called sAPPβ, as well as the CTFβ fragment that remains attached to the membrane. Then, CTFβ is proteolyzed by the γ-secretase enzyme to form Aβ-40 and Aβ-42 (225). In non-amyloidogenic pathway, as shown in Fig 1.3,

APP is proteolyzed by α-secretase and generates a soluble fragment from the extracellular N-terminal domain called sAPPα, which possesses different neurotropic and neuroprotective properties (226), in addition to the C-terminal fragment of APP that remains anchored to the membrane (CTFα), which again proteolyzed by the γ-secretase producing short p3 fragment. P3 fragment has low toxic properties (227).

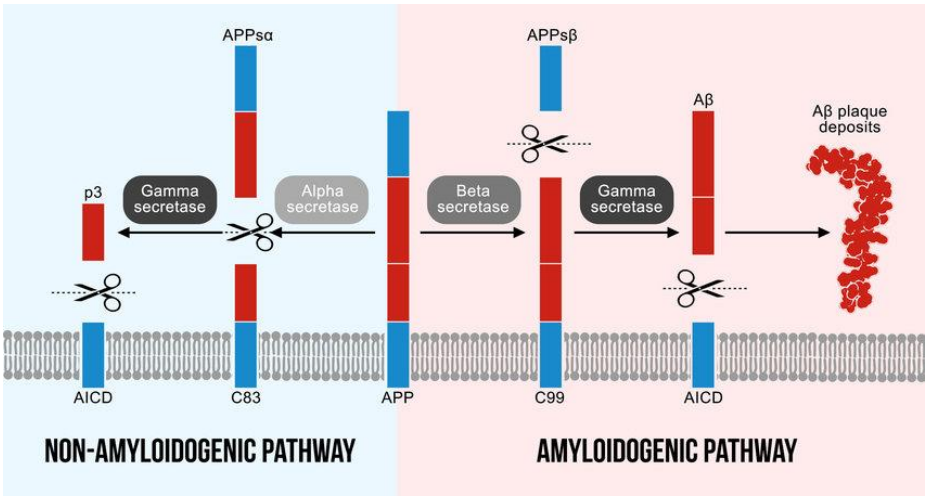

Fig 1. 3: Schematic representation of APP structure and metabolism showed amyloidogenic and non-amyloidogenic pathways. The red portion of APP signifies the toxic Aβ, which is cleaved in the non-amyloidogenic pathway (228). [URL: https://www.tandfonline.com/doi/full/10.1080/02648725.2018.1523521]

1.13. BBB

Blood vessels deliver oxygen and nutrients to organs and tissues throughout the body. CNS vessels are continuous non-fenestrated vessels, which tightly regulate molecules and ions within the CNS through a physical barrier called the BBB (229). The BBB is composed of the basement membrane, astrocytes, pericytes, and endothelial cells (ECs). ECs are tightly connected by junction proteins, such as Zo-1, claudin-5, and occludin. The BBB controls the passive and active transport mechanisms within the endothelium (230). This tightness is critical

for proper protection of the CNS from pathogens, injuries, and inflammation, and to maintain the neuronal function. However, due to the BBB nature, it could limit drugs delivery to the CNS, because of this obstacle, several studies and efforts have been made to modulate, overcome, or bypass the BBB to enhance CNS drugs delivery (231). BBB breakdown has been linked to AD due to disruption of the TJs, which alter the transport and movement of toxic molecules between blood and brain and vice versa, vessel regression aberrant, brain hypoperfusion, angiogenesis, and inflammatory responses (232). Targeting BBB has been considered as a novel therapeutic approach to cure AD.

1.14. Aβ clearance across the BBB

Functional BBB allows the transport of Aβ from brain interstitial space to the blood and vice versa (Fig 1.4). Soluble Aβ is transferred from the interstitium to the brain through LRP1, and P-gp (233). Several studies suggested that both transporters have been strongly involved in Aβ clearance across the BBB (234). On the other hand, free Aβ transfers to the brain across the BBB through the advanced glycosylation end product-specific receptor (RAGE) (235). In AD, the accumulation of brain Aβ could be due to an imbalance between its production and clearance. Several other mechanisms are associated with Aβ clearance across the BBB, including insulin-degrading enzyme (IDE), the soluble form of RAGE (sRAGE), and serum amyloid P component (236), as shown in Fig 1.4.

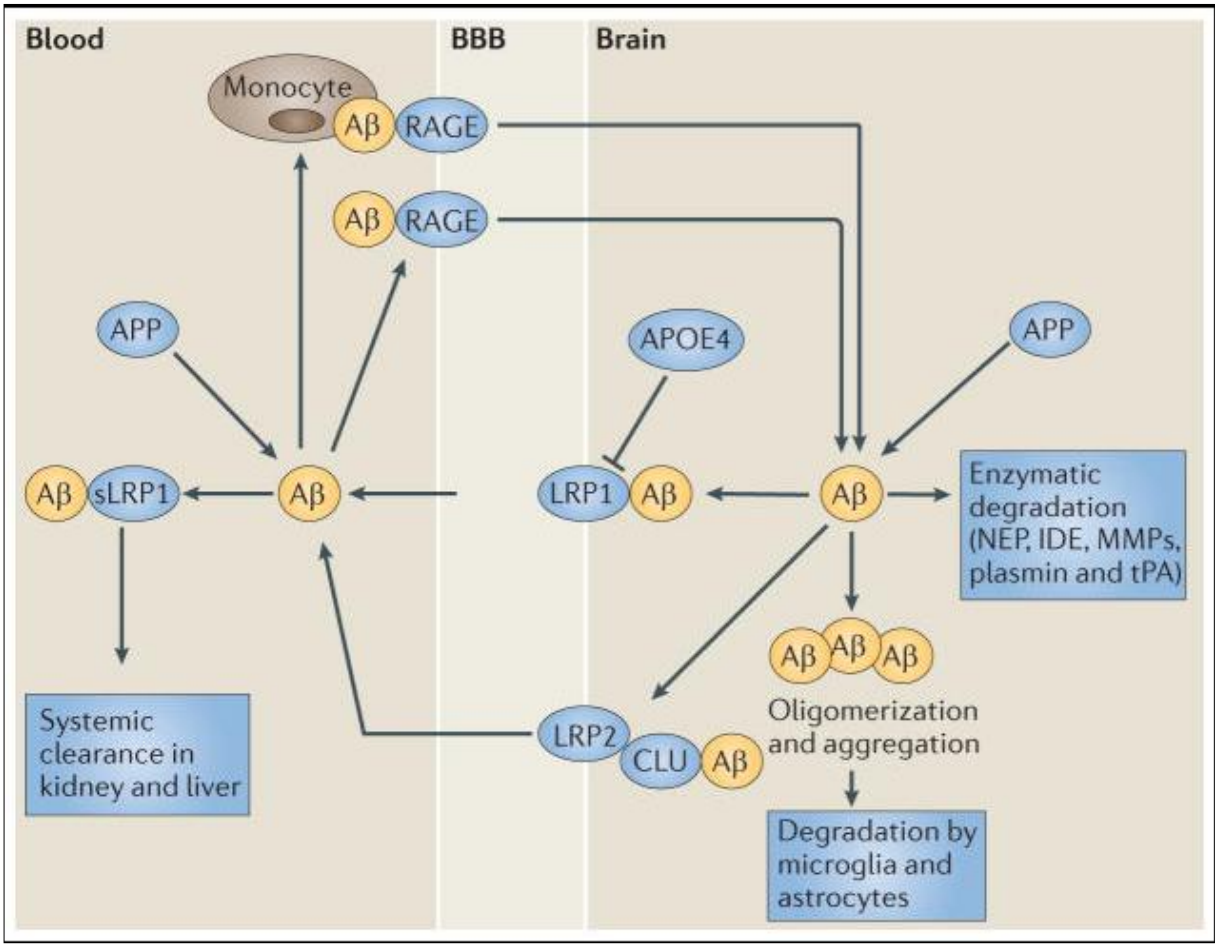

Fig 1. 4: Aβ efflux and influx through the BBB. LRP1 mediates the rapid efflux of a free, unbound form of Aβ. (APOE2). Several cells in the brain, including EC's, pericytes, neurons, astrocytes, and microglia, express different Aβ degrading enzymes, which contribute to Aβ clearance and maintain the brain levels low. In the circulation, Aβ bounds mainly to sLRP1, which normally prevent its entry to the brain and mediates its removal by the liver and kidney. At the same time, the unbound Aβ could return to the brain through RAGE. Taken from reference (237). [URL: https://pubmed.ncbi.nlm.nih.gov/22048062/).

1.15. History of olive leaf biophenols

Plants not only provide food macromolecules such as carbohydrates, proteins, and lipids, they also provide a variety of other compounds, which play diverse roles in health promotion (238). Plants provide us with numerous bioactive compounds that maintain health or prevent diseases. Among those bioactive compounds, biophenols have received an enormous amount of interest due to their multipurpose actions (239). Over the last three decades, they have been extensively investigated in a large number of studies for their biological activities. Experimental and clinical evidence suggests that olive oil biophenols may play a pivotal role in maintaining health or preventing disease (240-242).

Olive leaves and leaf extracts have been used for centuries, as complementary medicines for the treatment of different diseases including malaria fever, alopecia, colic, hypertension, rheumatic pain, sciatica, paralysis, arrhythmia, and cancer (243-246). Several biophenols have been reported in olive products (fruits, oil, and leaves). The concentrations of these biophenols vary in different products. Olive leaves are a richer source of biophenols than olive oil, and can contain up to 2% of total phenols on a fresh weight basis (246).

Evergreen trees belonging to the family Oleaceae, olive trees can grow up to 9 m tall. They have a lifespan of up to 2,000 years and can produce fruit for over a thousand years with minimum care (247). There are about 2500 known varieties of olives, but only 250 cultivars have been classified as commercial cultivars by the International Olive Oil Council (248). Olives can be grown in the cold as well as in warmer climates, but for most varieties, some winter frost is preferred (249). For most of the olive-growing regions of the world, the average maximum temperature in the hottest month is about 30°C; however, very high temperatures of up to 45°C have minimal effect on mature olives (249).

1.16. The role of biophenols in health

Consumption of olive fruits, oil, and leaves have never been restricted to dietary and culinary applications. Olive oil and leaf extract have been continuously incorporated in cosmetic and traditional medicine recipes since antiquity (250). The active ingredients responsible for the observed biological activities have been identified as phenolic in nature (251). Olive phenolic compounds, i.e., olive biophenols, are very well prized for their antioxidant properties (252). With the introduction of the oxidative theory of aging and the role of oxidative stress in disease pathology, biophenols are discovered for potential disease prevention and health promotion (246, 253).

1.17. Oleuropein and neuroprotective effect on AD

Oleuropein, $C_{25}H_{32}O_{13}$ (Fig 1.5), a secoiridoid (monoterpene), is an ester of hydroxytyrosol (HT) with the oleoside skeleton. It is the major biophenol found in olive leaves (244, 254-256). The pharmacological properties of oleuropein have been extensively studied. Oleuropein is associated with most of the health-promoting properties of olive leaves (257, 258). The glycosylated form of Oleuropein gives rise to many compounds found in olive fruit and leaves via aglycon, through the opening of the elenolic acid ring (259). Its quantity is almost negligible in olive oil as compared to olive leaves, because of its extensive enzymatic degradation during oil extraction and low partitioning in oil (260).

Oleuropein accounts for about 25% of the total biophenols of olive leaf (244). The concentration of oleuropein is lower in ripe olives due to hydrolysis and/or conversion to other compounds (243). During virgin oil extraction, glycosylated oleuropein (OLEG) is hydrolyzed to a number of compounds, including HT, elenolic acid, oleuropein aglycone (OLEA, Fig. 1.5), and glucose based on the hydrolysis conditions.

In AD, olive leaf extract (OLE) improved the neurologic deficit scores in rats after transient middle cerebral artery occlusion and cerebroprotection from ischemic reperfusion as well as reduced BBB permeability, brain edema, and LDL/HDL ratio (260). Another study reported that oleuropein has a potential anti-amyloidogenic effect as it forms a noncovalent highly stable complex with Aβ and prevents its aggregation (261). Schaffer and colleagues reported that 100 mg/kg of HT-rich olive extract for 12 days enhanced resistance of dissociated brain cells to oxidative stress in mice and reduced basal and stress-induced lipid peroxidation (262).

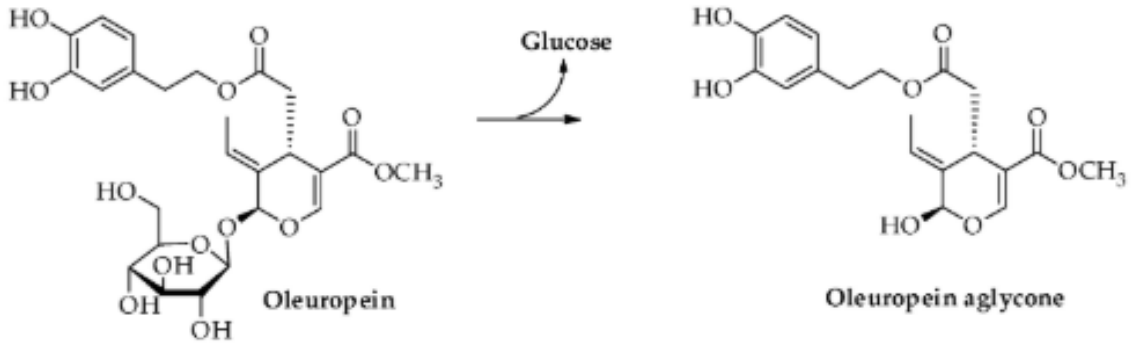

Fig 1. 5: Oleuropein and Oleuropein Aglycone Structures. Modified from the (Annalisa Romani, 2019) article (263). [URL: https://www.ncbi.nlm.nih.gov/pmc/articles/PMC6724211/]

1.18. Pharmacological activity of olive leaf extract

1.18.1. Antimicrobial activity

OLE is reported to be an effective antimicrobial agent against a variety of pathogens, such as viruses, bacteria, fungi, and protozoa. In addition, it can activate the immune system response against all microbes and directly stimulate phagocytosis (264), as well as interfere with the critical amino acid production necessary for microbes. Olive leaf extract reportedly counteracts antibiotic-resistant strains of bacteria and yeast; it is also useful against microorganisms that produce chronic fatigue and immune dysfunction syndromes (264).

1.18.2. Cardiovascular Protection

It has been established that consuming a Mediterranean diet (MD), which is rich in biophenols is associated with a reduced risk of cardiovascular diseases (CVDs) (245, 265). It has been proposed that polyphenols impede biochemical events that are associated with atherosclerotic disease (266). Biophenols may protect the cardiovascular system from free radical damage by scavenging ROS (267). They are believed to inhibit the oxidation process of low-density lipoprotein (LDL) (268), which is responsible for atherosclerosis, suggesting olive leaf biophenols can play a vital role in decreasing the risk of cardiovascular diseases.

Oleuropein has been shown to increase coronary flow and left intraventricular pressure in rabbit myocardium (269). Due to the antioxidant effects, oleuropein is considered a cardioprotective agent to prevent the acute complication post coronary obstruction (270). Oleuropein is involved in inhibition of 5-lipooxygenase and 12-lipooxygenase, and eicosanoid production (244). Oleuropein prevents the membrane lipid peroxidation and protects against oxidation-related myocardial injury due to either ischemia or reperfusion. A significant reduction of oxidized glutathione was observed in ischemic hearts pre-treated with oleuropein. The cardioprotective role of it to counteract the oxidation surge post-ischemic was examined by detecting the level of oxidized glutathione, which is a reliable indicator of cardio-myocyte's exposure to oxidative stress in the coronary effluent (270).

1.18.3. Antioxidant

Oxidative stress is defined as a disturbance in the balance between the production of toxic species like free radicals and the antioxidants. This imbalance diminishes the biological system's ability to get rid of these harmful products or efficiently fix the resulting injury (250, 271). The active phenolic ingredients in the olive extract, belong to secoiridoid family, are responsible for scavenging H_2O_2 (265). The antioxidant capacity of the olive extract is higher than that of vitamin C, vitamin E or hydroxytyrosol. Le Tutour and colleagues found that the olive leaf extract contains a large amount of oleuropein, as well as hydroxytyrosol, that are more effective than vitamin E in extending the induction period for oxidation (253). In was found that oleuropein-rich extracts from olive leaves, significantly decreased thiobarbituric acid reactive substances content of liver, heart, kidneys, and aorta, increased the activities of superoxide dismutase and liver catalase, as well as improved the serum antioxidant potential in rats (272). It was suggested that oleuropein, oleuropein aglycone, and hydroxytyrosol-rich extracts could delay the lipid peroxidation process and increase the activity of antioxidant enzymes.

1.18.4. Anti-inflammatory activity

Oxidative stress plays a vital role in inflammatory processes as it activates NF-κB signaling pathway (250, 273). Biophenols possess anti-inflammatory activity and act as modifiers of signal transduction pathways, modulate pro-inflammatory gene expression, and important cellular signaling processes (273). It has been proposed that these anti-inflammatory effects are due to various mechanisms including: scavenging effect of ROS directly or via glutathione peroxidase activity and modulation of nuclear redox factor activation, inhibition of pro-inflammatory enzymes, such as COX-2, lipoxygenase and inducible nitric oxide synthase

(iNOS), downregulation of various pro-inflammatory cytokines such as TNF-α, IL-1β and IL-6 and inhibition of NF-κB signaling pathway (264, 273). Oleuropein and hydroxytyrosol were found to reverse chronic inflammation and oxidative stress (274), suggesting that olive leaves may have a therapeutic potential in the treatment of inflammatory diseases.

2. Introduction

Alzheimer's disease (AD) is a progressive, most prevalent neurodegenerative disorder and the most common cause of dementia (1). While the cause of AD is not clear, several factors play a role solely or in a combination of lifestyle, environmental, and genetic factors (278). Worldwide, AD cases account for 60-80% of dementia cases (279), while in the United States, AD is considered the sixth leading cause of death, and the fifth among Americans above 65 years old (280). To date, no effective treatments exist. With the lack of a clear understanding of AD pathogenesis, it is difficult to find a cure as the available drugs treat the symptoms, not the underlying causes of the disease. AD is characterized by the deposition and accumulation of amyloid-beta (Aβ) peptides in the brain (281, 282), hyperphosphorylated tau protein (p-tau) aggregation, cerebral amyloid angiopathy (CAA), astrogliosis, microglial activation, synaptic dysfunction and neuronal loss (283, 284).

Aβ peptides are derived from the proteolytic cleavage in the amyloid precursor protein (APP) to form mainly $A\beta_{40}$ and $A\beta_{42}$ isoforms (285). Accumulation of Aβ could directly induce neuroinflammation by activating the NF-κB that could cause BBB disruption (286). Astrocytes and microglia are major cellular components of the innate immune of the CNS, and they have a vital role in the neuroinflammation processing in AD (286).

Disruption in the BBB results in neuronal toxicity associated with Aβ accumulation and reduced the clearance across the BBB, as well as neuroinflammation leading to AD progression. Therefore, to maintain a healthy BBB function and/or improve BBB function could provide a novel strategy to prevent or treat AD.

Functional BBB is composed of the basement membrane, astrocytes, pericytes, and endothelial cells (ECs). ECs are tightly connected at a junctional complex via tight junction (TJs) and

adherence junction proteins (231), which prevent the transport of solutes from blood to the brain and vice versa (287). Aβ peptides can be transported bi-directionally across the BBB (231); it has been reported that Aβ transport from the brain to blood across the BBB requires carrier- or receptor- mediated transport systems (287). Efflux transporters, P-gp, and low-density lipoprotein receptor-related protein-1 (LRP-1) regulate the traffic across BBB and play a key role in brain Aβ homeostasis (288).

In AD, neuroinflammation also plays a pivotal contribution to disease progression. Several pieces of evidence have demonstrated that activation of astrocytes can secrete a high level of pro-inflammatory cytokines, such as IL-1β, TNF-α, and IL-6 (115). Studies suggest that blocking the signaling pathway of IL-1β significantly reduced the development of AD progression, as well as cognitive dysfunction. IL-1β exerts its function upon maturation from caspase-1, which itself is activated by cytosolic mutliprotein complexes named NLR family pyrin domain containing 3 inflammasome (NLRP3). NLRP3 acts as an upstream protein that activates IL-1β, IL-18, and regulates caspase-1 molecule, the importance of NLRP3 has been studied and documented in human disease, but the exact mechanism of NLRP3 activation remains unclear. NLRP3 activation has been observed by the continuous presence of a stimulus, such as Aβ in AD brains, which promotes the formation of the inflammasome complex results in the production of the pro-inflammatory cytokines IL-1β, IL-6 through caspase -1 (289-291).

Two steps are required for NLRP3 activation, the first step called the priming signal that activates the NLRP3 and releases the pro-inflammatory cytokines through activation of NF-κB signaling pathway, the second signal through various stimuli including; PAMPs and DAMPs, which directly activate NLRP3 inflammasomes (292, 293). NF-κB has been involved in AD progression (294). Bauernfeind and colleagues suggested that activation of NLRP3

inflammasomes is mediated by NF-κB signaling (295), where the activation of NF-κB and NLRP3 inflammasome contributes to inflammation and tissue damage in AD. Previous studies have shown that inhibition of inflammatory pathways could rescue AD neuropathology in mice models (296, 297). Thus, targeting NF-κB and NLRP3 signaling pathways could serve as a novel therapeutic approach to slow, prevent, or treat AD.

Recent epidemiological studies have reported that long-term adherence to the MD could protect from neurodegeneration (298, 299). Adherence to MD is one of the top five modifiable factors against cognitive decline (300). MD demonstrated its beneficial effects in preventing age-related defects, including AD, and cardiovascular diseases (301). In 2011, a 4 years study in New York (2258 participant) showed that increased adherence to MD reduced the risk of conversion of mild cognitive impairment (MCI) to AD where participant who adheres to MD had a 40-50% lower risk of progression to AD compared to non-adherent (302). Another study conducted by the Bordeaux center for people above 65 years of age (1410 participant) investigated the effect of adherence to MD on changes to cognitive performance; results showed MD resulted in a reduction in cognitive impairment as measured by the cognitive test Mini-Mental State Examination (303). This neuroprotective effect was associated with several types of food from MD, including high intake of whole cereals, fruits, vegetables, and fish, and extra-virgin olive oil (EVOO) as the main source of fats, which exerts an anti-inflammatory and anti-oxidant effect in addition to other health benefits (304-307).

Secoiridoids found in EVOO, such as oleocanthal (OC), oleuropein aglycone (OLEA), and hydroxythyrosol (HT) have been suggested to be responsible for the positive effect of the EVOO (308-310). Studies from our lab showed that EVOO added to the diet of AD mouse models 5xFAD and TgSwDI significantly reduced Aβ-related pathology, enhanced Aβ

clearance and reduced its production, reduced Aβ deposits in cerebral vessels and restored the BBB function (311-313).

Glycosylated oleuropein (OLEG) is the major polyphenol in the olive leaves and olive fruits, while EVOO contains oleuropein aglycone (OLEA) and its derivatives, demethyloleuropein and ligstroside (314). OLEA interferes with Aβ, tau, and amylin (308, 315-319). In particular, Rigacci and his colleagues showed that OLEA did not induce the release of Aβ oligomers, and was effective when added at the beginning of Aβ aggregations, suggesting that OLEA as an anti-aggregate molecule (308). In TgCRND8, a mouse model of AD, diet supplementation with (8 mg/kg B.W. daily dose OLEA) for 8 weeks results in a significant reduction in Aβ load, reactive astrocytes, cognitive impairment, and autophagy induction (320). Another study found that OLEA mixed with olive oil in TgCRND8 for 2 months reduced Aβ plaques in mice hippocampi and cortexes and showed a neuroprotection effect in a dose-dependent manner (320, 321).

The beneficial effects of olive oil biophenols and OLEA on AD disease models, mainly at the early and middle stages of the disease, have been studied (320, 321). In addition, studies from our lab showed OC and EVOO significantly reduced Aβ-related pathology in early and late stages of AD in mice models (313, 322, 323). However, the effect of OLE and the mechanism(s) by which it exerts its beneficial effects against Aβ pathology remain unclear. The aim of this study was to evaluate the beneficial effect of 3-months consumption of OLE on memory function and Aβ-related pathology in 5XFAD mice, and to identify potential mechanism(s) for the observed effects.

5XFAD mouse model rapidly develops severe Aβ-related pathology. These mice accumulate high levels of Aβ, beginning around 1.5 months of age (324). Astrogliosis and microgliosis

begin at 2 months of age, developing in parallel with Aβ plaque deposition (324). As the purpose of this work is to evaluate OLE as a treatment of AD, 5XFAD mice were treated with OLE at the age of 3 months i.e. after developing AD associated pathological hallmarks including Aβ deposition and gliosis in order to study OLE effect on brain Aβ load and inflammation. This is unlike prevention studies where treatment should start before the development of the pathological hallmarks. OLE treatment continued for 3 month until they reached the age of 6 months where at this age 5XFAD are characterized with memory impairment, and this is important in order to be able to evaluate OLE effect on modulating cognitive function.

OLE dose selection was based on the dietary intake of olive oil in Greek population (50 ml/day)(325), which corresponds to 20µL/day/30g mouse body weight considering a 75 kg human body weight. Based on the olive oil we received, which contains about 550 mg/L (550 µg/ml) of OLEG, this means that each mouse approximately received 11 µg/mouse OLEG corresponding to 366 µg/kg body weight.

Brain inflammation markers selected for analysis included astrogliosis, gliosis, and proinflammatory cytokines including IL-1β and IL-6, which are characteristics of and produced in the brains of 5XFAD mice. It has been reported that cytokines levels increase as the pathology advance in 5XFAD mice as confirmed by Angel and colleagues who showed at 6 months of age, 5XFAD mice demonstrated a significant memory impairment correlated with upregulation in pro-inflammatory cytokines such as IL-1β and IL-6 (326). Changes in the cytokines IL-1β and IL-6, as well as HGMB1 which is a cytokine mediator of inflammation (327), are linked to the activation of NLRP3 inflammasomes and NF-κB (157). Thus, in our study besides these pro-inflammatory cytokines, the expression levels of NLRP3

inflammasomes and NF-κB pathways were investigated as a potential mechanism of the anti-inflammatory effect of OLE in 5XFAD. Besides, RAGE, an inflammatory receptor, is highly expressed in activated astrocytes, which induces neuroinflammation by releasing a high level of inflammatory cytokines (328). RAGE recognizes multiligand implicated in diverse chronic inflammatory states (329). RAGE binds and mediates the cellular response to a range of damage-associated molecular pattern molecules (DAMPs) including HMGB1 (329). Several studies reported that RAGE/NF-κB signaling pathway is involved in AD surrounding the Aβ plaques (146, 330). Thus, changes in RAGE levels was also investigated in our study.

2.1. Hypothesis and Aims

Aβ is considered one of the key pathological hallmarks of AD; its accumulation as deposits has been suggested to induce neuroinflammation and progressive memory impairment (275-277). Evidence (or several pieces of evidence) suggested that OLE polyphenols have a neuroprotective effect. However, the mechanism of this protective effect is not fully evaluated. Thus, we hypothesized that OLE reduces neuroinflammation by reducing the activation of NLRP3 inflammasomes in an AD mouse model via NF-κB signaling pathway. To test this hypothesis, the following aims were investigated:

Aim 1: Effects of OLE on memory function in 5xFAD mice.

Aim 2: Effects of OLE on Aβ-related pathology and neuroinflammation.

Aim 3: Mechanism by which OLE reduces neuroinflammation in 5xFAD mice.

3. Methodology

3.1. Material and chemicals

The material sources and reagents used in this study are listed in (Table 3.1) below.

Table 3. 1: Materials and chemicals used

Materials/Chemicals	Company	Country
Oleuropein glycosylated (OLEG)	Selleckchem	USA
Oleuropein aglycone (OLEA)	Gift from Dr. Khalid El-Sayed (University of Louisiana at Monroe)	LA, USA
Refined olive oil, and refined olive oil enriched with olive leaf extract (OLE)	Boundary Bend Olive	Australia
NP-40 lysis buffer	Alfa Aesar	MA, USA
RIPA buffer	Thermo-fisher Scientific	IL, USA
Bovine Serum Albumin (BSA)	Millipore Sigma	OH, USA
Non-fat dry milk	SCBT	TX, USA
PBS liquid (pH=7.4)	Corning	VA, USA
Protease arrest	G-Biosciences	MO, USA
EDTA (ACS grade)	Alfa Aesar	MA, USA
Donkey serum	Sigma Aldrich	Mo, USA
10x Tris-Glycine-SDS	Bio-Rad	USA
10x Tris-Glycine	Bio-Rad	USA
Resolving gel buffer	Bio-Rad	USA
Stacking gel buffer	Bio-Rad	USA
30% Acrylamide	Bio-Rad	USA
Tetramethylethylenediamine (TEMED)	Bio-Rad	USA
Ammonium persulfate (APS)	Bio-Rad	Japan
4x Laemmli sample buffer	Alfa Aesar	MA, USA
Pierce™ ECL WB substrate	Thermo-fisher Scientific	IL, USA
FemtoLUCENT™ PLUS-HRP	G-Biosciences	MO, USA

Polyvinylidene fluoride (PVDF)	Millipore Sigma	Ireland
Thioflavin S	Sigma Aldrich	MO, USA
Primers	Invitrogen	USA
Master mix	Promega	CA, USA
Tissue kit O.C.T	Sakura	CA, USA
Anti-fade mounting with DAPI	Vector Laboratories	CA, USA
Ketathesia (Ketamine HCL)	HENRY SCHEIN	Ohio, USA
Anased injection (Xylazine)	AKORN	IL, USA
MWM Tub	PanLab-Harvard Apparatus	MA, USA
DNA ladder	Promega	USA
Protein ladder	Abcam	MA, USA
Methanol (ACS grade)	Millipore Sigma	MA, USA
Acetonitrile (LC-MS grade)	Millipore Sigma	MA, USA
Ethyl Alcohol (ACS grade)	VWR	PA, USA
Tris-Boric acid-EDTA (TBE)	Growcells	CA, USA
Agarose	VWR	PA, USA
SyberSafe	EDVO-TEK	USA
Nuclease free water	Promega	USA
DNA extraction reagent	Quanta	USA
DNA stabilization buffer	Quanta	USA

3.2. Preparation of food with olive oil spiked with olive leaf extract

Refined olive oil spiked with olive leaf extract (OLE) enriched with oleuropein (550 ppm = 0.55 mg/ml), was delivered in multiple bottles from the same batch, each bottle contains 50 ml, closed and sealed. The 50 ml bottle aliquoted into 4 ml vials and stored at room temperature. For mice treatment, the food mixture was prepared by the geometric dilution method. One milliliter of OLE was added to 30 g of food and mixed for 5 min, followed by adding another 30 g food to the mixture with mixing for another 5 min. This procedure continued by adding 30 g food to the mixture with mixing to prepare the final amount of 250 g food containing OLE. This preparation will yield a daily dose of 366 µg/kg b.w. for 5g food. The mice dose was calculated bases on dietary intake of olive oil in the Greek population (50g/day) (325), in addition to previous studies that showed the effect of different doses of OLEA namely 8, 2 and 0.08 mg/kg b.w. on Aβ-related pathology (320, 321). In these studies, OLEA administered at 8 and 2 mg/kg b.w showed a significant reduction in Aβ level in TgCRND8 mice, a mouse model of AD, while at 0.08 mg/kg b.w. OLEA did not show effect. Thus, in our study, we chose to evaluate at a dose that is lower than 2 mg/kg and higher than 0.08 mg/kg b.w. Prepared food was changed daily. The major bioactive compound in OLE is OLEG representing about 50% of phenolic content, as described in Table 3.2.

Table 3. 2: The bioactive compounds in OLE

Biophenols (ppm)	Refined Oil	OLE
Hydroxytyrosol		93.66
Tyrosol		0
Vanillic acid & Caffeic acid		0
Vanillin		13.82
Para-coumaric acid		0
Hydroxytyrosyl acetate		0
Ferulic acid		81.66
Ortho-coumaric acid		0
Decarboxymethyl oleuropein aglycone, oxidised dialdehyde form		159.63
Oleacein		105.08
Oleuropein glycoslated (OLEG)		549.56
Oleuropein aglycone, dialdehyde form		0
Tyrosol acetate		0
Decarboxymethyl ligstroside aglycone, oxidised dialdehyde form		0
Oleocanthal		5.02
Pinoresinol, 1 acetoxy-pinoresinol		0
Cinnamic acid		0
Ligstroside aglycone, dialdehyde form		0
Oleuropein aglycone, oxidised aldehyde and hydroxylic form		14.91
Luteolin		18.51
Oleuropein aglycone, aldehyde and hydroxylic form		0
Ligstroside aglycone, oxidised aldehyde and hyroxylic form		0
Apigenin		0
Methyl-luteolin		0
Ligstoside aglycone, aldehyde and hydroxylic form		0
Total biophenol content mg/kg	**< 10**	**1041.848**

3.3. Mice

All animal treatment and surgical procedures were conducted in this study are approved according to the Institutional Animal Care and Use Committee (IACUC protocol 2018-3296) of Auburn University, and according to the public health services (PHS) guidelines. Transgenic 5xFAD mice were purchased from Jackson Laboratory (Ban Harbor, ME) and were maintained on C57Bl/6 background. Mice delivered to the biological research facility (BRF) for animal care at Auburn University. Mice were cross-breed, and pups were isolated for genotyping analysis.

3.4. Mice genotyping

At three weeks of age (21 days), pups were weaned and divided into different cages and tattooed for genomic DNA analysis. Genomic DNA was isolated from the tail biopsies according to the approved IACUC protocol. For each mouse, 0.2-0.3 cm of mouse tail was cut into small pieces, then 75µl of extraction reagent was added to ensure that the tail pieces are submerged within the extraction reagent. The samples were heated at 95^{o}C for 30 min. After heating, samples were settled down and cooled to room temperature. An equal volume, 75µl, of stabilization buffer was then added. For DNA quantification, 2 µl of the sample was measured by Nano-Drop spectrophotometer 2000C (Thermo-Scientific). Samples from 5xFAD mice that carry the transgene needed for this study were identified by Real-Time Polymerase-Chain-Reaction (qPCR) as follows: A reaction mixture including the DNA for PCR was setup according to (Table 3.3), and the sequences of the primers are listed in (Table 3.4). The PCR cycling protocol is listed in (Table 3.5). After this, samples from 5xFAD mice were subjected into agarose electrophoresis to determine transgenes as follow: 10x TBE was diluted to 1x TBE, then 3g of agarose was added to 100 ml of 1x TBE (89 mM Tris, 89 mM boric acid, 2 mM EDTA) and heated in a microwave for 1 min until the agarose dissolved completely, then cooled down to

reach 65ºC, followed by addition of 10 µl of SyberSafe to the 100 ml mixture. The gel was cast in a casting tray with a comb to form wells and solidified. After this, 15 µl from the PCR mixture were loaded into the wells. The agarose gel was run in a horizontal electrophoresis chamber (Bio-Rad). For size detection, two wells were filled with 10 µl of 100 bp DNA ladder and ran in TBE buffer for approximately 30 min at 110 V constant current. The agarose gel was visualized using the Chemi-Doc (Bio-Rad). Transgenic mice were identified according to the Jackson laboratory manual; only homozygous and WT mice were selected for this study.

Table 3. 3: PCR reaction mixture for DNA analysis

Reagent	Volume (µl)
The PCR mixture volume is 50 µl	
Gotaq green	25
Primer 23767	1.25
Primer 37589	1.25
Primer 37599	1.25
DNA	2
Nuclease free water	19.25

Table 3. 4: List of PCR primers

Primer	Sequence	Primer type
Primer 23767	CGG GCC TCT TCG CTA TTA C	Mutant Reverse
Primer 37598	ACC CCC ATG TCA GAG TTC CT	Common
Primer 37599	TAT ACA ACC TTG GGG GAT GG	Wild Type Reverse

Table 3. 5: PCR cycling protocol

Steps	Temperature (ºC)	Duration (s)
1	94	120
2	94	20
3	65	15
4	68	10
5	Repeat Step (2-4)-10x	-
6	94	15
7	60	15
8	72	10
9	Repeat Step (6-8)-28x	-
10	72	120
11	4	Hold

3.5. Mice protocol and treatment

Homozygous 5xFAD and WT mice were used in this study. Mice had free access to water and food and maintained on a 12h: 12h light: dark cycle. At the age of three months, mice were divided into three groups as follows. WT control (Refined oil), vehicle-treated (Refined oil), and OLE treated 5xFAD mice group. The powdered food was changed daily to maintain the freshness for 3 months. During the treatment period, mice body weights and health status were measured weekly. Visual observation indicated mice were healthy, and mice body weights were not significantly different ranging from 27.4 ± 2.8g, and 27.1 ± 2.6g for OLE and vehicle-treated mice, respectively. At the end of the treatment period, behavioral studies were conducted to assess learning and cognitive performance, and then mice were sacrificed with ketamine anesthesia and decapitated for brain collections. In the experiments, male mice were used with n=5 for WT mice and n=7 for 5XFAD mice per treatment group.

3.6. Testing the homogeneity of OLE in powdered food

To ensure the homogeneity of mice food mixed with OLE, random samples from the preparation were selected for analysis. For food mixture preparation, we used the geometric dilution method. To a 30 g food, 1 ml of OLE was added and mixed on a clean plate with a spatula for about 5 min. Then, another 30 g of food was added to the mixture and mixed for another 5 min. We continued the addition of 30 g food to the mixture with mixing to prepare a final amount of 250 g food containing OLE. The homogeneity test was performed for 5 different preparations over 5 weeks with three random samples (1 g each) per preparation were taken from different areas as shown in (Fig 3.1). Sampled food was placed in tubes. To each tube, 2 ml of 50% ethanol (ETOH) was added, sonicated for 30 min, followed by centrifugation at 108,860 *x g* for 45 min to allow the precipitation of powdered-food at room temperature by

Beckman Coulter (Avanti JXN-30 centrifuge). The supernatant was removed, filtered. The quantitative analysis of OLEG was performed by HPLC as follows, Shimadzu HPLC equipped with SIL 20-AHT auto-sampler, SPD-20A UV/VIS detector, and LC-20AB pump connected to a DGU-20A3 degasser was used. The separation was carried out by Eclipse XDB- C18 column (Agilent, 4.6 × 150 mm, 5 µm particle size). HPLC analysis was performed with a flow rate 1.0 ml/min. The mobile phase composition was water-acetonitrile (65:35) (v/v). All solvents were filtered through a 0.2 µm Millipore filter before use and degassed in an ultrasonic bath. Volumes of 10 µl of each prepared solution and samples were injected into the column.

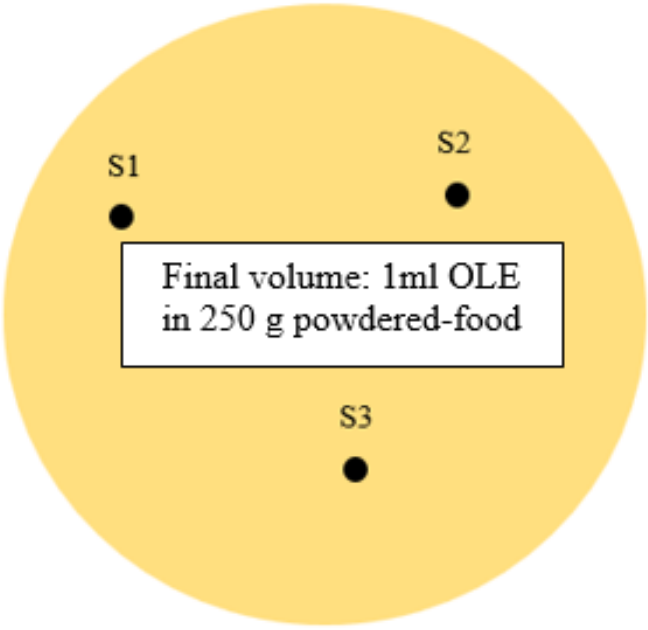

Fig 3. 1: Food homogeneity testing procedure.

3.7. OLEG stability

To assess OLE stability, OLEG was used as a biomarker to monitor OLE stability after extraction from the oil. OLEG represents 50% of the phenolic content in OLE. OLEG extraction was performed by adding 50% ethanol (1:10, respectively; v/v), vortexed for 5 min, followed

by centrifugation at 20,800 *x g* for 15 min at room temperature. The quantitative analysis of OLEG was performed by HPLC as described above, except the mobile phase was water-acetonitrile (75:25; v/v). Samples were filtered through a 0.2 µm Millipore filter before analysis. Volumes of 10 µl of each prepared solution and samples were injected into the column.

3.8. Brain collection

Mice brains were removed gently and divided into two halves. 2-Methyl-butane was used for snap-freezing for long-term storage at -80^{o}C for further biochemical and immunostaining analysis.

3.9. Mice brain homogenization

The weight of collected brains were measured and mixed with double volume (2:1, v/wt) of DPBS (137 mM NaCl, 8.1 mM Na_2HPO_4, 2.7 mM KCl, 0.9 mM $CaCl_2$, 5 mM D-glucose, 0.5 mM $MgCl_2$, 1.46 mM KH_2PO_4, and 1 mM Na-pyruvate) with protease arrest and homogenized using Omni International homogenizer (Omni International; Kennesaw, GA), then samples were aliquoted and stored at -80^{o}C.

3.10. SDS-PAGE immunoblotting

Samples for western blots were prepared from the stored brain homogenates in DPBS mixed with protease arrest in a dilution of 100:1. Then, 80 µl of brain homogenate were lysed with 160 µl of NP-40 on ice for 1h with vortex every 20 min. Samples supernatants were then collected after centrifugation at 20,800 *x g* for 20 min at 4^{o}C. Five microliters of each sample were used to measure the protein concentration using Pierce^{TM} BCA protein assay kit (Thermo-Fisher Scientific).

Thirty micrograms from each sample lysate were used for protein separation; samples were mixed with 4X Laemmli and NP-40 lysis buffer and boiled at 95^{o}C for 5 min for protein denaturation. Samples and pre-stained protein ladder were used for several protein separation. For low molecular weight proteins, 15% of Tris-Glycine-SDS polyacrylamide gels were used in SDS-PAGE gel chamber, and 10% of Tris-Glycine-SDS polyacrylamide gels for high molecular weight proteins as shown in Table 3.6. The Bio-Rad chamber designed to fit 4 gels at the same time, and the electrophoresis buffer consist of (5 mM Tris, 192 mM Glycine, and 0.1% SDS, pH 8.3). Once the samples and protein ladder loaded into the wells, the system ran for 90 min at 200 V.

At the end of separation, gels were removed from the electrophoresis chamber and soaked with a transfer buffer (25 mM Tris, 192 mM Glycine, and 20% (v/v) methanol, and water in a ratio of 1:2:7, respectively) for 10 min. Proteins were then transferred to PVDF membrane for 3h at 300 mA at 4^{o}C. Membranes were blocked with 2% non-fat dry milk in PBS for 1h at room temperature with gentle shaking, followed by the addition of primary antibodies in 2% non-fat dry milk for overnight at 4^{o}C. Used antibodies are listed in Table 3.7. On the next day, membranes were washed three times, each time 10 min with 0.05% Tween-PBS, and incubated with the 2% non-fat dry milk secondary antibodies for 1h at room temperature with shaking. Used secondary antibodies were goat anti-mouse IgG, goat anti-rabbit IgG (Invitrogen), and goat IgG HRP-conjugated (R&D) at a dilution of 1:1000. Membranes were then washed 3 times with 0.05% Tween-PBS. Images were captured by Chemi-Doc imaging system (Bio-Rad). The captured images were analyzed by Image Lab software v 6.0 (Bio-Rad), which measure bands intensity. Before samples analysis, the level of housekeeping proteins from different treatment groups were assessed for fixed amount of protein.

Table 3. 6: The polyacrylamide gel mixture

Reagents	10% Resolving gel	15% Resolving gel	Stacking gel
	Volume per (30 mls)	Volume per (30 mls)	Volume (10mls)
Water	11.9	6.9	6.8
30% Acrylamide	10	15	1.7
1.5 M Tris (pH 8.8)	7.5	7.5	1.2
10% SDS	0.3	0.3	0.1
10% APS	0.3	0.3	0.1
TEMED	0.012	0.012	0.01

Table 3. 7: A list of primary antibodies that been used in western blot analysis

Antibody	Dilution	Company
β-Actin	1:1000	Santa Cruz Biotechnology
Tubulin	1:200	Santa Cruz Biotechnology
GAPDH	1:1000	Invitrogen
PSD-95	1:2000	Invitrogen
SNAP-25	1:1000	Invitrogen
Synapsin-1	1:1000	Cell Signaling
sAPP-α	1:1000	Immuno-Biological Laboratories Co
sAPP-β	1:1000	Immuno-Biological Laboratories Co
Claudin-5	1:500	Invitrogen
Occludin	1:500	Invitrogen
ZO-1	1:500	Invitrogen
V-cadherin	1:200	Santa Cruz Biotechnology
P-gp	1:200	BioLegend
LRP1	1:1000	Abcam
NLRP3	1:1000	Cell Signaling
Pro-Caspase 1	1:200	Santa Cruz Biotechnology
RAGE	1:200	Santa Cruz Biotechnology
HMGb1	1:200	Santa Cruz Biotechnology
IκB-α	1:1000	Cell Signaling
p- IκB-α	1:1000	Cell Signaling
p-IKK	1:1000	Cell Signaling

3.11. Detection and quantification of cytokines by ELISA

ELISA was used to determine IL-1β and IL-6 levels by commercially available kits listed in (Table 3.8). Samples supernatants were prepared as described above under the brain homogenization section, diluted and optimized for each cytokine separately. Dilutions used were 1:10 for IL-1β and IL-6. The level of each cytokine was normalized to total protein measured by Pierce™ BCA protein assay kit (Thermo-Fisher Scientific). Levels of IL-1β, and IL-6 were expressed as pg/mg protein.

Table 3. 8: ELISA cytokines kits

ELISA Kit	Company
Mouse IL-6 Quantikine ELISA Kit	R&D Systems
Mouse IL-1 beta/IL-1F2 Quantikine ELISA Kit	R&D Systems

3.12. Detection and quantification of Aβ by ELISA

Samples supernatants were used to measure levels of $A\beta_{40}$ and $A\beta_{42}$ after dilution 1:10 and 1:40, respectively, in lysis buffer. The level of $A\beta_{40}$ and $A\beta_{42}$ was normalized to the total protein content by Pierce™ BCA protein assay kit (Thermo-Fisher Scientific) and expressed as pg/mg protein. Commercially available ELISA kits were used for the analysis and listed in Table 3.9.

Table 3. 9: ELISA kits for Aβ

ELISA Kit	Company
Human Amyloid beta (aa1-40) Quantikine ELISA Kit	R&D Systems
Human Amyloid beta (aa1-42) Quantikine ELISA Kit	R&D Systems

3.13. Immunohistochemistry (IHC)

3.13.1. Cryo-sectioning of mice brains

Frozen brains (by 2-methyl butane) were stored at -80^{o}C until analysis. One day before sectioning, the brains were embedded in optimal cutting temperature (O.C.T) liquid and kept on dry ice for 15 min, and then kept overnight at -80^{o}C. On the second day, the brain was placed in the Lecia CM3050S Research Cryostat at -20^{o}C and adjusted on the optimal angle to prepare sections by 16 µm thickness; three brain sections were placed on each slide and stored at -80^{o}C for different immunostaining purposes.

3.13.2. Aβ immunostaining

For total Aβ load, brain sections were fixed by 100% methanol for 15 min and washed gently five times with PBS to remove O.C.T remains, then blocked with 10% donkey serum diluted in PBS for 45 min. For the primary antibody, brain sections were immunostained with rabbit collagen IV antibody (Millipore) for 2h to stain the brain microvessels in a dilution of 1:200, then removed and washed five times with PBS followed by addition of the secondary antibody donkey polyclonal Alexa-Flour 675 anti-rabbit antibody in a dilution of 1:200 mixed with human-specific anti-Aβ (6E10) antibody conjugated to Alexa Flour-488 (BioLegend) at 1:1000 dilution in donkey serum for 2h. Sections were then washed five times with PBS, followed by an addition of 25 µl of 4′,6-diamidino-2-phenylindole (DAPI with antifade) to stain nuclear DNA. Lastly, 1.5 µm coverslips were placed on top of slides and were sealed with nail polish for fluorescence microscope images. Images were captured by an inverted fluorescence microscope (Nikon) at different magnification (4x, 10x, and 20x).

For Aβ plaques, brain sections were immunostained with 0.02% filtered thioflavin S (Sigma Aldrich) diluted in 70% ethanol for 30 min. Sections were washed with 70% ethanol alone for

another 15 min, followed by the addition of 25 µl DAPI Antifade. Images were captured inverted fluorescence microscope (Nikon).

3.13.3. Immunostaining of Astrocytes

To probe astrocytes activation, glial fibrillary acidic protein (GFAP) was probed. Brain sections were immunostained with the primary rabbit GFAP antibody (SCBT) at a dilution of 1:200 for 2h. Then, polyclonal Alexa Flour 647 anti-rabbit IgG antibody diluted 1:200 (Abcam) and 25 µl DAPI Antifade. Images were captured, and adjusted to the lowest background signal using the inverted fluorescence microscope (Nikon). For quantification, sections were normalized to the same background for hippocampi and cortexes regions. Images were analyzed by Image J software (NIH) that was set for mean value, minimum value, maximum value, and limit to the threshold, followed by analysis. Results showed the mean value, minimum value, maximum value, and area. The minimum value was similar in all sections; the density was then plotted as fold change in GFAP levels for hippocampi and cortexes.

3.13.4. Immunostaining of Microglia

To probe microglia activation, Iba1 (Abcam) as a primary antibody in a dilution of 1:200 for 2h was examined, followed by secondary donkey polyclonal Alexa Flour 647 anti-rabbit IgG antibody diluted 1:200 (Abcam) for another 2h, and 25 µl DAPI Antifade. Images were captured, and adjusted to the lowest background signal using the inverted fluorescence microscope (Nikon). For quantification, sections were normalized to the same background for hippocampi and cortexes regions. Images were analyzed by Image J software (NIH) that was set for mean value, minimum value, maximum value, and limit to the threshold, followed by analysis. Results showed the mean value, minimum value, maximum value, and area. The

minimum value was similar in all sections; the density was then plotted as fold change in Iba1 levels for hippocampi and cortexes.

3.14. Behavioral Study

The effect of treatment on spatial memory and learning was evaluated b Morris Water Maze (MWM). MWM is a round plastic tub (80x110 mm) filled with water (temperature; 22^{o}C). Maze testing was performed for six consecutive days, the visible day, followed by 4 days with an escape platform submerged 1.0 cm below the water line in a fixed location. Four visible cues in different shapes were placed at the wall around the Maze tub. On the first day, the mice were tested four times (4 trials) to measure the visibility, and the platform was placed on the same quadrant. Each mouse was entered the pool from four different starting positions (0, 45, 90, and 180^{o} from the platform) and allowed to swim until either the mouse finds submerged platform or reached a ceiling of 1 min in non-opaque water. If the mouse could not find the platform in 1.0 min, the mouse was gently guided to the platform and remained for 20 sec before being removed for the second trial. Four trials were completed each day for four days in opaque water, as demonstrated in Table 3.10 using white non-toxic water-based paint. On the probe day, the platform was removed from the maze tub, and mice were placed in the opposite quadrant and allowed them to swim for 1.0 min for one trial.

Table 3. 10: Morris Water Maze Protocol

	Day 1		Day 2	Day 3	Day 4	Day 5	Day 6
	Platform location	Starting point	Platform Location: SE starting location as follow:				No Platform
Trial 1	SW	S	S	S	N	N	N
Trial 2	NW	N	S	W	E	S	
Trial 3	NE	E	N	E	W	E	
Trial 4	SE	W	W	N	N	E	

All videos were recorded for behavioral analysis. The visible day was performed to ensure that no visual or motor deficits were contributed to mice performance. Collected data was used to determine changes in escape latency (sec), time spent in the target quadrant (%), and swimming speed (cm/sec). Smart V 3.0 tracking software (PanLab-Harvard Apparatus; Holliston, MA) was used to measure all MWM parameters.

3.15. Determination of OLEG and OLEA in mice plasma and brains by HPLC analysis

We conducted a feasibility study to obtain preliminary data for OLEG and OLEA penetration to the brain. OLEA is the main product of OLEG hydrolysis. A method was developed, however, it was not thoroughly validated. Plasma and brain levels of OLEG and OLEA in WT type mice were evaluated. Mice were divided into groups according to blood collection time points with n=3 mice. Mice received a single IV injection of OLEG at a dose of 10 mg/kg. Blood samples were collected at 0, 5, 10, 30, 60, and 240 min (n=3 per time point). In addition, brain tissues were collected at the same time points after mice decapitation. Plasma was immediately removed and stored at -80^{o}C until analysis. Mice brains were flash-frozen in 2-methyl butane, placed on dry ice, and stored at -80^{o}C until processing.

Extraction method

Brain tissues were homogenized in phosphate buffer saline in 1:1 ratio (wt/v). OLEG and OLEA were extracted plasma and brain homogenate tissues by precipitation method with acetonitrile in 1:1 ratio (v/v), sonicated and centrifuged at 20,800 *x g* for 10 min. Then, the supernatant was collected and placed in inserts. Calibration curves were prepared by serial dilution from the highest to the lowest dilution. Volumes of 10 µl of each prepared sample was injected onto the column.

Analytical method

Stock solutions of OLEG and OLEA were prepared in water and acetonitrile, respectively. Calibration curves were prepared in blank mouse plasma and brain homogenate. The mobile phase composition of OLEG and OLEA was water-acetonitrile at 75:25 and 64:34 (v/v), respectively, with a flow rate 1.0 ml/min. The separation was carried out by Eclipse XDB- C18 column (Agilent, 4.6 × 150 mm, 5 µm particle size) at wavelength of 200 nm. Volumes of 10

µl of each prepared sample was injected onto the column. The method was not adequately validated, however, the accuracy for each standard in the calibration curve was calculated and expressed as percentage value of the ratio between the measured concentration from the calibration curve and the theoretical concentration; in addition the limit of quantification (LOQ) was determined as the lowest concentration in the calibration curve that could be quantified.

Pharmacokinetics parameters

PK parameters for OLEG were obtained by non-compartmental method. Area under the curve from zero to infinity for concentrations vs time ($AUC_{0\text{-}inf}$) for OLEG in plasma was calculated using the linear trapezoidal rule extrapolated to infinite time; AUC from zero to last time point ($AUC_{0\text{-}t}$) for OLEA in plasma was calculated, while in the brain the ($AUC_{0\text{-}t}$) was calculated after correcting the obtained concentrations for cerebral blood volume in the brain which represent 4% of the total brain homogenate. Non-compartmental model assumes that elimination follows first order, thus terminal elimination rate constant (k_{el}) was calculated from the last three points as the negative slope of the non-weighted least squares curve fit to logarithmically transformed concentration vs time, from k_{el}, elimination half-life ($t_{1/2}$) was calculated from the equation $0.693/k_{el}$. Total clearance (CL) was determined by the equation dose/ $AUC_{0\text{-}inf}$, and volume of distribution (V_D) was determined from dose/Cp^o, Cp^o is extrapolated concentration at time zero.

3.16. Statistical Analysis

All values were expressed as mean ± SEM. Statistical analysis was done by GraphPad Prism V 5.0 software. The statistical significance for all results was assessed by student's t-test or one-way ANOVA, and two-way ANOVA. A *p*-value of < 0.05 was considered statistically significant.

4. Results

4.1. Testing OLE homogeneity in the powdered food preparation for 5xFAD mice

The importance of testing OLEG, as a representative compound in OLE, in powdered-food mixed with olive oil spiked in OLE is to confirm mixing homogeneity and similar distribution of the oil in the food. OLEG concentration in powdered-food was evaluated and analyzed by HPLC over 5 weeks. Fig 4.1.A shows the percentage of 3 different samples randomly selected from each preparation. Results showed that the prepared mixture was homogenous within the same preparation, where the percentage of OLEG concentration did not change in the same week. In addition to that, we tested the percentage of OLEG concentration between all preparations over the 5 weeks as shown in Fig 4.1.B; there were no difference in the concentration of OLEG over the 5 weeks preparation (94.8% ± 3.3; 91% ± 2; 98.8% ± 0.6; 95.4% ± 6.1; and 92.9% ± 4.7).

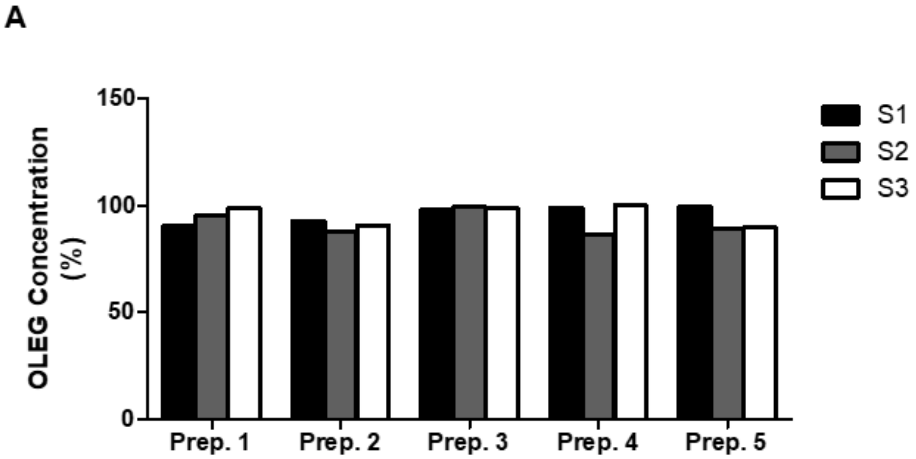

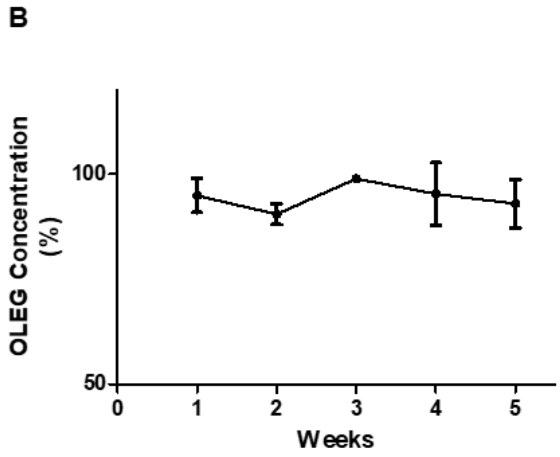

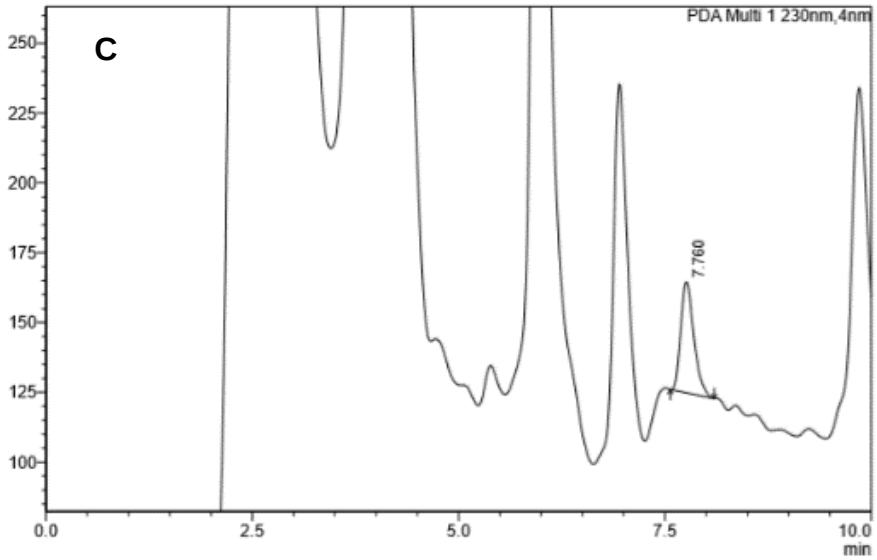

Fig 4. 1: OLE preparation was homogenous during the mice treatment period. **(A)** Randomly selected samples within and from different preparations over 5 weeks. Results showed no statistically significant difference in the OLEG concentration in all preparations. **(B)** OLE quantification from all samples over 5 weeks. **(C)** A representative chromatogram of food spiked with OLE showing OLEG at retention time 7.76 min.

4.2. Testing OLE stability

The stability of OLE was monitored by evaluating OLEG stability within one year of receiving the samples. The initial concentration of OLEG was determined as 550 ppm (0.55 mg/ml). One year later, OLEG concentration was evaluated at 0.502 mg/ml ± 0.01, suggesting OLEG, and thus OLE is stable.

Initial Conc.	Conc. (1 year)
0.55 mg/ml	0.502 mg/ml ± 0.01

4.3. Genotyping of mice for the study

To determine the mutant allele in 5xFAD mice strain, genotyping analysis by PCR was performed. The colony started with 5xFAD$^{+/-}$ parents. For study purposes, only mutant 5xFAD mice (MW; 129bp) that show the aggressive Aβ level at an early stage were used in the experiments. In addition to WT mice from the same background (MW; 216) were selected, as shown in Fig 4.2 below.

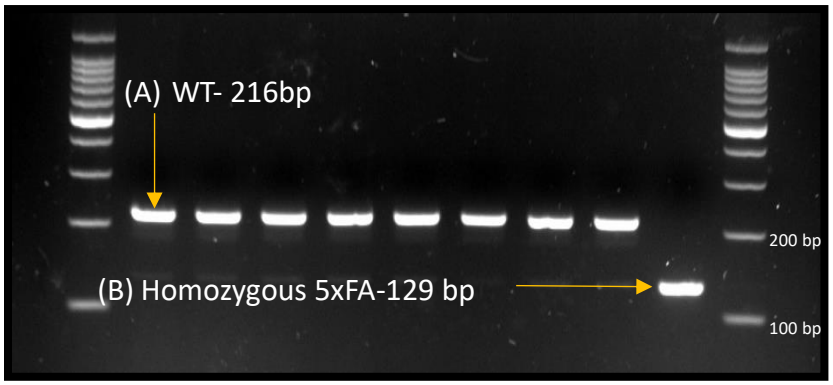

Fig 4. 2: Genotyping analysis using PCR for 5xFAD mice. **(A)** WT mice- 216 bp. **(B)** Homozygous 5xFAD mice- 129 bp.

4.4. Treatment with OLE enhanced the spatial learning and memory function in 5xFAD mice

To investigate the effect of OLE treatment on learning and memory function, MWM test was performed in mice divided into three groups: WT (refined oil, n=5 male mice), Vehicle (refined oil, n=7 male mice) and OLE (n=7 male mice). Learning abilities and memory were assessed at the end of treatments. Parameters analyzed include the time a mouse takes to find the hidden platform area (Escape Latency, sec), time spent in the target quadrant (%), and swimming speed (cm/sec). On training days, 5xFAD mice treated with OLE showed significant improvement and found the platform faster compared to the vehicle-treated group, as shown in Fig 4.3.A. This effect was also analyzed and compared to WT. WT mice showed a better performance compare to Veh treated mice. In addition, OLE treatment improved the cognitive function nearly as WT mice (Fig 4.3.A).

On the probe day, the time spent in the platform quadrant were analyzed, and results showed a significant improvement where mice treated with OLE spent a longer time in the target quadrant when compared to vehicle-treated group, as shown in Fig 4.3.B (p <0.05). Compared to WT mice, the time spent in the target quadrant of OLE treated mice was comparable to WT. These results demonstrated that OLE treatment improved memory function in 5xFAD mice. On the other hand, swimming speed didn't change (ns) between all groups, as shown in Fig 4.3.C, which excludes the motor changes as a cause of the observed improvement.

A

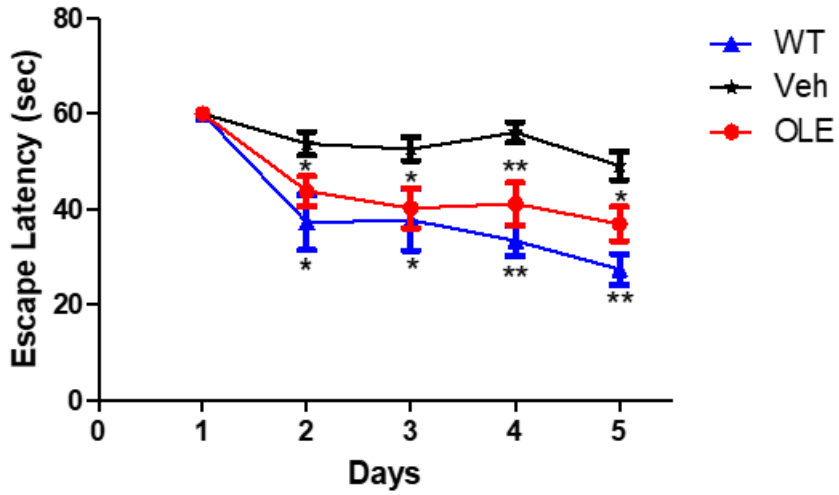
Escape Latency (sec)
80
60
40
20
0
0
1
2
3
4
5
Days
WT
Veh
OLE
*
*
*
*
**
**
*
**

B

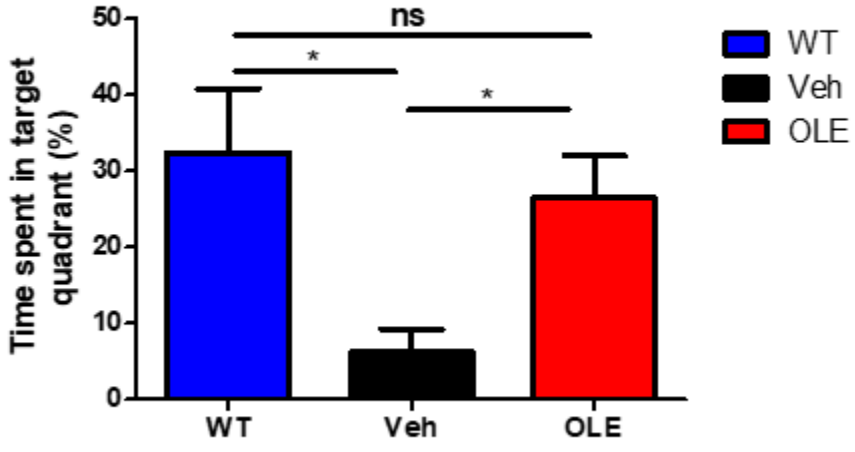
Time spent in target quadrant (%)
50
40
30
20
10
0
ns
*
*
WT
Veh
OLE
WT
Veh
OLE

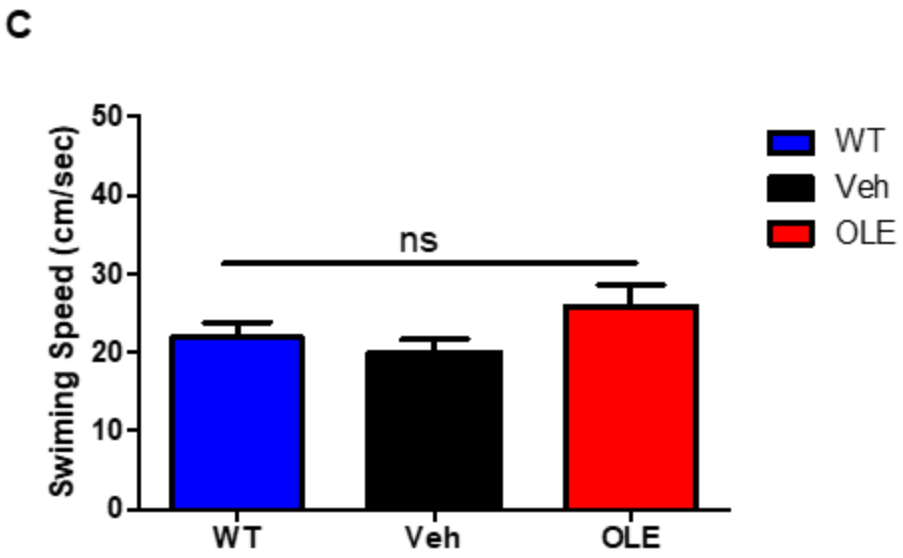

Fig 4. 3: OLE improves memory function in homozygous 5xFAD mice after 3 months treatment period. **(A)** Escape latency to search for the hidden (submerged) platform in 5xFAD mice was significantly reduced nearly as WT compared to vehicle-treated mice (Veh). **(B-C)** Probe trial for time spent in the target quadrant and swimming speed were analyzed. OLE treatment increased the time spent in the target quadrant **(B)** without changing the swimming speed **(C)** between all mice groups WT, Veh, and OLE (n=5-7). Data presented as means ± SEM. * $p < 0.05$, ** $p < 0.01$.

4.5. Treatment with OLE increased the tight junction proteins in 5xFAD mice brains

To investigate the effect of OLE on the expression of tight junction (TJs) including claudin-5, occludin, and ZO-1, in addition to adherence junction protein VE-cadherin were evaluated by western blot. The tight junction proteins were evaluated in mice treated with OLE, vehicle-treated (refined oil) in 5xFAD mice, and were compared to WT. OLE treatment significantly induced the expression of VE-cadherin, claudin-5, occludin, and ZO-1 compared to vehicle-treated group (p<0.05). Compared to WT, protein expressions of claudin-5, occludin, and ZO-1 were significantly lower in vehicle-treated mice that were enhanced by OLE treatment almost to WT levels. These results suggest OLE enhanced the brain tightness, as demonstrated by TJs upregulation, as shown in Fig 4.4.

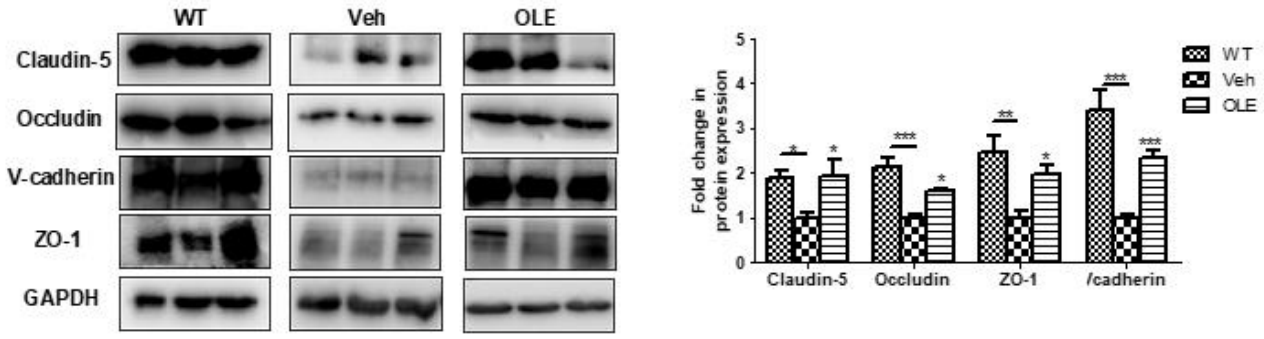

Fig 4. 4: OLE treatment significantly increased the tight junction proteins expression in 5xFAD mice brain homogenate. Representative western blot and densitometry analysis of claudin-5, occludin, ZO-1, and V-cadherin. Results showed significant upregulation in TJ proteins in OLE –treated mice); this effect was restored to basal protein levels observed in WT mice. Mice were treated with OLE 366 µg/kg daily for 3 months. Data represented as mean ± SEM for n=6 mice. * p < 0.05, ** p < 0.01, *** p < 0.001.

4.6. The effect of OLE treatment on Aβ major transporter proteins in 5xFAD mice brains

To evaluate and confirm the effect of OLE on Aβ major efflux transporter proteins, namely P-gp and LRP1, western blot in brain homogenate of 5xFAD mice was performed. As shown in Fig 4.5., OLE treatment induced the expression of LRP1, but did not reach a significant level, while the effect on P-gp was significantly increased in OLE-treated mice by 81 % ($p < 0.05$) compared to vehicle-treated mice Compared to WT, the expression of P-gp and LRP1 was significantly lower in vehicle-treated mice and were enhanced by OLE treatment.

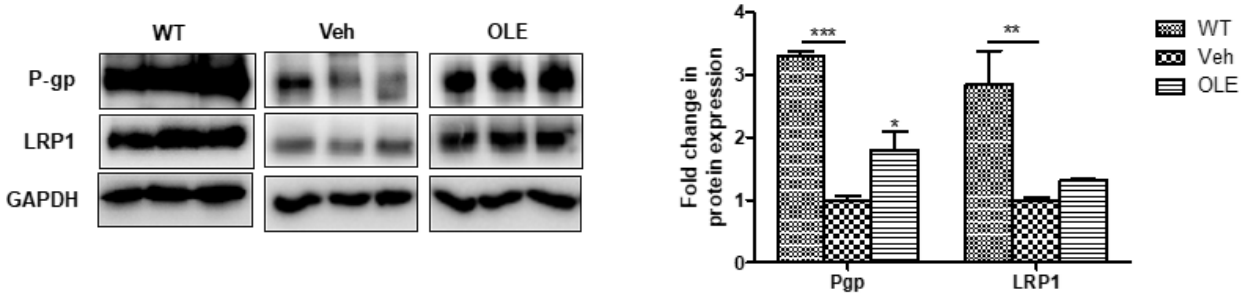

Fig 4. 5: The effect of OLE on Aβ major efflux transporter proteins (P-gp and LRP1). Representative western blot and densitometry analysis of P-gp and LRP. Results showed that OLE treatment significantly increased the expression of P-gp and LRP1 (n=6) compared to vehicle-treated 5xFAD mice; this effect was slightly restored to basal protein levels observed in WT mice. Mice were treated with OLE 366 µg/kg daily for 3 months. All proteins were measured from the brain homogenate and normalized to GAPDH. Data represented as mean ± SEM. * $p < 0.05$, ** $p < 0.01$, *** $p < 0.001$.

4.7. Effect of OLE treatment on Aβ Production in 5xFAD mice brains

The effect of OLE on Aβ production was evaluated by western blot to measure the expression of sAPPα, sAPPβ, and ADAM-10. APP processing undergoes several enzymatic cleavages by α, β, and γ secretases; the neuroprotective effect through APP processing is mediated by α-secretase (ADAM-10) to produce sAPPα, while sAPPβ is produced by β-secretase followed by another cleavage to form Aβ peptides. The processing of APP was evaluated in 5XFAD mice treated with OLE and was compared to vehicle-treated mice (refined oil) Finding from this study showed that OLE treatment significantly induced the expression of both ADAM10 and sAPPα by 50 and 99 % ($p < 0.001$) and reduced the expression of sAPPβ by 25 % ($p < 0.05$) compared to vehicle-treated mice as shown in Fig 4.6.

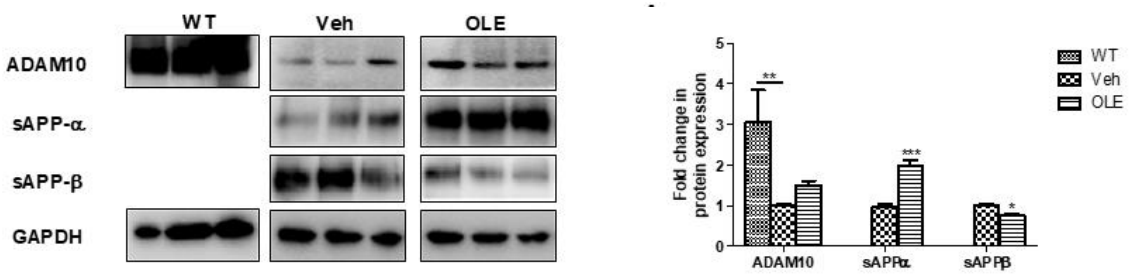

Fig 4. 6: The effect of OLE treatment on the Aβ production through APP processing in 5xFAD brain homogenate. **(A)** Representative western blot and densitometry analysis of ADAM-10, sAPP-α and sAPP-β in 5XFAD mice brains demonstrated that level of ADAM-10 was increased in 5xFAD males (n=6) with a significant upregulation in sAPP-α expression and a significant reduction in the expression of sAPP-β. sAPP-α and sAPP-β were not detected in the WT mice brains as their antibodies are human-specific. Mice were treated with OLE 366 µg/kg daily for 3 months. All proteins were measured from the brain homogenate and normalized to GAPDH. Data represented as mean ± SEM. * $p < 0.05$, ** $p < 0.01$ and *** $p < 0.001$.

4.8. Treatment with OLE decreased Aβ burden in 5xFAD mice brains

The effect of OLE on total Aβ level was evaluated by ELISA and immunohistochemical (IHC) analysis. Soluble Aβ levels in brain homogenates were determined and analyzed by ELISA using commercially available kits for $A\beta_{40}$ and $A\beta_{42}$. Results showed that compared to vehicle-treated 5xFAD mice, OLE consumption significantly decreased the levels of soluble $A\beta_{40}$ ($p < 0.05$)), while $A\beta_{42}$ decreased in OLE-treated mice, but didn't reach the significant level compared to vehicle group as shown in Fig 4.7.A.

For IHC, total Aβ and Aβ plaques have been evaluated in males. Our results showed that mice treated with OLE had a significantly reduced total Aβ deposits in brain sections detected by 6E10 antibody in the hippocampus and cortex regions compared to vehicle-treated mice, as shown in Fig 4.7.B. In addition to that, Aβ plaques in the 5xFAD mice brains were detected by Thioflavin S and showed a significant decrease in the hippocampi and cortexes of mice brains treated with OLE when compared to the vehicle group (Fig 4.7.C).

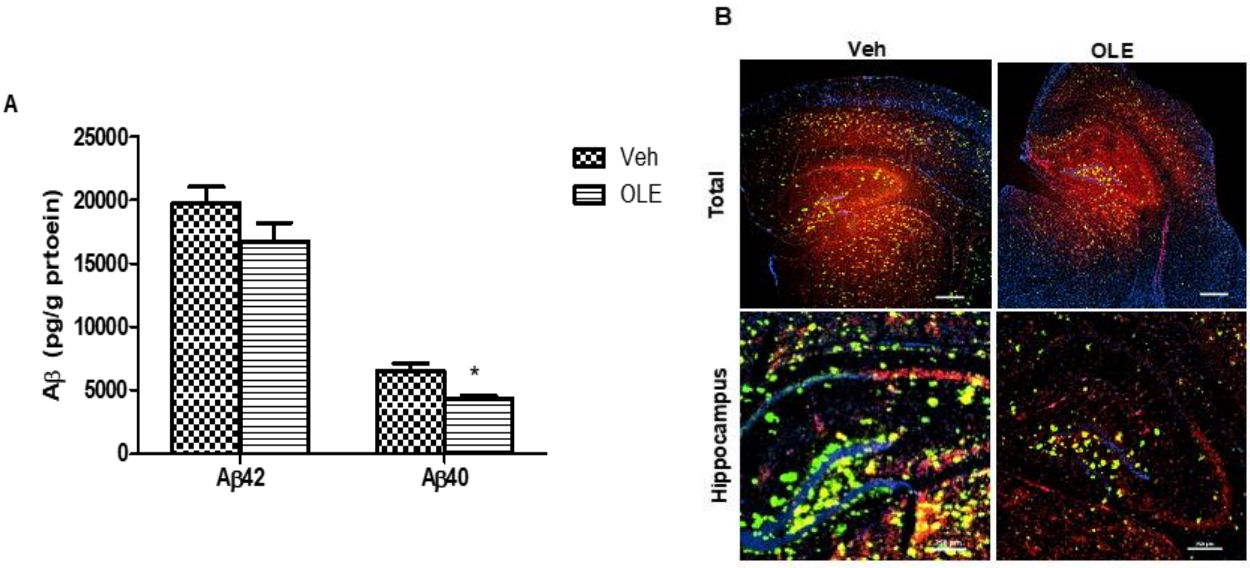

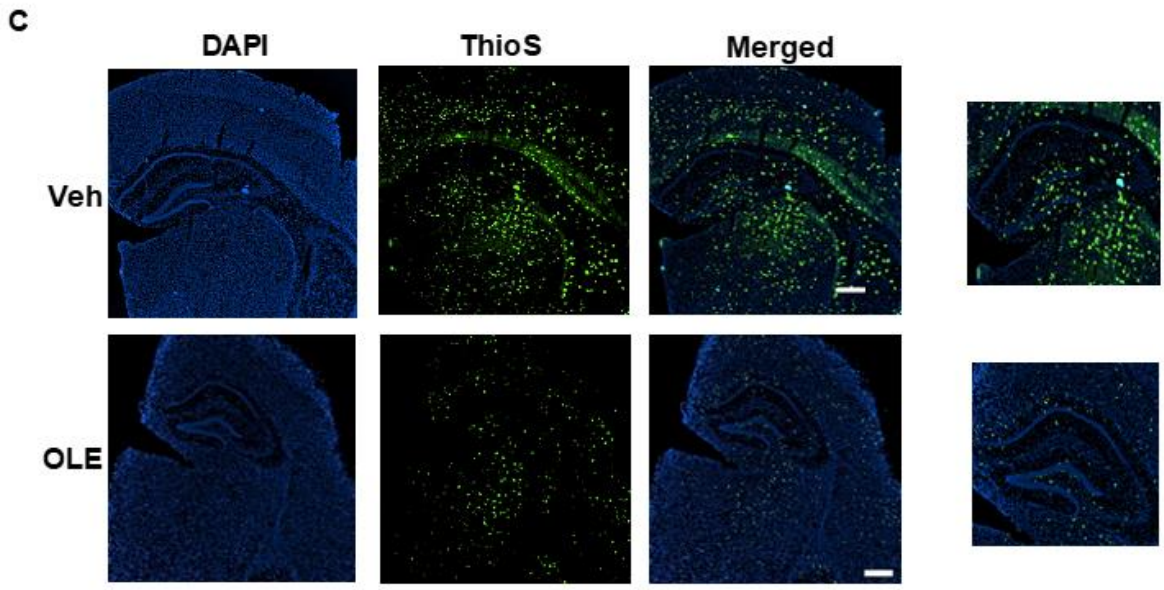

Fig 4. 7: Effect of OLE treatment (366 µg/kg) for 3 months on Aβ burden in 5xFAD mice. **(A)** ELISA for $A\beta_{40}$ and $A\beta_{42}$ (n=4 males). Results showed OLE treatment significantly reduced the $A\beta_{40}$ in male mice brain homogenate, while the $A\beta_{42}$ was reduced in males, but the effect was not significant (ns). **(B)** Representative brain sections of 5xFAD mice treated with refined oil as the vehicle or OLE stained with 6E10 antibody to detect total Aβ load (green), anti-collagen IV antibody to detect microvessels (red) and DAPI (blue), Scale bar= 250µm. **(C)** Representative brain sections of 5xFAD mice treated with refined oil as the vehicle or OLE stained with Thioflavin S to quantify total Aβ plaques (green) and DAPI (blue), Scale bar= 500µm. Data represented as mean ± SEM, * $p < 0.05$.

4.9. Treatment with OLE decreased astrogliosis in 5xFAD mice brains

The effect of OLE on astrogliosis was evaluated by monitoring the levels of glial fibrillary acidic protein (GFAP), as a marker for activation of astrocytes following injury or stress in the CNS. GFAP level was determined by IHC analysis. Activated astrocytes become more intense and branchy in the brains of AD patients. Our findings showed that astrocytes activation as detected by GFAP in mice hippocampi and cortexes (measured by density for each specific region) significantly decreased with OLE treatment (Fig 4.8.A & B) in 5xFAD mice compared to vehicle-treated mice.

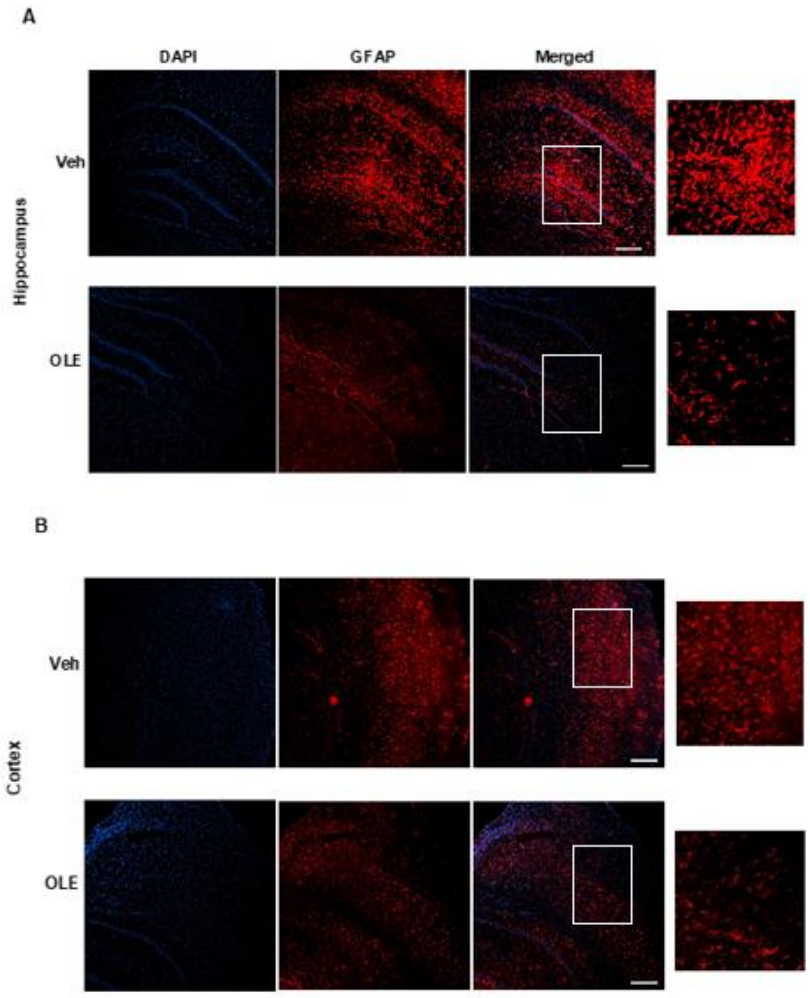

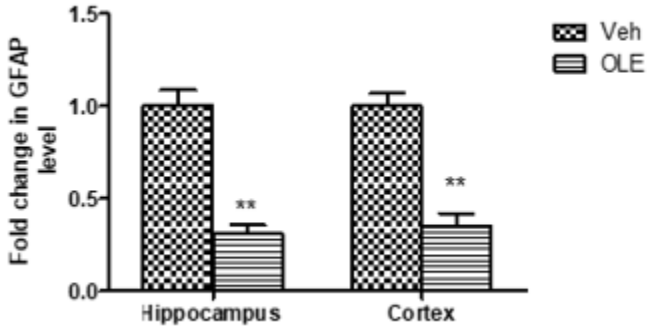

Fig 4. 8: Effect of OLE treatment on astrogliosis. Mice treated with OLE at 366 µg/kg for 3 months. **(A-B)** Representative brain sections with semi-quantitative analysis of 5xFAD mice treated with refined oil as the vehicle or OLE stained with GFAP antibody to detect activated astrocytes (Red). Counterstained with DAPI (blue), Scale bar= 250µm. Results showed the density of activated astrocytes were significantly reduced with OLE treatment compared to vehicle-treated mice in the hippocampi and cortexes of males 5xFAD mice. Small boxes are magnified on the right side for clarification. Data is presented as mean± SEM. Males (n=3) ** $p < 0.01$.

4.10. Treatment with OLE decreased microglial activation in 5xFAD mice brains

The effect of OLE on the activation of microglia was evaluated by monitoring the ionized calcium-binding adaptor molecule-1 (Iba-1). Iba-1 level was determined by IHC analysis. Microglia becomes more intense upon activation. Our findings showed that microglial cells activation as detected by Iba-1 in mice hippocampi and cortexes (measured by density for each specific region) decreased with OLE treatment (Fig 4.9.A & B) in 5xFAD mice compared to vehicle-treated mice.

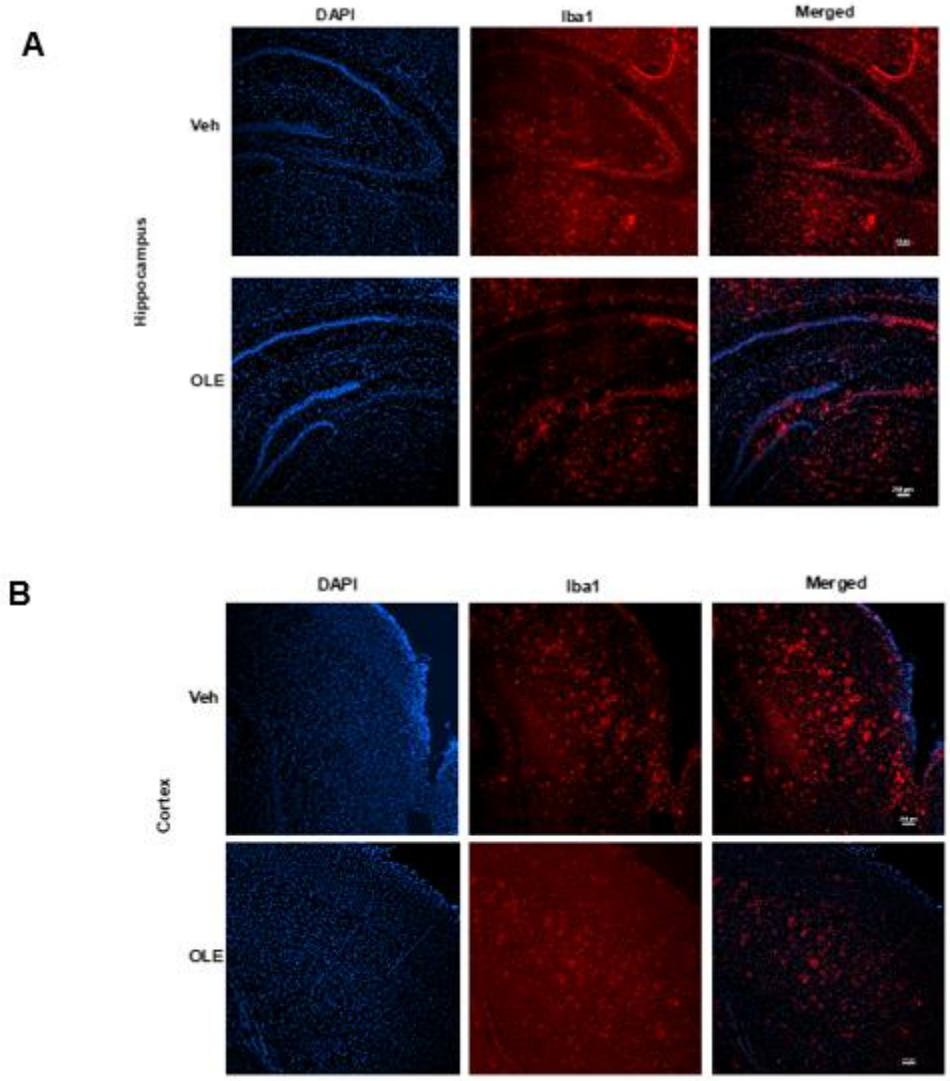

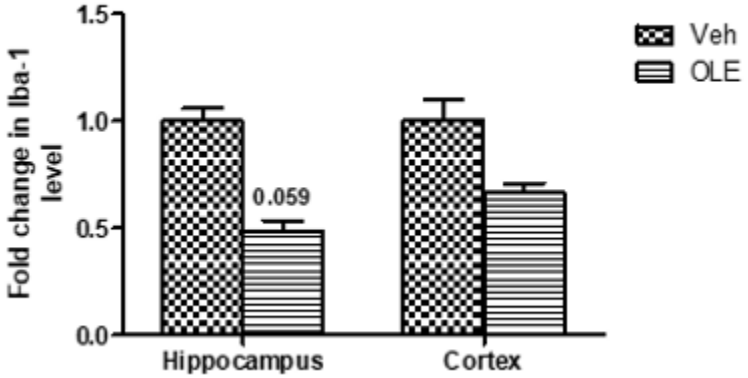

Fig 4. 9: Effect of OLE treatment on microglial cells activation. Mice treated with OLE at 366 µg/kg daily for 3 months. **(A-B)** Representative brain sections with quantitative analysis of 5xFAD mice treated with refined oil as the vehicle or OLE stained with Iba-1 antibody to detect activated microglia (Red). Counterstained with DAPI (blue), Scale bar= 250µm. Results showed the density of activated microglia was reduced with OLE treatment compared to vehicle-treated mice in the hippocampi and cortexes of 5xFAD mice. Data represented as mean± SEM. Male mice (n=3).

4.11. Treatment with OLE increased synaptic markers in 5xFAD mice brains

To investigate the effect of OLE on synaptic protein expression, two pre-synaptic markers (SNAP-25, and Synapsin-1), and one post-synaptic marker (PSD-95) were evaluated by western blot. The levels of synaptic markers were evaluated in males (n=6) in the brain homogenate of 5xFAD mice treated with OLE, Veh-treated (refined oil), and WT treated (refined oil). Results demonstrated that OLE treatment significantly induced the expression of presynaptic markers SNAP-25 and Synapsin-1 by 118 and 41 % ($p < 0.05$) in 5xFAD mice, respectively, compared to vehicle-treated mice. In addition, OLE treated group increased the expression of PSD -95 by 264 % ($p < 0.001$. Compared to male WT mice, the expression of SNAP-25, Synapsin-1, and PSD-95 was significantly reduced in the vehicle-treated group by 77, 175 and 356 % ($p < 0.05$). These results suggest OLE treatment rectified synaptic loss associated with Aβ-related pathology in 5xFAD mice, as shown in Fig 4.10.

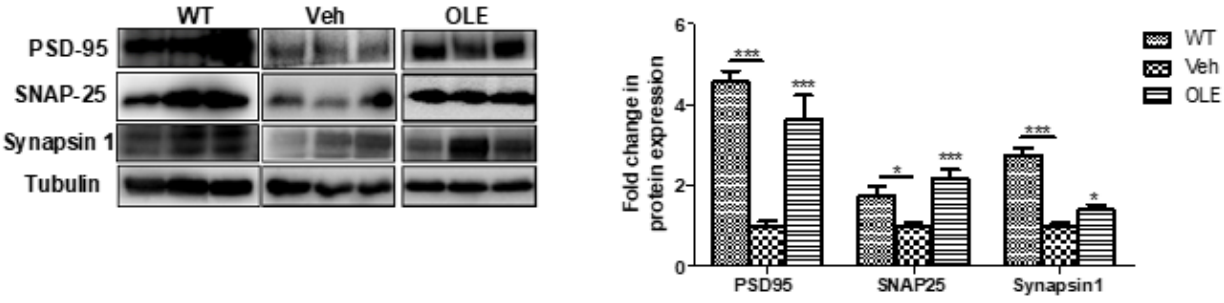

Fig 4. 10: Treatment with OLE (366 µg/kg) for 3 months increased the expression of synaptic markers in 5xFAD mice brains. Representative western blot and densitometry analysis of synaptic markers in mice brain homogenate showed a significant upregulation in SNAP-25, Synapsin-1, and PSD-95 in males (n=6). This effect was restored to the level of WT mice. All proteins were measured from the brain homogenate and normalized to Tubulin. Data represented as mean± SEM. * p <0.05, ** p < 0. 01 and *** p < 0.001.

4.12. Treatment with OLE decreased IL-1β and IL-6 levels

In AD, neuroinflammation contributes to disease pathogenesis. It has been reported that the presence of stimuli such as Aβ and pro-inflammatory cytokines IL-1β and IL-6 activates NLRP3 and promotes the formation of the inflammasome complex. Thus, in this work, we investigated the effect of OLE on the production of pro-inflammatory cytokines in 5xFAD mice. The major pro-inflammatory cytokines were evaluated by ELISA. OLE treatment significantly reduced IL-1β level by 76 % ($p < 0.001$). In addition, a significant reduction in IL-6 by 57 % ($p < 0.05$) was observed (Fig 4.11.A). To explain reduced levels of the inflammatory cytokines, the effect of OLE treatment on NLRP3 inflammasome activation was evaluated. As demonstrated in Fig 4.11.B, OLE reduced NLRP3 significantly by 24 % in 5xFAD mice ($p <0.01$), an effect that was also associated with a significant reduction in pro-caspase 1 by 39 % ($p <0.05$) compared to vehicle-treated group. Compared to male WT mice, the expression of NLRP3 and pro-caspase 1 was significantly increased in the vehicle-treated group ($p <0.05$), suggesting that OLE treatment reduced the neuroinflammation associated with Aβ-related pathology in 5xFAD mice via NLRP3 pathway.

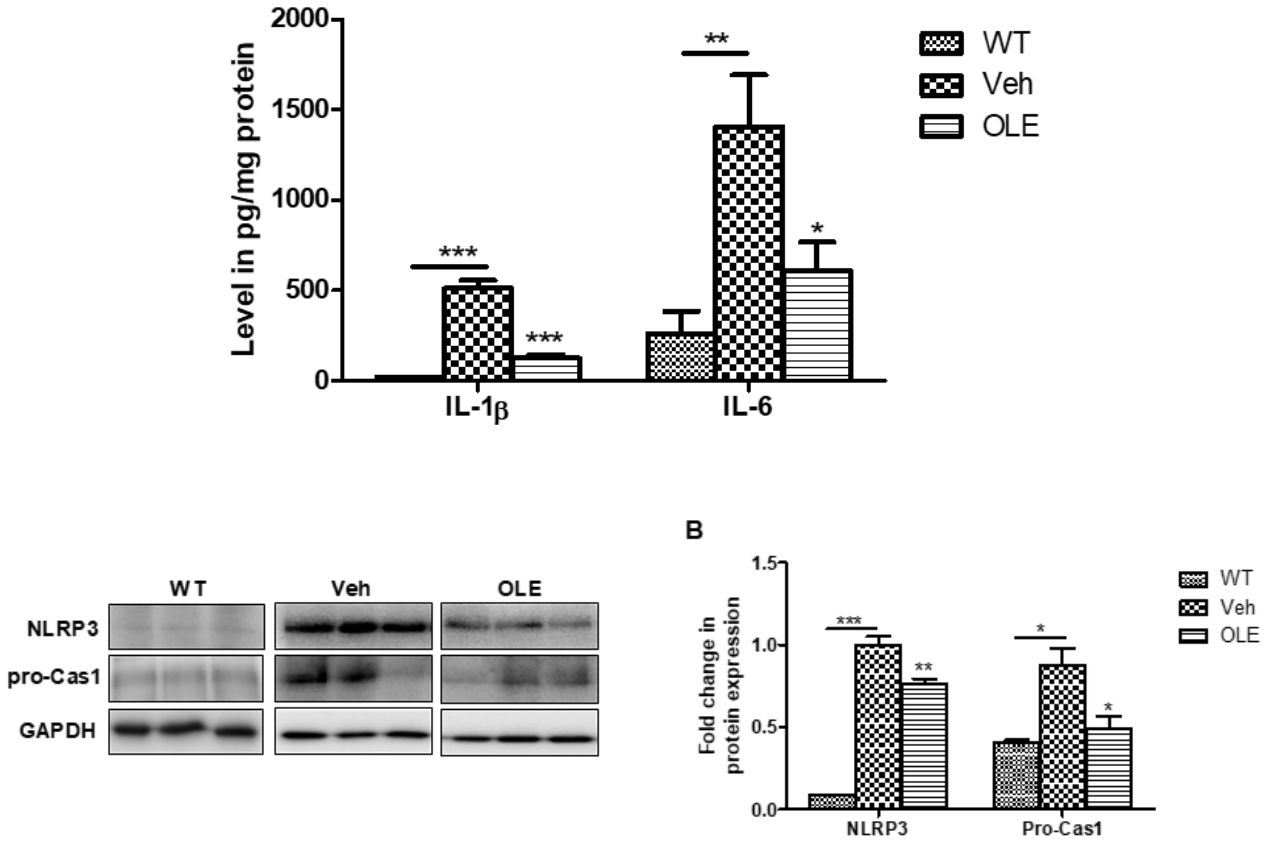

Fig 4. 11: Treatment with OLE (366 µg/kg) for 3 months reduced the neuroinflammation in 5xFAD mice. **(A)** ELISA for pro-inflammatory cytokines, IL-1β, and IL-6 (n=4, males). Results showed OLE treatment significantly reduced IL-1β and IL-6 levels. **(B)** Representative western blot and densitometry analysis of NLRP3 and pro-caspase 1 in 5xFAD mice brain homogenate. Results showed a significant reduction in NLRP3 and pro-caspase 1 in males (n=6 mice). All proteins were measured from the brain homogenate and normalized to GAPDH. Data represented as mean± SEM. * $p < 0.05$, ** $p < 0.01$ and *** $p < 0.001$.

4.13. Treatment with OLE reduced RAGE/HMGb1 expression in 5xFAD mice brains

In AD, RAGE has been studied extensively as a major source of Aβ entry to the brain. Other ligands, including Aβ and HMGb1, interact with RAGE and directly induce inflammation. Thus, here we examined the effect of OLE on the expression of RAGE and HMGb1 in homogenate samples from 5XFAD mice. RAGE expression was significantly decreased by 49 (p<0.01) in 5XFAD mice. In addition, the expression of HMGb1 was significantly reduced by 30 % ($p < 0.05$) compared to vehicle-treated mice. Compared to male WT mice, the expression of RAGE and HMGb1 was significantly increased in the vehicle-treated group by 47 and 65% ($p < 0.01$), as shown in Fig 4.12.

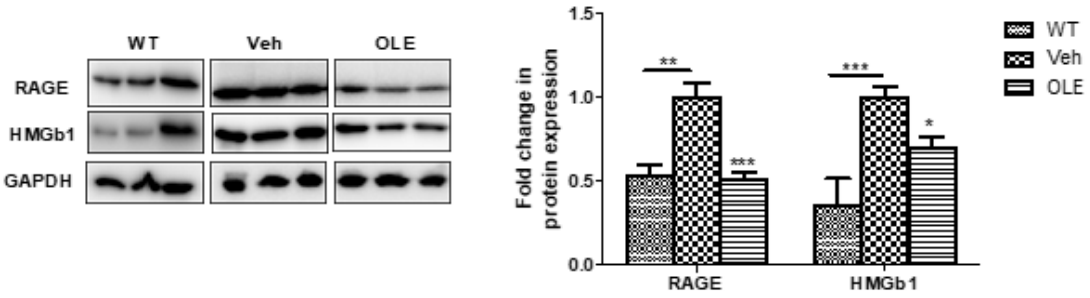

Fig 4. 12: Treatment with OLE (366 µg/kg) for 3 months reduced the neuroinflammation in 5xFAD mice. Representative western blot and densitometry analysis of RAGE and HMGb1 in 5xFAD mice brain homogenate. Results showed a significant reduction in RAGE and HMGb1 in males (n=6); this effect reduced to WT level. All proteins were measured from the brain homogenate and normalized to GAPDH. Data represented as mean± SEM. * p < 0.05, ** p < 0. 01 and *** p < 0.001.

4.14. Treatment with OLE reduced neuroinflammation markers in 5xFAD mice brains through NF-κB signaling pathway

To determine the underlying mechanism by which OLE reduced neuroinflammation markers, we evaluated the effect of the treatment on the NF-κB signaling pathway. Three major proteins from the NF-κB pathway were measured, including IκBα, p-IκBα (Ser32), and p-IKKβ. Results showed the expression of p-IKKβ was significantly reduced in males by 65 % ($p < 0.01$) compared to vehicle-treated mice. This significant reduction in p-IKKβ was associated with increased levels of total IκBα and reduced p-IκBα. The expression of p-IκBα significantly decreased by 25 % ($p < 0.01$), while IκBα level was significantly increased by 89% ($p < 0.01$), when compared to vehicle-treated mice (Fig 4.13). Compared to male WT mice, the expression of IκBα was significantly reduced in vehicle-treated group ($p <0.01$), which was associated with upregulation of p-IκBα and p-IKK ($p <0.01$), suggesting that OLE treatment reduced the neuroinflammation associated with Aβ-related pathology in 5xFAD mice via NF-κB signaling pathway.

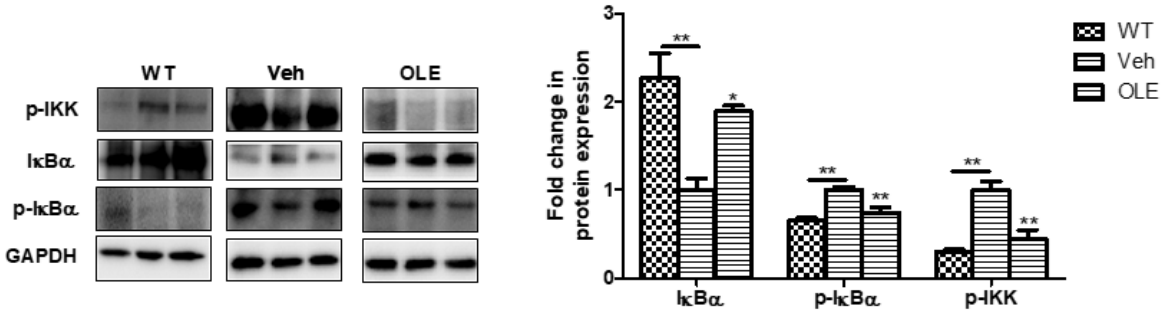

Fig 4. 13: Treatment with OLE (366 µg/kg) for 3 months reduced the neuroinflammation through inactivation of NF-κB signaling pathway in 5xFAD mice brain homogenates. Representative western blot and densitometry analysis of IκBα, p-IκBα (Ser32), and p-IKKβ in 5xFAD mice brain homogenates. Results showed a significant reduction in p-IKKβ and p-IκBα (Ser32), and upregulation in IκBα in males (n=6) compared to vehicle-treated mice. All proteins were measured from the brain homogenate and normalized to GAPDH. Data represented as mean± SEM. * $p < 0.05$, ** $p < 0.01$ and *** $p < 0.001$.

4.15. Plasma and brain levels of OLEG and OLEA following IV administration of OLEG

To exert its effect in the brain, a CNS drug should enter the brain to reach its target. OLEG rapidly hydrolyzes to the aglycone form OLEA. Several studies evaluated OLEA plasma and brain disposition and found that OLEA crosses the BBB (319, 332). In this study, plasma and brain levels of OLEG and OLEA in WT type mice were evaluated. Mice were divided into groups according to blood collection time points with n=3 mice per one-time point. Mice received a single IV injection of OLEG at a dose of 10mg/kg. Blood samples were collected at 0, 5, 10, 30, 60, and 240 min (n=3 per time point). In addition, brain tissues were collected at the same time points after mice decapitation. Plasma samples were analyzed for OLEG and OLEA by HPLC. To analyze samples obtained from plasma and brain tissues, one calibration curve was prepared from OLEG starting from 1.25-10µg/ml with linear regression equation (y = 4623.6x - 2918.3) as shown in (Table 4.1) before analyzing the plasma levels of OLEG in the same day. For OLEA, one calibration curve was prepared from OLEA starting from 6.25-25 µg/ml with linear regression equation (y = 343.41x - 819) as shown in (Table 4.1) before analyzing the plasma levels of OLEA in the same day. In the brain, OLEA was evaluated, one calibration curve was prepared starting from 1.25-5 µg/ml with a linear regression of y = 2999.5x - 1324.5) before analyzing the brain levels of OLEA in the same day as shown in (Table 4.1). The accuracy was calculated from each point in the calibration curves as shown in (4.1) The LOQ, which represents the lowest concentration in the calibration curves was 1.25 µg/ml in plasma for OLEG, and was 6.25 µg/ml in plasma and 1.25 in brain homogenate for OLEA. All calibration curve standards, plasma and brain samples were analyzed by HPLC.

OLEG plasma levels rapidly reduced and was only detected up to 60 min with the highest concentration at 5 min measured at 0.93 ± 0.7 µg/ml (Fig 4.14.A). The hydrolysis product of OLEG, namely OLEA, was detected in plasma starting at 10 min with 2.2 ± 1.9 µg/ml concentration that was detected up to 240 min (Fig 4.14.B). While OLEG was not detected in the brain, OLEA was detected at 60 and 240 min (Fig 4.14.C). The partition coefficient (Kp) ratio of brain to plasma was 11.4%, which is comparable to findings from a previous study reporting a Kp value of 9% (319). Blank samples from the plasma of OLEG and OLEA, and blank brain samples of OLEA were used. A representative chromatograms are shown in (Fig 4.13.D). These finding showed that all drug concentration in plasma and brain were below the LOQ with a variation ≥25%, suggesting further studies are necessary to evaluate concentrations of OLEG and OLEA in plasma and brain.

Table 4. 1: Plasma and brain spiked calibration curve from OLEG and OLEA

OLEG-Plasma			
$y = 4623.6x - 2918.3$ $R^2 = 0.999$			
CC (µg/ml)	Area	BC	Accuracy (%)
1.25	2533	0.63	50
2.5	9379	1.18	47
5	19667	2.66	53
10	43441	4.88	49
OLEA-Plasma			
$y = 343.41x - 819$ $R^2 = 0.9977$			
CC (µg/ml)	Area	BC	Accuracy (%)
6.25	1445	6.59	105
12.5	3297	11.99	96
25	7825	25.17	100
OLEA-Brain			
$y = 2999.5x - 1324.5$ $R^2 = 0.9928$			
CC (µg/ml)	Area	BC	Accuracy (%)
1.25	2057	1.13	90
2.5	6726	2.68	107
5	13489	4.94	99

BC: back calculation of area using the linear regression equation.

Table 4. 2: Pharmacokinetic parameters of OLEG and OLEA following a single intravenous administration of 10mg/kg OLEG.

		OLEG	OLEA			
Parameter	Unit		Parameter	Unit	Plasma	Brain
$t_{1/2}$	min	49				
$AUC_{0\text{-}inf}$	µg.min/ml	53.4	$AUC_{0\text{-}240}$	µg.min/ml	592	67.4
k_{el}	min^{-1}	0.014				
CL	ml/min	5.6				
Vd	ml	300				

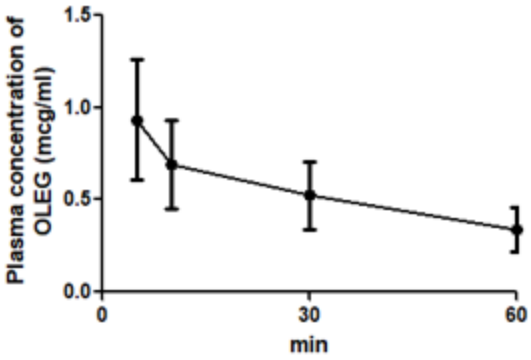
Plasma concentration of OLEG (mcg/ml)
1.5
1.0
0.5
0.0
0
30
60
min

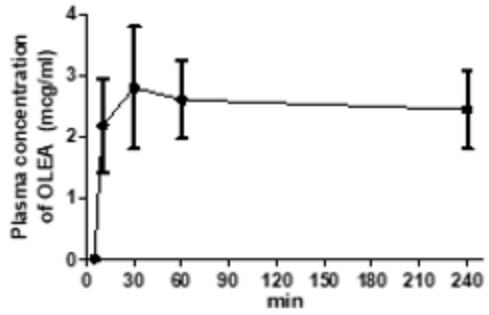
Plasma concentration of OLEA (mcg/ml)
4
3
2
1
0
0 30 60 90 120 150 180 210 240
min

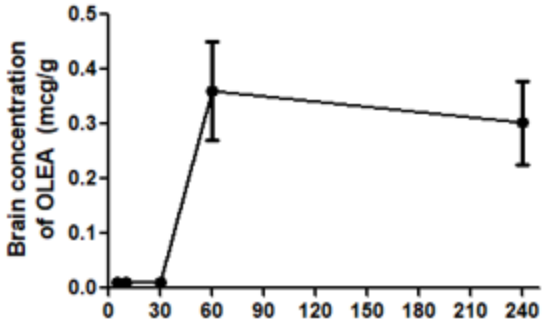
Brain concentration of OLEA (mcg/g
0.5
0.4
0.3
0.2
0.1
0.0
0 30 60 90 120 150 180 210 240

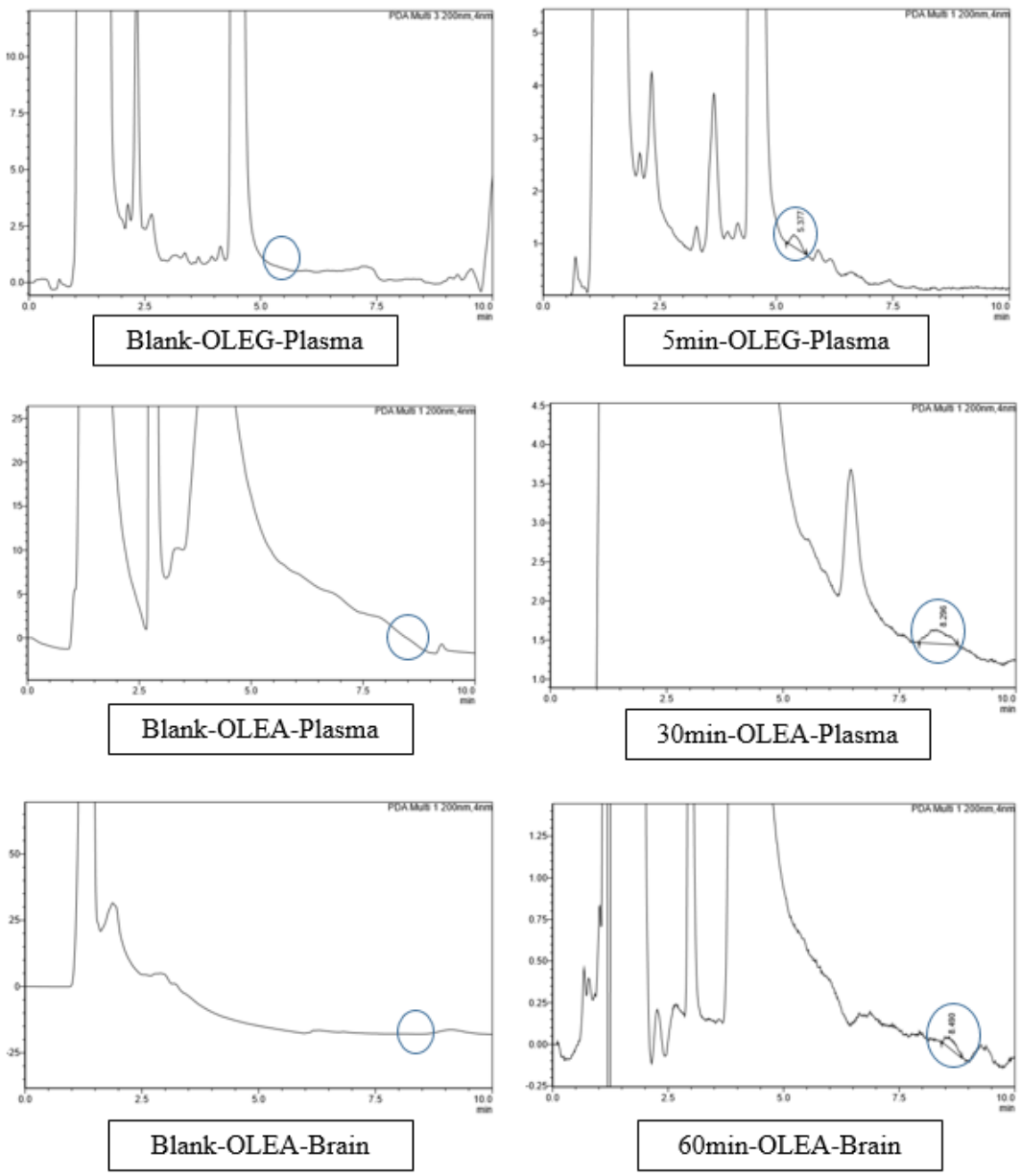

Fig 4. 14: Plasma and brain levels of OLEG and OLEA following IV administration of OLEG. **(A)** Time-plasma concentration profile of OLEG after a single IV dose 10 mg/kg. **(B)** Time-plasma concentration profile of OLEA. **(C)** Time-brain concentration profile of OLEA. Results showed OLEA crossed the BBB. **D)** Representative chromatograms of blank and plasma samples of OLEG at retention time 5.4 min and brain sample of OLEA at retention time 8.3 min. Data are expressed as mean ± SD from (n=3) for each time point.

4.16. The effect of OLE on Aβ-related pathology and neuroinflammation in female 5xFAD mice

Recently, a growing body of evidence suggested sex differences in AD mouse models with female mice demonstrating increased Aβ accumulation compared to male mice (4), which could alter male and female mice's response to therapeutic treatments. Here, I was interested in evaluating whether OLE effect is different between male and female mice on Aβ and related pathology and neuroinflammation. To create preliminary data, I used a limited number of female 5xFAD mice (n=3/group) for vehicle-treated (refined oil) and OLE groups. All methods described above, including food preparation, animal procedures, and biochemical analysis were applied. Results are shown in Supplementary data (end of the dissertation). Preliminary findings showed that in female mice, OLE enhanced the tight junction proteins, reduced Aβ accumulation, and reduced neuroinflammation. This effect was consistent with that observed in male 5xFAD mice. Presented data are considered preliminary and requires further clarification with a larger number of female mice with the inclusion of WT female mice. All figures from these experiments are shown in the supplemental data chapter.

5. Discussion

AD is a complex neurodegenerative disorder characterized by multiple environmental and genetic factors that could influence the incidence and prevalence of disease susceptibility (1). Several hypotheses and theories suggested major hallmarks of AD, including but not limited to compromised BBB, Aβ plaques, NFT, widespread of activated astrocytes and microglial cells, synaptic dysfunction, neuronal damage, oxidative stress and neuroinflammation (229, 276, 332). Available medicines only temporarily alleviate some symptoms but do not target the underlying cause(s) of the disease, and to date, all evaluated therapies failed to treat the disease. Neuroinflammation significantly contributes to AD pathology and development, which could lead to neurodegeneration and cognitive decline (333). Thus, targeting neuroinflammatory pathways could be essential to stop or delay disease progression.

In the last few decades, MD has been studied extensively and was proven to have several beneficial effects, such as anti-inflammatory, anti-oxidant, and neuroprotective effects (301, 302, 304, 308). Greater adherence to MD has been associated with a slower rate of cognitive impairment and dementia (303, 334). Olive oil is considered as the major source of fat in MD, contains more than 100 different biophenolic compounds (247, 335). Previous studies reported the beneficial effect of biophenols present in olive oil using different transgenic mouse models of AD, such as 5xFAD and TgSwDI mice (311-313, 322, 323). Results showed mice treated with EVOO or OC enhanced the BBB function, enhanced tightness of endothelial cells, increased Aβ clearance across the BBB by increasing the expression of Aβ major transport proteins, reduced the accumulation of Aβ, and reduced neuroinflammation (323). In comparison, OLE contains a higher amount of bioactive compounds than those found in EVOO, and showed a pivotal role in enhancing health outcomes (336). The major bioactive compound

in OLE is OLEG, which undergoes hydrolysis to OLEA in the blood. Several studies investigated the effect of OLEA in AD mouse models and reported that at the doses of (2 and 8 mg/kg b.w.) reduced Aβ oligomers, astrocytes activation, and cognitive impairment (320, 321), but still, the exact mechanism is not fully understood.

In the current study, our goal was to evaluate the effect of OLE added to powdered food on Aβ-related pathology, cognitive function, and neuroinflammation in 5xFAD mice with advanced AD pathology. Furthermore, we investigated the potential mechanism by which OLE reduced Aβ-related pathology.

Different dosage regimens have been previously studied for the effect of OLE and OLEA on Aβ-related pathology mouse model (320, 321, 337)**.** Briefly, one study investigated the effect of OLE on APPswe/PS1dE9 mouse model at dose of 8mg/kg b.w. administered for 4 months, results showed the level of Aβ reduced significantly in hippocampi and cortexes, but the mechanism by which OLE produce the observed positive effect has not been identified (337). Other studies used the pure oleuropein aglyone (OLEA) using different dosage regimen namely 8, 2 and 0.08 mg/kg b.w. for 2 months on Aβ-related pathology (320, 321). In these studies, OLEA administered at 8 and 2 mg/kg b.w showed a significant reduction in Aβ level in TgCRND8 mice, a mouse model of AD, while at 0.08 mg/kg b.w. OLEA did not show effect. Thus, in our study, we chose to evaluate at a dose that is lower than 2 mg/kg and higher than 0.08 mg/kg b.w. of OLEG, taken into consideration that OLE contains other biophenolic compounds that could also produce an additive or synergistic effect.

Mice were fed daily, with 366 µg/kg b.w. To confirm food homogeneity and ensure all mice received the same dose every day with the assumption of the same consumed food amount, after mixing OLE with food, we tested the levels of OLEG in 3 randomly selected portions of

the food. This process was repeated for 5 preparations over 5 weeks. OLE concentration was consistent between the portions of each preparation and between preparations confirming food homogeneity.

With the reported beneficial effect of polyphenols against neurodegenerative diseases (338-340), studies focused on their BBB penetration are limited. While many open questions are in need to be answered regarding the action of major phenolic compounds present in olive oil and leaf extract once ingested and absorbed, to exert the desired effect, these compounds should reach the brain. In this study, we performed a feasibility study to evaluate the ability of OLEG, as a major bioactive compound in OLE to cross the BBB in WT mice after a single IV dose. Following IV administration, while plasma levels of OLEG decreased with time, OLEA levels increased and detected after 10 min of dosing. In the brain, OLEA levels were detected at 1 and 4 h in low concentrations at levels lower than LOQ due to the low method sensitivity. Our preliminary findings are consistent with Molitova and colleagues, who found after a single dose of olive oil phenolic compounds prepared in a cake (3g/kg b.w.) in treated rats, was absorbed and distributed to different tissues including the brain (319). The authors were able to detect oleuropein at 1, 2, and 4 h following oral consumption. Further studies are needed to thoroughly evaluate OLEA penetration to the brain across the BBB.

In aging and AD, changes in BBB functionality and supporting cells from the neurovascular unit (NVU) lead to BBB dysfunction in a more progressed disease stage (110, 230, 236, 237, 341, 342). Several studies reported the alteration of BBB plays a pivotal role in AD (237, 343, 344), and suggested that breakdown is an early event in advanced aged human brains started in the hippocampus and contributes to cognitive decline (345). Previous work from our lab showed a significant upregulation in TJ protein expression with EVOO and OC (323). Our data here

showed a consistent trend. Treatment with OLE enriched with OLEG in 5xFAD mice restored the tight junction and adherence junction proteins to levels close to those observed in WT mice through significant upregulation of claudin-5, occludin, and Zo-1, as well as VE-cadherin.

The amyloidogenic hypothesis of AD, suggests that the formation, aggregation, and deposition of Aβ peptides (346). The imbalance between amyloid production and clearance is responsible for cognitive impairment and neuronal death (346-347). Therefore, we examined the effect of OLE treatment on the clearance of $A\beta_{40}$ and $A\beta_{42}$, the most abundant pathogenic isoforms (348). Our treatments demonstrated a significant reduction in total Aβ and Aβ plaques accumulation in 5xFAD mice brains as detected by 6E10 and Thioflavin S, respectively. Such decrease in Aβ was associated with increased expression of Aβ major transport proteins responsible for Aβ clearance, named P-gp and LRP1 (284, 349-354). Efflux transporter proteins are reduced in age-related neurodegeneration (284). We found the expression of Aβ major transporter proteins are increased significantly in males with OLE treatment compared to vehicle-treated with refined oil.

Besides the effect on enhancing Aβ clearance, OLE treatment altered Aβ production by shifting the APP processing toward the non-amyloidogenic pathway. This effect was investigated with a long-term treatment of OLE for 3 months. From previously reported in vitro study, OLEA was evaluated on APPβ metabolism and other enzymes involved in AD into two different cell lines; human neuroblastoma (SK-N-SH) and human embryonic kidney cells (HEK293), results showed that OLEA effect in a concentration of (12.5, 25, 50 μM) significantly elevated the levels of sAPPα, α-secretase (ADAM-10), and significantly reduced Aβ oligomers (355). The observed effect was consistent with our study as OLE treatment showed significant induction of the expression of α-secretase (ADAM-10) and sAPPα, an effect that was associated with a

significant reduction in sAPPβ, which means that OLE treatment directed Aβ production toward the non-amyloidogenic pathway by increasing the activity of the α-secretase enzyme. In addition, we investigated the level of each Aβ isoforms ($A\beta_{40}$ and $A\beta_{42}$) by ELISA, and they were both significantly reduced compared to refined oil-treated mice. Thus, the effect of OLE treatment on the expression of synaptic markers was evaluated. Our findings demonstrated that the expression of both pre and post-synaptic markers, Synapsin-1, SNAP-25, and PSD-95 were upregulated significantly by the effect of OLE treatment, which could explain the improvement in learning abilities and memory function in 5xFAD mice.

The findings of this study also demonstrated that OLE treatment significantly improved memory function and reduced neuroinflammation. There is increasing evidence that neuroinflammation is a crucial factor in AD pathology (356). Neuroinflammation involves microglial and astrocyte cell activation. Glial cells have a phagocytic function under normal physiological conditions (357). But in AD brains, glial cells become activated, and they secrete several pro-inflammatory cytokines, ROS, and other oxidative stress markers and eventually cause neuronal death (358). GFAP expression changes during development, aging, and other various diseases, including AD (359). We assessed the effect of OLE treatment on the levels of GFAP as measured by the density of activated astrocytes in hippocampi and cortexes. Results showed a significant reduction in the levels of GFAP immunoreactivity in the cortex and hippocampus, and the effect was almost the same in both regions in OLE treated mice. In addition, microglial activation has been heavily studied for its contribution to Aβ phagocytosis. However, the microglial response also has been associated with detrimental effects mediated by proinflammatory cytokines, chemokines, and neurotoxins release (275, 253, 254). In an advanced Aβ-related pathology mouse model, the activation of microglial cells was

significantly reduced in both cortexes and hippocampi, which was consistent with a significant reduction in pro-inflammatory cytokines levels.

To clarify the mechanism by which OLE reduced neuroinflammation, we have evaluated several pathways that been associated with AD in relation to Aβ pathology. RAGE increased in aging and AD (360-364), known as influx transporter protein that responsible for entry of Aβ from the blood to the brain (237), as wells as a receptor of inflammation expressed on the astrocytes (329). In addition, RAGE is highly expressed in activated astrocytes in the brain which induce the neuroinflammation by releasing a high level of inflammatory cytokines (365). Besides, Lue and colleagues reported the expression of RAGE was observed in neurons and microglia (366). PAMPs and DAMPs ligands such as Aβ and HMGB1 have shown to interact and increase the expression and activity of RAGE (367-370). Several studies reported that RAGE/NF-κB signaling pathway is involved in AD surrounding the Aβ plaques (146, 330, 371). Several studies showed the implication of HMGb1 in AD pathology upon its release from various cells, including astrocytes and microglia, through its binding with RAGE and TLRs and activated the inflammatory response (372, 373). Upon interactions, Aβ and HMGb1 activate several inflammatory signaling pathways, including NF-κB and NADPH-oxidase, which lead to cell death (374-376). A study in 5xFAD mice at 6 months of age showed that RAGE induced the activation of NF-κB and initiate the inflammatory response (330). NF-κB activation promotes the expression of pro-inflammatory cytokines to induce a prolonged activation and promotion of signaling mechanisms for cell damage, in addition to regulating NLRP3 inflammasome activation (377), which has been activated in AD mouse model (168). Therefore, reducing the activity of NLRP3 could effectively interfere with the AD progression and inhibits the activation of NF-κB inflammatory pathways. Our findings showed that OLE treatment

caused a significant reduction in the pro-inflammatory cytokines IL-1β and IL-6, compared to vehicle-treated with refined oil. This effect was accompanied by a significant reduction in both NF-κB and NLRP3. Collectively, and based on our findings, we propose the scheme below (Scheme 1) for the potential mechanism by which OLE reduced neuroinflammation by targeting the NLRP3/ RAGE/NF-κB pathway.

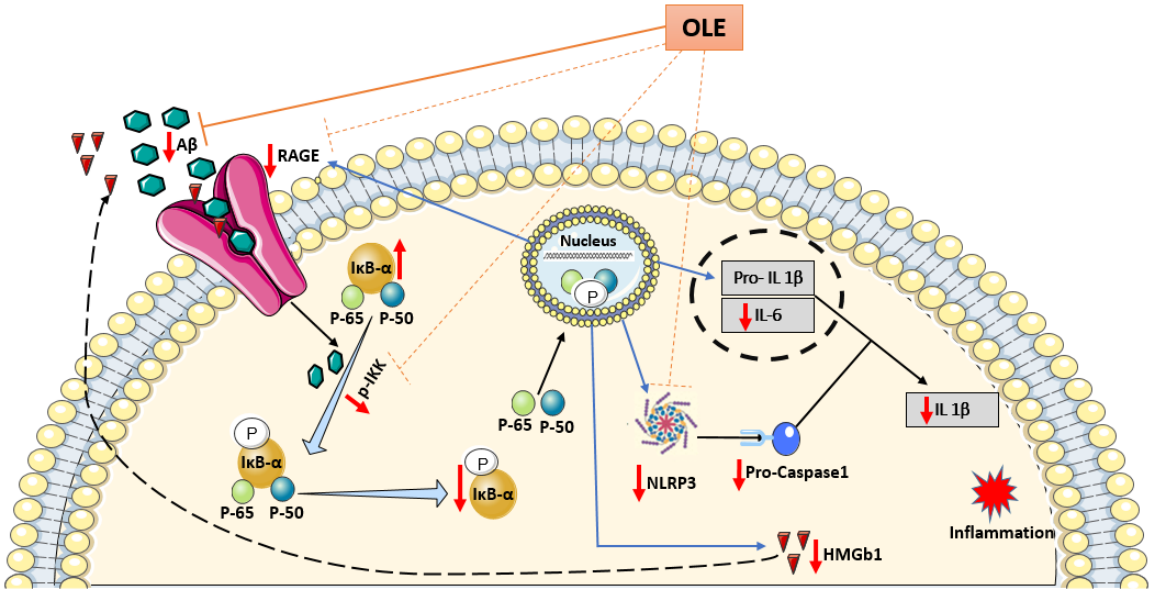

Scheme 1: The potential mechanism of OLE by targeting NLRP3/ RAGE/NF-κB pathway (Prepared by Ihab Abdallah).

Limitations and challenges: Findings from our studies confirmed the beneficial effect of OLE against Aβ and related pathology in a mouse model of AD, however, we acknowledge that there are few limitations associated with this work as described below.

In the behavioral studies to assess the spatial learning and memory function, we found OLE treatment improved the learning abilities of mice in the training days and the test day (probe day), but on the probe day to (i.e. in the absence of platform in the target quadrant), we found that vehicle treated mice spent time less than 25% chance, and WT and OLE treated mice time spent was higher but close to the 25% chance. This effect could be due to room size that caused closer cues to the tub that mice could not adequately see them. Another limitation is the small number of mice used in our experiments (n=7 mice), where for behavior studies, it is usually recommended to have $n \geq 10$ mice.

A CNS drug should enter the brain to reach its target, and exert its effect in the brain. In our feasibility study for OLEG and OLEA for its penetration to the brain, the developed method to quantify compounds levels was not fully and thoroughly validated. For OLEA penetration to the brain, brains vessels were not flushed to remove the blood containing the compound, which could overestimated the drug concentration in the brain. However, in the experiment, to compensate for the blood vessels volume, the compound amount was corrected for the blood volume by multiplying the compound concentration by 4% (estimated blood vessels volume in the brain) to determine the Kp of OLEA. To overcome this issue, in future studies, flushing brain vessels or adding a non-BBB permeable marker such as Evans blue could be used to normalize vascular pool in the brain. For BBB integrity, we only measured the effect of OLE on tight junction and transport proteins, however, for additional studies could be necessary for functional study including injection of Evans blue or large molecular weight markers like

Dextran 40K. Furthermore, additional studies that compare both sexes with a larger number of mice are necessary.

6. Conclusion and future directions

AD is a complex disorder associated with many pathological factors that communicate together and start a long time before the disease onset. Factors such as accumulation of Aβ and neuroinflammation plays a significant role in AD pathology and results in neuronal toxicity, cognitive impairment, and, eventually, dementia. Due to the complexity of AD, current therapies are not effective and only treat the disease symptoms. Thus, targeting multiple pathological events may reduce the progression of AD.

In the past few decades, a growing body of evidence showed the beneficial effect of bioactive polyphenols found in olive oil and OLE in experimental and clinical research. OLE contains a higher number of bioactive polyphenols compared to olive oil. The major bioactive compound, named oleuropein, showed a beneficial effect by reducing Aβ level in an AD mouse model, but the exact mechanism was not fully elucidated. Finding from this work showed the positive effect of OLE against several pathological hallmarks of AD. Mice treated with OLE showed a significant improvement in memory function associated with increased synaptic markers. In addition, our study added further support for the important role of bioactive polyphenols against Aβ and related pathology. For example, OLE significantly reduced Aβ levels as determined by IHC and ELISA, an effect that could be linked to increased clearance and reduced production. In addition, OLE increased the expression of TJs and efflux transport proteins with long-term consumption of OLE. OLE also reduced neuroinflammation as determined by monitoring astrogliosis, microgliosis, and cytokines levels, which showed a significant reduction compared to vehicle-treated mice. Indeed, additional studies are necessary to clarify whether the observed effect is due to OLE direct effect against neuroinflammation and/or indirect that is mediated by reduced Aβ brain levels. To shed some light on the potential mechanism of the observed effect,

we demonstrated that OLE (directly and/or indirectly) reduced the activation of NLRP3 inflammasomes, possibly via reducing NF-κB pathway activation which leads to reduced RAGE and HMGb1.

7. References

1- Citron M. Alzheimer's disease: strategies for disease modification. Nature reviews Drug discovery. 2010 May;9(5):387-98.

2- Strassnig M, Ganguli M. About a peculiar disease of the cerebral cortex: Alzheimer's original case revisited. Psychiatry (Edgmont). 2005 Sep;2(9):30.

3- Marsh J, Alifragis P. Synaptic dysfunction in Alzheimer's disease: the effects of amyloid beta on synaptic vesicle dynamics as a novel target for therapeutic intervention. Neural regeneration research. 2018 Apr;13(4):616.

4- Alzheimer's Association. 2019 Alzheimer's disease facts and figures. Alzheimer's & Dementia. 2019 Mar;15(3):321-87.

5- Hebert LE, Weuve J, Scherr PA, Evans DA. Alzheimer disease in the United States (2010–2050) estimated using the 2010 census. Neurology. 2013 May 7;80(19):1778-83.

6- Bayer TA, Wirths O. Intracellular accumulation of amyloid-Beta-a predictor for synaptic dysfunction and neuron loss in Alzheimer's disease. Frontiers in aging neuroscience. 2010 Mar 10;2:8.

7- St George-Hyslop, P. H., Haines, J. L., Rogaev, E. I., Mortilla, M., Vaula, G., Pericak-Vance, M., ... & Rainero, I. (1992). Genetic evidence for a novel familial Alzheimer's disease locus on chromosome 14. *Nature genetics*, *2*(4), 330-334.

8- Levy-Lahad E, Lahad A, Wijsman EM, Bird TD, Schellenberg GD. Apolipoprotein E genotypes and age of onset in early-onset familial Alzheimer's disease. Annals of Neurology: Official Journal of the American Neurological Association and the Child Neurology Society. 1995 Oct;38(4):678-80.

9- Chakrabarti S, Khemka VK, Banerjee A, Chatterjee G, Ganguly A, Biswas A. Metabolic risk factors of sporadic Alzheimer's disease: implications in the pathology, pathogenesis and treatment. Aging and disease. 2015 Aug;6(4):282.

10- Mendez MF. Early-onset Alzheimer disease. Neurologic clinics. 2017 May 1;35(2):263-81.

11- Tanzi RE. The genetics of Alzheimer disease. Cold Spring Harbor perspectives in medicine. 2012 Oct 1;2(10):a006296.

12- De Strooper B, Iwatsubo T, Wolfe MS. Presenilins and γ-secretase: structure, function, and role in Alzheimer disease. Cold Spring Harbor perspectives in medicine. 2012 Jan 1;2(1):a006304.

13- O'Brien RJ, Wong PC. Amyloid precursor protein processing and Alzheimer's disease. Annual review of neuroscience. 2011 Jul 21;34:185-204.

14- Chen GF, Xu TH, Yan Y, Zhou YR, Jiang Y, Melcher K, Xu HE. Amyloid beta: structure, biology and structure-based therapeutic development. Acta Pharmacologica Sinica. 2017 Sep;38(9):1205-35.

15- Bekris LM, Yu CE, Bird TD, Tsuang DW. Genetics of Alzheimer disease. Journal of geriatric psychiatry and neurology. 2010 Dec;23(4):213-27.

16- Isik AT, Bozoglu E, Naharci MI, Eker D. Cardiac safety of rivastigmine in patients with late onset Alzheimer's disease. Journal of Geriatrics and Geriatric Neuropsychiatry. 2010;1(3):21-6.

17- Saunders AM, Strittmatter WJ, Schmechel D, George-Hyslop PS, Pericak-Vance MA, Joo SH, Rosi BL, Gusella JF, Crapper-MacLachlan DR, Alberts MJ, Hulette C.

Association of apolipoprotein E allele ϵ4 with late-onset familial and sporadic Alzheimer's disease. Neurology. 1993 Aug 1;43(8):1467-.

18- Corder EH, Saunders AM, Strittmatter WJ, Schmechel DE, Gaskell PC, Small G, Roses AD, Haines JL, Pericak-Vance MA. Gene dose of apolipoprotein E type 4 allele and the risk of Alzheimer's disease in late onset families. Science. 1993 Aug 13;261(5123):921-3.

19- Holtzman DM. CSF biomarkers for Alzheimer's disease: current utility and potential future use. Neurobiology of aging. 2011 Dec 1;32:S4-9.

20- van der Flier WM, Pijnenburg YA, Fox NC, Scheltens P. Early-onset versus late-onset Alzheimer's disease: the case of the missing APOE ε4 allele. The Lancet Neurology. 2011 Mar 1;10(3):280-8.

21- Karrasch M, Sinervä E, Grönholm P, Rinne J, Laine M. CERAD test performances in amnestic mild cognitive impairment and Alzheimer's disease. Acta Neurologica Scandinavica. 2005 Mar;111(3):172-9.

22- Fuld PA. Test profile of cholinergic dysfunction and of Alzheimer-type dementia. Journal of Clinical and Experimental Neuropsychology. 1984 Nov 1;6(4):380-92.

23- Khachaturian ZS. Diagnosis of Alzheimer's disease. Archives of neurology. 1985 Nov 1;42(11):1097-105.

24- Saint-Aubert L, Barbeau EJ, Péran P, Nemmi F, Vervueren C, Mirabel H, Payoux P, Hitzel A, Bonneville F, Gramada R, Tafani M. Cortical florbetapir-PET amyloid load in prodromal Alzheimer’s disease patients. EJNMMI research. 2013 Dec 1;3(1):43.

25- Hampel H, Bürger K, Teipel SJ, Bokde AL, Zetterberg H, Blennow K. Core candidate neurochemical and imaging biomarkers of Alzheimer's disease. Alzheimer's & Dementia. 2008 Jan 1;4(1):38-48.

26- Liu PP, Xie Y, Meng XY, Kang JS. History and progress of hypotheses and clinical trials for Alzheimer's disease. Signal transduction and targeted therapy. 2019 Aug 23;4(1):1-22.

27- Tang-Wai DF, Graff-Radford NR, Boeve BF, Dickson DW, Parisi JE, Crook R, Caselli RJ, Knopman DS, Petersen RC. Clinical, genetic, and neuropathologic characteristics of posterior cortical atrophy. Neurology. 2004 Oct 12;63(7):1168-74.

28- McMonagle P, Kertesz A. Exploded drawing in posterior cortical atrophy. Neurology. 2006 Nov 28;67(10):1866-.

29- Alladi S, Xuereb J, Bak T, Nestor P, Knibb J, Patterson K, Hodges JR. Focal cortical presentations of Alzheimer's disease. Brain. 2007 Oct 1;130(10):2636-45.

30- Koedam EL, Lauffer V, van der Vlies AE, van der Flier WM, Scheltens P, Pijnenburg YA. Early-versus late-onset Alzheimer's disease: more than age alone. Journal of Alzheimer's Disease. 2010 Jan 1;19(4):1401-8.

31- Cacace R, Sleegers K, Van Broeckhoven C. Molecular genetics of early-onset Alzheimer's disease revisited. Alzheimer's & Dementia. 2016 Jun 1;12(6):733-48.

32- Bennett DA, Schneider JA, Tang Y, Arnold SE, Wilson RS. The effect of social networks on the relation between Alzheimer's disease pathology and level of cognitive function in old people: a longitudinal cohort study. The Lancet Neurology. 2006 May 1;5(5):406-12.

33- Selkoe DJ. The molecular pathology of Alzheimer's disease. Neuron. 1991 Apr 1;6(4):487-98.

34- Norfray JF, Provenzale JM. Alzheimer's disease: neuropathologic findings and recent advances in imaging. American Journal of Roentgenology. 2004 Jan;182(1):3-13.

35- Selkoe DJ. Alzheimer's disease is a synaptic failure. Science. 2002 Oct 25;298(5594):789-91.

36- Jack CR, Petersen RC, Xu YC, Waring SC, O'Brien PC, Tangalos EG, Smith GE, Ivnik RJ, Kokmen E. Medial temporal atrophy on MRI in normal aging and very mild Alzheimer's disease. Neurology. 1997 Sep 1;49(3):786-94.

37- Alves L, Correia AS, Miguel R, Alegria P, Bugalho P. Alzheimer’s disease: a clinical practice-oriented review. Frontiers in neurology. 2012 Apr 20;3:63.

38- Holtzman DM, Morris JC, Goate AM. Alzheimer’s disease: the challenge of the second century. Science translational medicine. 2011 Apr 6;3(77):77sr1-.

39- Singh SK, Srivastav S, Yadav AK, Srikrishna S, Perry G. Overview of Alzheimer’s disease and some therapeutic approaches targeting Aβ by using several synthetic and herbal compounds. Oxidative medicine and cellular longevity. 2016 Oct;2016.

40- Braak H, Braak E. Neuropathological stageing of Alzheimer-related changes. Acta neuropathologica. 1991 Sep 1;82(4):239-59.

41- Murray ME, Graff-Radford NR, Ross OA, Petersen RC, Duara R, Dickson DW. Neuropathologically defined subtypes of Alzheimer's disease with distinct clinical characteristics: a retrospective study. The Lancet Neurology. 2011 Sep 1;10(9):785-96.

42- Shibata M, Yamada S, Kumar SR, Calero M, Bading J, Frangione B, Holtzman DM, Miller CA, Strickland DK, Ghiso J, Zlokovic BV. Clearance of Alzheimer’s amyloid-β

1-40 peptide from brain by LDL receptor–related protein-1 at the blood-brain barrier. The Journal of clinical investigation. 2000 Dec 15;106(12):1489-99.

43- Glabe C. Intracellular mechanisms of amyloid accumulation and pathogenesis in Alzheimer's disease. Journal of molecular neuroscience. 2001 Oct 1;17(2):137-45.

44- Potter R, Patterson BW, Elbert DL, Ovod V, Kasten T, Sigurdson W, Mawuenyega K, Blazey T, Goate A, Chott R, Yarasheski KE. Increased in vivo amyloid-β42 production, exchange, and loss in presenilin mutation carriers. Science translational medicine. 2013 Jun 12;5(189):189ra77-.

45- Dawkins E, Small DH. Insights into the physiological function of the β-amyloid precursor protein: beyond Alzheimer's disease. Journal of neurochemistry. 2014 Jun;129(5):756-69.

46- Yamaguchi H, Hirai S, Morimatsu M, Shoji M, Ihara Y. A variety of cerebral amyloid deposits in the brains of the Alzheimer-type dementia demonstrated byβ protein immunostaining. Acta neuropathologica. 1988 Nov 1;76(6):541-9.

47- Small GW. The pathogenesis of Alzheimer's disease. The Journal of clinical psychiatry. 1998 Jan 1;59:7-14.

48- Hardy J, Selkoe DJ. The amyloid hypothesis of Alzheimer's disease: progress and problems on the road to therapeutics. science. 2002 Jul 19;297(5580):353-6.

49- Bamburg JR, Bloom GS. Cytoskeletal pathologies of Alzheimer disease. Cell motility and the cytoskeleton. 2009 Aug;66(8):635-49.

50- Puzzo D, Privitera L, Fa' M, Staniszewski A, Hashimoto G, Aziz F, Sakurai M, Ribe EM, Troy CM, Mercken M, Jung SS. Endogenous amyloid-β is necessary for hippocampal synaptic plasticity and memory. Annals of neurology. 2011 May;69(5):819-30.

51- KITAZAWA M, YAMASAKI TR, LAFERLA FM. Microglia as a Potential Bridge between the Amyloid β-Peptide and Tau. Annals of the New York Academy of Sciences. 2004 Dec;1035(1):85-103.

52- Vukic, V., Callaghan, D., Liu, H., & Zhang, W. (2012). Molecular mechanisms of neuroinflammation in Alzheimer's disease.

53- Craft JM, Watterson DM, Van Eldik LJ. Human amyloid β-induced neuroinflammation is an early event in neurodegeneration. Glia. 2006 Apr 1;53(5):484-90.

54- Atamna H, Boyle K. Amyloid-β peptide binds with heme to form a peroxidase: Relationship to the cytopathologies of Alzheimer's disease. Proceedings of the National Academy of Sciences. 2006 Feb 28;103(9):3381-6.

55- Jana A, Pahan K. Fibrillar amyloid-β-activated human astroglia kill primary human neurons via neutral sphingomyelinase: implications for Alzheimer's disease. Journal of Neuroscience. 2010 Sep 22;30(38):12676-89.

56- Hu J, Ferreira A, Van Eldik LJ. S100β induces neuronal cell death through nitric oxide release from astrocytes. Journal of neurochemistry. 1997 Dec;69(6):2294-301.

57- Van Wagoner NJ, Oh JW, Repovic P, Benveniste EN. Interleukin-6 (IL-6) production by astrocytes: autocrine regulation by IL-6 and the soluble IL-6 receptor. Journal of Neuroscience. 1999 Jul 1;19(13):5236-44.

58- Götz J, Probst A, Spillantini MG, Schäfer T, Jakes R, Bürki K, Goedert M. Somatodendritic localization and hyperphosphorylation of tau protein in transgenic mice expressing the longest human brain tau isoform. The EMBO journal. 1995 Apr;14(7):1304-13.

59- Kimura T, Whitcomb DJ, Jo J, Regan P, Piers T, Heo S, Brown C, Hashikawa T, Murayama M, Seok H, Sotiropoulos I. Microtubule-associated protein tau is essential for long-term depression in the hippocampus. Philosophical Transactions of the Royal Society B: Biological Sciences. 2014 Jan 5;369(1633):20130144.

60- Goedert M, Spillantini MG. A century of Alzheimer's disease. science. 2006 Nov 3;314(5800):777-81.

61- Buée L, Bussière T, Buée-Scherrer V, Delacourte A, Hof PR. Tau protein isoforms, phosphorylation and role in neurodegenerative disorders. Brain Research Reviews. 2000 Aug 1;33(1):95-130.

62- Iqbal K, Alonso AD, Chen S, Chohan MO, El-Akkad E, Gong CX, Khatoon S, Li B, Liu F, Rahman A, Tanimukai H. Tau pathology in Alzheimer disease and other tauopathies. Biochimica et Biophysica Acta (BBA)-Molecular Basis of Disease. 2005 Jan 3;1739(2-3):198-210.

63- Lee G, Neve RL, Kosik KS. The microtubule binding domain of tau protein. Neuron. 1989 Jun 1;2(6):1615-24.

64- Billingsley ML, Kincaid RL. Regulated phosphorylation and dephosphorylation of tau protein: effects on microtubule interaction, intracellular trafficking and neurodegeneration. Biochemical Journal. 1997 May 1;323(3):577-91.

65- Kimura T, Yamashita S, Fukuda T, Park JM, Murayama M, Mizoroki T, Yoshiike Y, Sahara N, Takashima A. Hyperphosphorylated tau in parahippocampal cortex impairs place learning in aged mice expressing wild-type human tau. The EMBO journal. 2007 Dec 12;26(24):5143-52.

66- Nordberg A. Amyloid plaque imaging in vivo: current achievement and future prospects. European journal of nuclear medicine and molecular imaging. 2008 Mar 1;35(1):46-50.

67- Abbott NJ, Patabendige AA, Dolman DE, Yusof SR, Begley DJ. Structure and function of the blood–brain barrier. Neurobiology of disease. 2010 Jan 1;37(1):13-25.

68- Bernacki, J., Dobrowolska, A., Nierwiñska, K., & Malecki, A. (2008). Physiology and pharmacological role of the blood-brain barrier. *Pharmacol Rep*, *60*(5), 600-22.

69- Hawkins BT, Egleton RD. Pathophysiology of the blood–brain barrier: animal models and methods. Current topics in developmental biology. 2007 Jan 1;80:277-309.

70- Stewart PA. Endothelial vesicles in the blood–brain barrier: are they related to permeability?. Cellular and molecular neurobiology. 2000 Apr 1;20(2):149-63.

71- Daneman R, Prat A. The blood–brain barrier. Cold Spring Harbor perspectives in biology. 2015 Jan 1;7(1):a020412.

72- Storck SE, Hartz AM, Bernard J, Wolf A, Kachlmeier A, Mahringer A, Weggen S, Pahnke J, Pietrzik CU. The concerted amyloid-beta clearance of LRP1 and ABCB1/P-gp across the blood-brain barrier is linked by PICALM. Brain, Behavior, and Immunity. 2018 Oct 1;73:21-33.

73- Demeule M, Currie JC, Bertrand Y, Ché C, Nguyen T, Régina A, Gabathuler R, Castaigne JP, Béliveau R. Involvement of the low-density lipoprotein receptor-related protein in the transcytosis of the brain delivery vector Angiopep-2. Journal of neurochemistry. 2008 Aug;106(4):1534-44.

74- Silverberg GD, Messier AA, Miller MC, Machan JT, Majmudar SS, Stopa EG, Donahue JE, Johanson CE. Amyloid efflux transporter expression at the blood-brain barrier

declines in normal aging. Journal of Neuropathology & Experimental Neurology. 2010 Oct 1;69(10):1034-43.

75- Moura RP, Martins C, Pinto S, Sousa F, Sarmento B. Blood-brain barrier receptors and transporters: an insight on their function and how to exploit them through nanotechnology. Expert opinion on drug delivery. 2019 Mar 4;16(3):271-85.

76- Persidsky Y, Ramirez SH, Haorah J, Kanmogne GD. Blood–brain barrier: structural components and function under physiologic and pathologic conditions. Journal of Neuroimmune Pharmacology. 2006 Sep 1;1(3):223-36.

77- Cirrito JR, Deane R, Fagan AM, Spinner ML, Parsadanian M, Finn MB, Jiang H, Prior JL, Sagare A, Bales KR, Paul SM. P-glycoprotein deficiency at the blood-brain barrier increases amyloid-β deposition in an Alzheimer disease mouse model. The Journal of clinical investigation. 2005 Nov 1;115(11):3285-90.

78- Wardlaw JM, Smith EE, Biessels GJ, Cordonnier C, Fazekas F, Frayne R, Lindley RI, T O'Brien J, Barkhof F, Benavente OR, Black SE. Neuroimaging standards for research into small vessel disease and its contribution to ageing and neurodegeneration. The Lancet Neurology. 2013 Aug 1;12(8):822-38.

79- Raji CA, Lopez OL, Kuller LH, Carmichael OT, Becker JT. Age, Alzheimer disease, and brain structure. Neurology. 2009 Dec 1;73(22):1899-905.

80- Price JL, Ko AI, Wade MJ, Tsou SK, McKeel DW, Morris JC. Neuron number in the entorhinal cortex and CA1 in preclinical Alzheimer disease. Archives of neurology. 2001 Sep 1;58(9):1395-402.

81- Giannakopoulos P, Herrmann FR, Bussière T, Bouras C, Kövari E, Perl DP, Morrison JH, Gold G, Hof PR. Tangle and neuron numbers, but not amyloid load, predict cognitive status in Alzheimer's disease. Neurology. 2003 May 13;60(9):1495-500.

82- Aimone JB, Wiles J, Gage FH. Potential role for adult neurogenesis in the encoding of time in new memories. Nature neuroscience. 2006 Jun;9(6):723-7.

83- Terry RD, Masliah E, Salmon DP, Butters N, DeTeresa R, Hill R, Hansen LA, Katzman R. Physical basis of cognitive alterations in Alzheimer's disease: synapse loss is the major correlate of cognitive impairment. Annals of Neurology: Official Journal of the American Neurological Association and the Child Neurology Society. 1991 Oct;30(4):572-80.

84- Tsai J, Grutzendler J, Duff K, Gan WB. Fibrillar amyloid deposition leads to local synaptic abnormalities and breakage of neuronal branches. Nature neuroscience. 2004 Nov;7(11):1181-3.

85- Scheff SW, Price DA, Schmitt FA, DeKosky ST, Mufson EJ. Synaptic alterations in CA1 in mild Alzheimer disease and mild cognitive impairment. Neurology. 2007 May 1;68(18):1501-8.

86- DeKosky ST, Scheff SW. Synapse loss in frontal cortex biopsies in Alzheimer's disease: correlation with cognitive severity. Annals of Neurology: Official Journal of the American Neurological Association and the Child Neurology Society. 1990 May;27(5):457-64.

87- Andreyev AY, Kushnareva YE, Starkov AA. Mitochondrial metabolism of reactive oxygen species. Biochemistry (Moscow). 2005 Feb 1;70(2):200-14.

88- Halliwell B. Reactive oxygen species and the central nervous system. Journal of neurochemistry. 1992 Nov;59(5):1609-23.

89- Huang, W. J., Zhang, X. I. A., & Chen, W. W. (2016). Role of oxidative stress in Alzheimer's disease. *Biomedical reports*, *4*(5), 519-522.

90- Pratico D. Oxidative stress hypothesis in Alzheimer's disease: a reappraisal. Trends in pharmacological sciences. 2008 Dec 1;29(12):609-15.

91- Nunomura A, Perry G, Pappolla MA, Wade R, Hirai K, Chiba S, Smith MA. RNA oxidation is a prominent feature of vulnerable neurons in Alzheimer's disease. Journal of Neuroscience. 1999 Mar 15;19(6):1959-64.

92- Gabbita SP, Lovell MA, Markesbery WR. Increased nuclear DNA oxidation in the brain in Alzheimer's disease. Journal of neurochemistry. 1998 Nov;71(5):2034-40.

93- Praticò D, Sung S. Lipid peroxidation and oxidative imbalance: early functional events in Alzheimer's disease. Journal of Alzheimer's Disease. 2004 Jan 1;6(2):171-5.

94- Smith KJ, Kapoor R, Felts PA. Demyelination: the role of reactive oxygen and nitrogen species. Brain pathology. 1999 Jan;9(1):69-92.

95- Marcus DL, Thomas C, Rodriguez C, Simberkoff K, Tsai JS, Strafaci JA, Freedman ML. Increased peroxidation and reduced antioxidant enzyme activity in Alzheimer's disease. Experimental neurology. 1998 Mar 1;150(1):40-4.

96- Griffin WS, Stanley LC, Ling CH, White L, MacLeod V, Perrot LJ, White C3, Araoz C. Brain interleukin 1 and S-100 immunoreactivity are elevated in Down syndrome and Alzheimer disease. Proceedings of the National Academy of Sciences. 1989 Oct 1;86(19):7611-5.

97- Rogers J, Luber-Narod J, Styren SD, Civin WH. Expression of immune system-associated antigens by cells of the human central nervous system: relationship to the pathology of Alzheimer's disease. Neurobiology of aging. 1988 Jan 1;9:339-49.

98- Wyss-Coray T, Yan F, Lin AH, Lambris JD, Alexander JJ, Quigg RJ, Masliah E. Prominent neurodegeneration and increased plaque formation in complement-inhibited Alzheimer's mice. Proceedings of the National Academy of Sciences. 2002 Aug 6;99(16):10837-42.

99- Beard CM, Waring SC, O'Brien PC, Kurland LT, Kokmen E. Nonsteroidal anti-inflammatory drug use and Alzheimer's disease: a case-control study in Rochester, Minnesota, 1980 through 1984. InMayo Clinic Proceedings 1998 Oct 1 (Vol. 73, No. 10, pp. 951-955). Elsevier.

100- Breitner JC, Gau BA, Welsh KA, Plassman BL, McDonald WM, Helms MJ, Anthony JC. Inverse association of anti-inflammatory treatments and Alzheimer's disease: initial results of a co-twin control study. Neurology. 1994 Feb 1;44(2):227-.

101- Rich JB, Rasmusson DX, Folstein MF, Carson KA, Kawas C, Brandt J. Nonsteroidal anti-inflammatory drugs in Alzheimer's disease. Neurology. 1995 Jan 1;45(1):51-5.

102- McGeer PL, McGeer EG. NSAIDs and Alzheimer disease: epidemiological, animal model and clinical studies. Neurobiology of aging. 2007 May 1;28(5):639-47.

103- Miguel-Álvarez M, Santos-Lozano A, Sanchis-Gomar F, Fiuza-Luces C, Pareja-Galeano H, Garatachea N, Lucia A. Non-steroidal anti-inflammatory drugs as a treatment for Alzheimer’s disease: a systematic review and meta-analysis of treatment effect. Drugs & aging. 2015 Feb 1;32(2):139-47.

104- McGeer PL, Rogers J. Anti-inflammatory agents as a therapeutic approach to Alzheimer's disease. Neurology. 1992 Feb 1;42(2):447-9.

105- Zotova E, Nicoll JA, Kalaria R, Holmes C, Boche D. Inflammation in Alzheimer's disease: relevance to pathogenesis and therapy. Alzheimers Res Ther. 2010 Feb;2(1):1-9.

106- Kim YS, Joh TH. Microglia, major player in the brain inflammation: their roles in the pathogenesis of Parkinson's disease. Experimental & molecular medicine. 2006 Aug;38(4):333-47.

107- Goldgaber D, Harris HW, Hla T, Maciag T, Donnelly RJ, Jacobsen JS, Vitek MP, Gajdusek DC. Interleukin 1 regulates synthesis of amyloid beta-protein precursor mRNA in human endothelial cells. Proceedings of the National Academy of Sciences. 1989 Oct 1;86(19):7606-10.

108- Plassman BL, Havlik RJ, Steffens DC, Helms MJ, Newman TN, Drosdick D, Phillips C, Gau BA, Welsh–Bohmer KA, Burke JR, Guralnik JM. Documented head injury in early adulthood and risk of Alzheimer's disease and other dementias. Neurology. 2000 Oct 24;55(8):1158-66.

109- Quintanilla RA, Orellana DI, González-Billault C, Maccioni RB. Interleukin-6 induces Alzheimer-type phosphorylation of tau protein by deregulating the cdk5/p35 pathway. Experimental cell research. 2004 Apr 15;295(1):245-57.

110- Abbott NJ, Rönnbäck L, Hansson E. Astrocyte–endothelial interactions at the blood–brain barrier. Nature reviews neuroscience. 2006 Jan;7(1):41.

111- Volterra A, Meldolesi J. Astrocytes, from brain glue to communication elements: the revolution continues. Nature Reviews Neuroscience. 2005 Aug;6(8):626-40.

112- Liu W, Tang Y, Feng J. Cross talk between activation of microglia and astrocytes in pathological conditions in the central nervous system. Life sciences. 2011 Aug 1;89(5-6):141-6.

113- Allaman I, Bélanger M, Magistretti PJ. Astrocyte–neuron metabolic relationships: for better and for worse. Trends in neurosciences. 2011 Feb 1;34(2):76-87.

114- Sofroniew MV, Vinters HV. Astrocytes: biology and pathology. Acta neuropathologica. 2010 Jan 1;119(1):7-35.

115- Akiyama H, Barger S, Barnum S, Bradt B, Bauer J, Cole GM, Cooper NR, Eikelenboom P, Emmerling M, Fiebich BL, Finch CE. Inflammation and Alzheimer's disease. Neurobiology of aging. 2000 May 1;21(3):383-421.

116- Kuchibhotla KV, Lattarulo CR, Hyman BT, Bacskai BJ. Synchronous hyperactivity and intercellular calcium waves in astrocytes in Alzheimer mice. Science. 2009 Feb 27;323(5918):1211-5.

117- Abramov AY, Canevari L, Duchen MR. Changes in intracellular calcium and glutathione in astrocytes as the primary mechanism of amyloid neurotoxicity. Journal of Neuroscience. 2003 Jun 15;23(12):5088-95.

118- Garwood CJ, Pooler AM, Atherton J, Hanger DP, Noble W. Astrocytes are important mediators of A β-induced neurotoxicity and tau phosphorylation in primary culture. Cell death & disease. 2011 Jun;2(6):e167-.

119- Fuller S, Steele M, Münch G. Activated astroglia during chronic inflammation in Alzheimer's disease—do they neglect their neurosupportive roles?. Mutation research/fundamental and molecular mechanisms of mutagenesis. 2010 Aug 7;690(1-2):40-9.

120- Hartlage-Rübsamen M, Zeitschel U, Apelt J, Gärtner U, Franke H, Stahl T, Günther A, Schliebs R, Penkowa M, Bigl V, Rossner S. Astrocytic expression of the Alzheimer's disease β-secretase (BACE1) is stimulus-dependent. Glia. 2003 Jan 15;41(2):169-79.

121- Roßner S, Apelt J, Schliebs R, Perez-Polo JR, Bigl V. Neuronal and glial β-secretase (BACE) protein expression in transgenic Tg2576 mice with amyloid plaque pathology. Journal of neuroscience research. 2001 Jun 1;64(5):437-46.

122- Chan WY, Kohsaka S, Rezaie P. The origin and cell lineage of microglia—new concepts. Brain research reviews. 2007 Feb 1;53(2):344-54.

123- Ransohoff RM, Perry VH. Microglial physiology: unique stimuli, specialized responses. Annual review of immunology. 2009 Apr 23;27:119-45.

124- Streit WJ, Sammons NW, Kuhns AJ, Sparks DL. Dystrophic microglia in the aging human brain. Glia. 2004 Jan 15;45(2):208-12.

125- De Haas AH, Boddeke HW, Biber K. Region-specific expression of immunoregulatory proteins on microglia in the healthy CNS. Glia. 2008 Jun;56(8):888-94.

126- Nimmerjahn A, Kirchhoff F, Helmchen F. Resting microglial cells are highly dynamic surveillants of brain parenchyma in vivo. Science. 2005 May 27;308(5726):1314-8.

127- Chew LJ, Takanohashi A, Bell M. Microglia and inflammation: impact on developmental brain injuries. Mental retardation and developmental disabilities research reviews. 2006;12(2):105-12.

128- Orihuela R, McPherson CA, Harry GJ. Microglial M1/M2 polarization and metabolic states. British journal of pharmacology. 2016 Feb;173(4):649-65.

129- Bolós M, Perea JR, Avila J. Alzheimer’s disease as an inflammatory disease. Biomolecular concepts. 2017 Mar 1;8(1):37-43.

130- Okello A, Edison P, Archer HA, Turkheimer FE, Kennedy J, Bullock R, Walker Z, Kennedy A, Fox N, Rossor M, Brooks DJ. Microglial activation and amyloid deposition in mild cognitive impairment: a PET study. Neurology. 2009 Jan 6;72(1):56-62.

131- Cherry JD, Olschowka JA, O'Banion MK. Neuroinflammation and M2 microglia: the good, the bad, and the inflamed. Journal of neuroinflammation. 2014 Dec 1;11(1):98.

132- Mrak RE, Griffin WS. Interleukin-1, neuroinflammation, and Alzheimer's disease. Neurobiology of aging. 2001 Nov 1;22(6):903-8.

133- Griffin WS, Mrak RE. Interleukin-1 in the genesis and progression of and risk for development of neuronal degeneration in Alzheimer's disease. Journal of leukocyte biology. 2002 Aug;72(2):233-8.

134- Sheng JG, Jones RA, Zhou XQ, McGinness JM, Van Eldik LJ, Mrak RE, Griffin WS. Interleukin-1 promotion of MAPK-p38 overexpression in experimental animals and in Alzheimer's disease: potential significance for tau protein phosphorylation. Neurochemistry international. 2001 Nov 1;39(5-6):341-8.

135- Hirano T, Yasukawa K, Harada H, Taga T, Watanabe Y, Matsuda T, Kashiwamura SI, Nakajima K, Koyama K, Iwamatsu A, Tsunasawa S. Complementary DNA for a novel human interleukin (BSF-2) that induces B lymphocytes to produce immunoglobulin. Nature. 1986 Nov;324(6092):73-6.

136- Spooren A, Kolmus K, Laureys G, Clinckers R, De Keyser J, Haegeman G, Gerlo S. Interleukin-6, a mental cytokine. Brain research reviews. 2011 Jun 24;67(1-2):157-83.

137- Tehranian R, Hasanvan H, Iverfeldt K, Post C, Schultzberg M. Early induction of interleukin-6 mRNA in the hippocampus and cortex of APPsw transgenic mice Tg2576. Neuroscience letters. 2001 Mar 23;301(1):54-8.

138- Huell M, Strauss S, Volk B, Berger M, Bauer J. Interleukin-6 is present in early stages of plaque formation and is restricted to the brains of Alzheimer's disease patients. Acta neuropathologica. 1995 Nov 1;89(6):544-51.

139- Bauer J, Strauss S, Schreiter-Gasser U, Ganter U, Schlegel P, Witt I, Berger M. Interleukin-6 and α-2-macroglobulin indicate an acute-phase state in Alzheimer's disease cortices. FEBS letters. 1991 Jul 8;285(1):111-4.

140- van Oijen M, Arp PP, de Jong FJ, Hofman A, Koudstaal PJ, Uitterlinden AG, Breteler MM. Polymorphisms in the interleukin 6 and transforming growth factor β1 gene and risk of dementia: the Rotterdam Study. Neuroscience letters. 2006 Jul 10;402(1-2):113-7.

141- He MX, Yang WL, Zhang MM, Lian YJ, Hua HY, Zeng JS, Zhang LR. Association between interleukin-6 gene promoter− 572C/G polymorphism and the risk of sporadic Alzheimer's disease. Neurological sciences. 2010 Apr 1;31(2):165-8.

142- Wang M, Jia J. The interleukin-6 gene− 572C/G promoter polymorphism modifies Alzheimer's risk in ApoE ε4 carriers. Neuroscience letters. 2010 Oct 4;482(3):260-3.

143- Del Bo R, Angeretti N, Lucca E, De Simoni MG, Forloni G. Reciprocal control of inflammatory cytokines, IL-1 and IL-6, and β-amyloid production in cultures. Neuroscience letters. 1995 Mar 16;188(1):70-4.

144- Brugg B, Dubreuil YL, Huber G, Wollman EE, Delhaye-Bouchaud N, Mariani J. Inflammatory processes induce beta-amyloid precursor protein changes in mouse brain. Proceedings of the National Academy of Sciences. 1995 Mar 28;92(7):3032-5.

145- Quintanilla RA, Orellana DI, González-Billault C, Maccioni RB. Interleukin-6 induces Alzheimer-type phosphorylation of tau protein by deregulating the cdk5/p35 pathway. Experimental cell research. 2004 Apr 15;295(1):245-57.

146- Kaltschmidt B, Uherek M, Volk B, Baeuerle PA, Kaltschmidt C. Transcription factor NF-κB is activated in primary neurons by amyloid β peptides and in neurons surrounding early plaques from patients with Alzheimer disease. Proceedings of the National Academy of Sciences. 1997 Mar 18;94(6):2642-7.

147- Terai K, Matsuo A, McGeer PL. Enhancement of immunoreactivity for NF-κB in the hippocampal formation and cerebral cortex of Alzheimer's disease. Brain research. 1996 Sep 30;735(1):159-68.

148- Samuelsson M, Fisher L, Iverfeldt K. β-Amyloid and interleukin-1β induce persistent NF-κB activation in rat primary glial cells. International journal of molecular medicine. 2005 Sep 1;16(3):449-53.

149- Bonaiuto C, McDonald PP, Rossi F, Cassatella MA. Activation of nuclear factor-κB by β-amyloid peptides and interferon-γ in murine microglia. Journal of neuroimmunology. 1997 Jul 1;77(1):51-6.

150- Sen R, Baltimore D. Inducibility of κ immunoglobulin enhancer-binding protein NF-κB by a posttranslational mechanism. Cell. 1986 Dec 26;47(6):921-8.

151- Kopitar-Jerala N. Innate immune response in brain, NF-kappa B signaling and cystatins. Frontiers in molecular neuroscience. 2015 Dec 9;8:73.

152- Samuelsson M, Fisher L, Iverfeldt K. β-Amyloid and interleukin-1β induce persistent NF-κB activation in rat primary glial cells. International journal of molecular medicine. 2005 Sep 1;16(3):449-53.

153- Paudel YN, Angelopoulou E, Piperi C, Othman I, Aamir K, Shaikh M. Impact of HMGB1, RAGE, and TLR4 in Alzheimer's Disease (AD): From Risk Factors to Therapeutic Targeting. Cells. 2020 Feb;9(2):383.

154- Harris HE, Andersson U, Pisetsky DS. HMGB1: a multifunctional alarmin driving autoimmune and inflammatory disease. Nature Reviews Rheumatology. 2012 Apr;8(4):195.

155- Magna M, Pisetsky DS. The role of HMGB1 in the pathogenesis of inflammatory and autoimmune diseases. Molecular medicine. 2014 Jan 1;20(1):138-46.

156- Balosso S, Liu J, Bianchi ME, Vezzani A. Disulfide-containing high mobility group box-1 promotes N-methyl-D-aspartate receptor function and excitotoxicity by activating Toll-like receptor 4-dependent signaling in hippocampal neurons. Antioxidants & redox signaling. 2014 Oct 20;21(12):1726-40.

157- Nan K, Han Y, Fang Q, Huang C, Yu L, Ge W, Xiang F, Tao YX, Cao H, Li J. HMGB1 gene silencing inhibits neuroinflammation via down-regulation of NF-κB signaling in primary hippocampal neurons induced by Aβ25–35. International Immunopharmacology. 2019 Feb 1;67:294-301.

158- Falcão AS, Carvalho LA, Lidónio G, Vaz AR, Lucas SD, Moreira R, Brites D. Dipeptidyl vinyl sulfone as a novel chemical tool to inhibit HMGB1/NLRP3-inflammasome and inflamma-miRs in Aβ-mediated microglial inflammation. ACS chemical neuroscience. 2017 Jan 18;8(1):89-99.

159- Fujita K, Motoki K, Tagawa K, Chen X, Hama H, Nakajima K, Homma H, Tamura T, Watanabe H, Katsuno M, Matsumi C. HMGB1, a pathogenic molecule that induces

neurite degeneration via TLR4-MARCKS, is a potential therapeutic target for Alzheimer’s disease. Scientific reports. 2016 Aug 25;6(1):1-5.

160- Jang A, Liew H, Kim YM, Choi H, Kim S, Hyung Lee S, Ohshima T, Mikoshiba K, Suh YH. p35 deficiency accelerates HMGB-1-mediated neuronal death in the early stages of an Alzheimer's disease mouse model. Current Alzheimer Research. 2013 Oct 1;10(8):829-43.

161- Meneghini V, Bortolotto V, Francese MT, Dellarole A, Carraro L, Terzieva S, Grilli M. High-mobility group box-1 protein and β-amyloid oligomers promote neuronal differentiation of adult hippocampal neural progenitors via receptor for advanced glycation end products/nuclear factor-κB axis: relevance for Alzheimer's disease. Journal of Neuroscience. 2013 Apr 3;33(14):6047-59.

162- Pirzada RH, Javaid N, Choi S. The Roles of the NLRP3 Inflammasome in Neurodegenerative and Metabolic Diseases and in Relevant Advanced Therapeutic Interventions. Genes. 2020 Feb;11(2):131.

163- Franchi L, Eigenbrod T, Muñoz-Planillo R, Ozkurede U, Kim YG, Chakrabarti A, Gale M, Silverman RH, Colonna M, Akira S, Núñez G. Cytosolic double-stranded RNA activates the NLRP3 inflammasome via MAVS-induced membrane permeabilization and K+ efflux. The Journal of Immunology. 2014 Oct 15;193(8):4214-22.

164- Vandanmagsar B, Youm YH, Ravussin A, Galgani JE, Stadler K, Mynatt RL, Ravussin E, Stephens JM, Dixit VD. The NLRP3 inflammasome instigates obesity-induced inflammation and insulin resistance. Nature medicine. 2011 Feb;17(2):179.

165- Freeman LC, Ting JP. The pathogenic role of the inflammasome in neurodegenerative diseases. Journal of neurochemistry. 2016 Jan;136:29-38.

166- Halle A, Hornung V, Petzold GC, Stewart CR, Monks BG, Reinheckel T, Fitzgerald KA, Latz E, Moore KJ, Golenbock DT. The NALP3 inflammasome is involved in the innate immune response to amyloid-β. Nature immunology. 2008 Aug;9(8):857.

167- Nakanishi A, Kaneko N, Takeda H, Sawasaki T, Morikawa S, Zhou W, Kurata M, Yamamoto T, Akbar SM, Zako T, Masumoto J. Amyloid β directly interacts with NLRP3 to initiate inflammasome activation: identification of an intrinsic NLRP3 ligand in a cell-free system. Inflammation and regeneration. 2018 Dec 1;38(1):27.

168- Heneka MT, Kummer MP, Stutz A, Delekate A, Schwartz S, Vieira-Saecker A, Griep A, Axt D, Remus A, Tzeng TC, Gelpi E. NLRP3 is activated in Alzheimer's disease and contributes to pathology in APP/PS1 mice. Nature. 2013 Jan;493(7434):674-8.

169- Yin J, Zhao F, Chojnacki JE, Fulp J, Klein WL, Zhang S, Zhu X. NLRP3 inflammasome inhibitor ameliorates amyloid pathology in a mouse model of Alzheimer's disease. Molecular neurobiology. 2018 Mar 1;55(3):1977-87.

170- Lue LF, Rydel R, Brigham EF, Yang LB, Hampel H, Murphy Jr GM, Brachova L, Yan SD, Walker DG, Shen Y, Rogers J. Inflammatory repertoire of Alzheimer's disease and nondemented elderly microglia in vitro. Glia. 2001 Jul;35(1):72-9.

171- Apelt J, Schliebs R. β-amyloid-induced glial expression of both pro-and anti-inflammatory cytokines in cerebral cortex of aged transgenic Tg2576 mice with Alzheimer plaque pathology. Brain research. 2001 Mar 9;894(1):21-30.

172- van der Flier, W. M., & Scheltens, P. (2005). Epidemiology and risk factors of dementia. *Journal of Neurology, Neurosurgery & Psychiatry*, *76*(suppl 5), v2-v7.

173- Kukull WA, Higdon R, Bowen JD, McCormick WC, Teri L, Schellenberg GD, van Belle G, Jolley L, Larson EB. Dementia and Alzheimer disease incidence: a prospective cohort study. Archives of neurology. 2002 Nov 1;59(11):1737-46.

174- Launer LJ, Andersen K, Dewey M, Letenneur L, Ott A, Amaducci LA, Brayne C, Copeland JR, Dartigues JF, Kragh-Sorensen P, Lobo A. Rates and risk factors for dementia and Alzheimer's disease: results from EURODEM pooled analyses. Neurology. 1999 Jan 1;52(1):78-.

175- Ganguli M, Dodge HH, Chen P, Belle S, DeKosky ST. Ten-year incidence of dementia in a rural elderly US community population: the MoVIES Project. Neurology. 2000 Mar 14;54(5):1109-16.

176- Kawas C, Gray S, Brookmeyer R, Fozard J, Zonderman A. Age-specific incidence rates of Alzheimer's disease: the Baltimore Longitudinal Study of Aging. Neurology. 2000 Jun 13;54(11):2072-7.

177- López-Pousa S, Vilalta-Franch J, Llinàs-Regla J, Garre-Olmo J, Román GC. Incidence of dementia in a rural community in Spain: the Girona cohort study. Neuroepidemiology. 2004;23(4):170-7.

178- Hebert LE, Scherr PA, Beckett LA, Albert MS, Pilgrim DM, Chown MJ, Funkenstein HH, Evans DA. Age-specific incidence of Alzheimer's disease in a community population. Jama. 1995 May 3;273(17):1354-9.

179- Corrada MM, Brookmeyer R, Paganini-Hill A, Berlau D, Kawas CH. Dementia incidence continues to increase with age in the oldest old: the 90+ study. Annals of neurology. 2010 Jan;67(1):114-21.

180- Wilson RS, De Leon CF, Barnes LL, Schneider JA, Bienias JL, Evans DA, Bennett DA. Participation in cognitively stimulating activities and risk of incident Alzheimer disease. Jama. 2002 Feb 13;287(6):742-8.

181- Breteler MM, van Amerongen NM, van Swieten JC, Claus JJ, Grobbee DE, Van Gijn J, Hofman A, van Harskamp F. Cognitive correlates of ventricular enlargement and cerebral white matter lesions on magnetic resonance imaging. The Rotterdam Study. Stroke. 1994 Jun;25(6):1109-15.

182- Wallin A, Roman GC, Esiri M, Kettunen P, Svensson J, Paraskevas GP, Kapaki E. Update on vascular cognitive impairment associated with subcortical small-vessel disease. Journal of Alzheimer's Disease. 2018 Jan 1;62(3):1417-41.

183- Cheung ZH, Gong K, Ip NY. Cyclin-dependent kinase 5 supports neuronal survival through phosphorylation of Bcl-2. Journal of Neuroscience. 2008 May 7;28(19):4872-7.

184- Wen Y, Yang SH, Liu R, Perez EJ, Brun-Zinkernagel AM, Koulen P, Simpkins JW. Cdk5 is involved in NFT-like tauopathy induced by transient cerebral ischemia in female rats. Biochimica et Biophysica Acta (BBA)-Molecular Basis of Disease. 2007 Apr 1;1772(4):473-83.

185- Kalaria RN. Vascular basis for brain degeneration: faltering controls and risk factors for dementia. Nutrition reviews. 2010 Dec 1;68(suppl_2):S74-87.

186- Deane R, Wu Z, Sagare A, Davis J, Du Yan S, Hamm K, Xu F, Parisi M, LaRue B, Hu HW, Spijkers P. LRP/amyloid β-peptide interaction mediates differential brain efflux of Aβ isoforms. Neuron. 2004 Aug 5;43(3):333-44.

187- Luchsinger JA, Tang MX, Stern Y, Shea S, Mayeux R. Diabetes mellitus and risk of Alzheimer's disease and dementia with stroke in a multiethnic cohort. American journal of epidemiology. 2001 Oct 1;154(7):635-41.

188- Arvanitakis Z, Schneider JA, Wilson RS, Li Y, Arnold SE, Wang Z, Bennett DA. Diabetes is related to cerebral infarction but not to AD pathology in older persons. Neurology. 2006 Dec 12;67(11):1960-5.

189- Sacco RL, Benjamin EJ, MANOLIO T, WHISNANT J, WOLF P. Risk factors: Prevention and Rehabilitation of Stroke. Stroke (1970). 1997;28(7):1507-17.

190- Lovestone S, Smith U. Advanced glycation end products, dementia, and diabetes. Proceedings of the National Academy of Sciences. 2014 Apr 1;111(13):4743-4.

191- Farris W, Mansourian S, Chang Y, Lindsley L, Eckman EA, Frosch MP, Eckman CB, Tanzi RE, Selkoe DJ, Guénette S. Insulin-degrading enzyme regulates the levels of insulin, amyloid β-protein, and the β-amyloid precursor protein intracellular domain in vivo. Proceedings of the National Academy of Sciences. 2003 Apr 1;100(7):4162-7.

192- Park CR. Cognitive effects of insulin in the central nervous system. Neuroscience & Biobehavioral Reviews. 2001 Jun 1;25(4):311-23.

193- Femminella GD, Bencivenga L, Petraglia L, Visaggi L, Gioia L, Grieco FV, De Lucia C, Komici K, Corbi G, Edison P, Rengo G. Antidiabetic drugs in Alzheimer’s disease: Mechanisms of action and future perspectives. Journal of diabetes research. 2017 Oct;2017.

194- Coronado VG, McGuire LC, Sarmiento K, Bell J, Lionbarger MR, Jones CD, Geller AI, Khoury N, Xu L. Trends in traumatic brain injury in the US and the public health response: 1995–2009. Journal of safety research. 2012 Sep 1;43(4):299-307.

195- Fazel S, Wolf A, Pillas D, Lichtenstein P, Långström N. Suicide, fatal injuries, and other causes of premature mortality in patients with traumatic brain injury: a 41-year Swedish population study. JAMA psychiatry. 2014 Mar 1;71(3):326-33.

196- Mayeux R, Ottman R, Maestre G, Ngai C, Tang MX, Ginsberg H, Chun M, Tycko B, Shelanski M. Synergistic effects of traumatic head injury and apolipoprotein-epsilon4 in patients with Alzheimer's disease. Neurology. 1995 Mar 1;45(3):555-7.

197- Rasmusson DX, Brandt J, Martin DB, Folstein MF. Head injury as a risk factor in Alzheimer's disease. Brain Injury. 1995 Jan 1;9(3):213-9.

198- Schofield PW, Tang M, Marder K, Bell K, Dooneief G, Chun M, Sano M, Stern Y, Mayeux R. Alzheimer's disease after remote head injury: an incidence study. Journal of Neurology, Neurosurgery & Psychiatry. 1997 Feb 1;62(2):119-24.

199- Fleminger S, Oliver DL, Lovestone S, Rabe-Hesketh S, Giora A. Head injury as a risk factor for Alzheimer’s disease: the evidence 10 years on; a partial replication. Journal of Neurology, Neurosurgery & Psychiatry. 2003 Jul 1;74(7):857-62.

200- Mortimer JA, Van Duijn CM, Chandra V, Fratiglioni L, Graves AB, Heyman A, Jorm AF, Kokmen E, Kondo K, Rocca WA, Shalat SL. Head trauma as a risk factor for Alzheimer's disease: a collaborative re-analysis of case-control studies. International journal of epidemiology. 1991 Jan 1;20(Supplement_2):S28-35.

201- Franz G, Beer R, Kampfl A, Engelhardt K, Schmutzhard E, Ulmer H, Deisenhammer F. Amyloid beta 1-42 and tau in cerebrospinal fluid after severe traumatic brain injury. Neurology. 2003 May 13;60(9):1457-61.

202- Lithell, H., Hansson, L., Skoog, I., Elmfeldt, D., Hofman, A., Olofsson, B., ... & SCOPE Study Group. (2003). The Study on Cognition and Prognosis in the Elderly (SCOPE):

principal results of a randomized double-blind intervention trial. *Journal of hypertension*, *21*(5), 875-886.

203- Launer LJ, Feskens EJ, Kalmijn S, Kromhout D. Smoking, drinking, and thinking: the zutphen elderly study: the zutphen elderly study. American Journal of Epidemiology. 1996 Feb 1;143(3):219-27.

204- Merchant, C., Tang, M. X., Albert, S., Manly, J., Stern, Y., & Mayeux, R. (1999). The influence of smoking on the risk of Alzheimer's disease. *Neurology*, *52*(7), 1408-1408.

205- Ott A, Slooter AJ, Hofman A, van Harskamp F, Witteman JC, Van Broeckhoven C, Van Duijn CM, Breteler MM. Smoking and risk of dementia and Alzheimer's disease in a population-based cohort study: the Rotterdam Study. The Lancet. 1998 Jun 20;351(9119):1840-3.

206- Abner EL, Nelson PT, Jicha GA, Cooper GE, Fardo DW, Schmitt FA, Kryscio RJ. Tobacco smoking and dementia in a Kentucky cohort: a competing risk analysis. Journal of Alzheimer's Disease. 2019 Jan 1;68(2):625-33.

207- Ferini-Strambi L, Smirne S, Garancini P, Pinto P, Franceschi M. Clinical and epidemiological aspects of Alzheimer's disease with presenile onset: a case control study. Neuroepidemiology. 1990;9(1):39-49.

208- Tyas SL, Pederson LL. Psychosocial factors related to adolescent smoking: a critical review of the literature. Tobacco control. 1998 Dec 1;7(4):409-20.

209- Valavanidis A, Vlachogianni T, Fiotakis K. Tobacco smoke: involvement of reactive oxygen species and stable free radicals in mechanisms of oxidative damage, carcinogenesis and synergistic effects with other respirable particles. International journal of environmental research and public health. 2009 Feb;6(2):445-62.

210- Colonna M, Wang Y. TREM2 variants: new keys to decipher Alzheimer disease pathogenesis. Nature Reviews Neuroscience. 2016 Apr;17(4):201.

211- Paloneva J, Manninen T, Christman G, Hovanes K, Mandelin J, Adolfsson R, Bianchin M, Bird T, Miranda R, Salmaggi A, Tranebjærg L. Mutations in two genes encoding different subunits of a receptor signaling complex result in an identical disease phenotype. The American Journal of Human Genetics. 2002 Sep 1;71(3):656-62.

212- Guerreiro R, Wojtas A, Bras J, Carrasquillo M, Rogaeva E, Majounie E, Cruchaga C, Sassi C, Kauwe JS, Younkin S, Hazrati L. TREM2 variants in Alzheimer's disease. New England Journal of Medicine. 2013 Jan 10;368(2):117-27.

213- Bayer TA, Cappai R, Masters CL, Beyreuther K, Multhaup G. It all sticks together—the APP-related family of proteins and Alzheimer's disease. Molecular psychiatry. 1999 Nov;4(6):524-8.

214- Hartley D, Blumenthal T, Carrillo M, DiPaolo G, Esralew L, Gardiner K, Granholm AC, Iqbal K, Krams M, Lemere C, Lott I. Down syndrome and Alzheimer's disease: Common pathways, common goals. Alzheimer's & Dementia. 2015 Jun 1;11(6):700-9.

215- Van Giau V, Bagyinszky E, An SS, Kim SY. Role of apolipoprotein E in neurodegenerative diseases. Neuropsychiatric disease and treatment. 2015;11:1723.

216- Corder EH, Saunders AM, Strittmatter WJ, Schmechel DE, Gaskell PC, Small G, Roses AD, Haines JL, Pericak-Vance MA. Gene dose of apolipoprotein E type 4 allele and the risk of Alzheimer's disease in late onset families. Science. 1993 Aug 13;261(5123):921-3.

217- Deary IJ, Whiteman MC, Pattie A, Starr JM, Hayward C, Wright AF, Visscher PM, Tynan MC, Whalley LJ. Apolipoprotein e gene variability and cognitive functions at age

79: a follow-up of the Scottish mental survey of 1932. Psychology and aging. 2004 Jun;19(2):367.

218- Guo Z, Cupples LA, Kurz A, Auerbach SH, Volicer L, Chui H, Green RC, Sadovnick AD, Duara R, DeCarli C, Johnson K. Head injury and the risk of AD in the MIRAGE study. Neurology. 2000 Mar 28;54(6):1316-23.

219- O'Brien RJ, Wong PC. Amyloid precursor protein processing and Alzheimer's disease. Annual review of neuroscience. 2011 Jul 21;34:185-204.

220- Tanaka S, Nakamura S, Ueda K, Kameyama M, Shiojiri S, Takahashi Y, Kitaguchi N, Ito H. Three types of amyloid protein precursor mRNA in human brain: their differential expression in Alzheimer's disease. Biochemical and biophysical research communications. 1988 Dec 15;157(2):472-9.

221- Solà C, García-Ladona FJ, Sarasa M, Mengod G, Probst A, Palacios G, Palacios JM. βAPP gene expression is increased in the rat brain after motor neuron axotomy. European Journal of Neuroscience. 1993 Jul;5(7):795-808.

222- Tomita S, Kirino Y, Suzuki T. Cleavage of Alzheimer's amyloid precursor protein (APP) by secretases occurs after O-glycosylation of APP in the protein secretory pathway Identification of intracellular compartments in which APP cleavage occurs without using toxic agents that interfere with protein metabolism. Journal of Biological Chemistry. 1998 Mar 13;273(11):6277-84.

223- Moya KL, Benowitz LI, Schneider GE, Allinquant B. The amyloid precursor protein is developmentally regulated and correlated with synaptogenesis. Developmental biology. 1994 Feb 1;161(2):597-603.

224- Nalivaeva NN, Turner AJ. The amyloid precursor protein: a biochemical enigma in brain development, function and disease. FEBS letters. 2013 Jun 27;587(13):2046-54.

225- Pardossi-Piquard R, Checler F. The physiology of the β-amyloid precursor protein intracellular domain AICD. Journal of neurochemistry. 2012 Jan;120:109-24.

226- Lu DC, Rabizadeh S, Chandra S, Shayya RF, Ellerby LM, Ye X, Salvesen GS, Koo EH, Bredesen DE. A second cytotoxic proteolytic peptide derived from amyloid β-protein precursor. Nature medicine. 2000 Apr;6(4):397-404.

227- De Strooper B, Vassar R, Golde T. The secretases: enzymes with therapeutic potential in Alzheimer disease. Nature Reviews Neurology. 2010 Feb;6(2):99-107.

228- Sasmita AO. Current viral-mediated gene transfer research for treatment of Alzheimer's disease. Biotechnology and Genetic Engineering Reviews. 2019 Jan 2;35(1):26-45.

229- Zlokovic BV. The blood-brain barrier in health and chronic neurodegenerative disorders. Neuron. 2008 Jan 24;57(2):178-201.

230- Provias J, Jeynes B. Reduction in vascular endothelial growth factor expression in the superior temporal, hippocampal, and brainstem regions in Alzheimer's disease. Current neurovascular research. 2014 Aug 1;11(3):202-9.

231- M Larsen J, R Martin D, E Byrne M. Recent advances in delivery through the blood-brain barrier. Current topics in medicinal chemistry. 2014 May 1;14(9):1148-60.

232- Abbott NJ. Prediction of blood–brain barrier permeation in drug discovery from in vivo, in vitro and in silico models. Drug Discovery Today: Technologies. 2004 Dec 1;1(4):407-16.

233- Pascale CL, Miller MC, Chiu C, Boylan M, Caralopoulos IN, Gonzalez L, Johanson CE, Silverberg GD. Amyloid-beta transporter expression at the blood-CSF barrier is age-dependent. Fluids and Barriers of the CNS. 2011 Dec 1;8(1):21.

234- Ito S, Ohtsuki S, Murata S, Katsukura Y, Suzuki H, Funaki M, Tachikawa M, Terasaki T. Involvement of insulin-degrading enzyme in insulin-and atrial natriuretic peptide-sensitive internalization of amyloid-β peptide in mouse brain capillary endothelial cells. Journal of Alzheimer's Disease. 2014 Jan 1;38(1):185-200.

235- Cheng CL, Tang Y, Zheng Z, Liu X, Zengchun CY, Wang C, Lou TQ. Advanced glycation end-products activate the renin-angiotensin system through the RAGE/PI3-K signaling pathway in podocytes. Clinical and Investigative Medicine. 2012 Oct 6:E282-93.

236- Zlokovic BV. Neurodegeneration and the neurovascular unit. Nature medicine. 2010 Dec;16(12):1370-1.

237- Zlokovic BV. Neurovascular pathways to neurodegeneration in Alzheimer's disease and other disorders. Nature Reviews Neuroscience. 2011 Dec;12(12):723-38.

238- Hasler CM. Functional foods: benefits, concerns and challenges—a position paper from the American Council on Science and Health. The Journal of nutrition. 2002 Dec 1;132(12):3772-81.

239- Teodoro AJ. Bioactive compounds of food: their role in the prevention and treatment of diseases.

240- Santangelo C, Filesi C, Varì R, Scazzocchio B, Filardi T, Fogliano V, D'Archivio M, Giovannini C, Lenzi A, Morano S, Masella R. Consumption of extra-virgin olive oil rich in phenolic compounds improves metabolic control in patients with type 2 diabetes

mellitus: a possible involvement of reduced levels of circulating visfatin. Journal of Endocrinological Investigation. 2016 Nov 1;39(11):1295-301.

241- Ruano J, Lopez-Miranda J, Fuentes F, Moreno JA, Bellido C, Perez-Martinez P, Lozano A, Gómez P, Jiménez Y, Jiménez FP. Phenolic content of virgin olive oil improves ischemic reactive hyperemia in hypercholesterolemic patients. Journal of the American College of Cardiology. 2005 Nov 15;46(10):1864-8.

242- Covas MI, Nyyssönen K, Poulsen HE, Kaikkonen J, Zunft HJ, Kiesewetter H, Gaddi A, de la Torre R, Mursu J, Bäumler H, Nascetti S. The effect of polyphenols in olive oil on heart disease risk factors: a randomized trial. Annals of internal medicine. 2006 Sep 5;145(5):333-41.

243- Benavente-Garcıa, O., Castillo, J., Lorente, J., Ortuño, A. D. R. J., & Del Rio, J. A. (2000). Antioxidant activity of phenolics extracted from Olea europaea L. leaves. *Food chemistry*, *68*(4), 457-462.

244- Visioli F, Galli C. Biological properties of olive oil phytochemicals. Critical reviews in food science and nutrition. 2002 May 1;42(3):209-21.

245- Waterman E, Lockwood B. Active components and clinical applications of olive oil. Alternative medicine review. 2007 Dec 1;12(4).

246- Obied HK, Prenzler PD, Omar SH, Ismael R, Servili M, Esposto S, Taticchi A, Selvaggini R, Urbani S. Pharmacology of olive biophenols. InAdvances in molecular toxicology 2012 Jan 1 (Vol. 6, pp. 195-242). Elsevier.

247- http://www.oliveaustralia.com.au/About_Olive_Trees/about_olive_trees.html

248- IOOC Home Page (International Olive Oil Council Activities: World Olive Oil Figures: World Olive Oil Consumption) [accessed on 25 November 2011]. Available online: www.internationaloliveoil.org.

249- Olives and Olive Oils in Health and Disease Prevention (2010) book

250- Obied HK. Biography of biophenols: past, present and future. Functional Foods in Health and Disease. 2013 Jun 24;3(6):230-41.

251- Uccella N. Olive biophenols: novel ethnic and technological approach. Trends in Food Science & Technology. 2000 Sep 10;11(9-10):328-39.

252- Saija A, Uccella N. Olive biophenols: functional effects on human wellbeing. Trends in Food Science & Technology. 2000 Sep 10;11(9-10):357-63.

253- Le Tutour B, Guedon D. Antioxidative activities of Olea europaea leaves and related phenolic compounds. Phytochemistry. 1992 Apr 1;31(4):1173-8.

254- Bouaziz M, Sayadi S. Isolation and evaluation of antioxidants from leaves of a Tunisian cultivar olive tree. European Journal of Lipid Science and Technology. 2005 Aug;107(7-8):497-504.

255- Ranalli A, Contento S, Lucera L, Di Febo M, Marchegiani D, Di Fonzo V. Factors affecting the contents of iridoid oleuropein in olive leaves (Olea europaea L.). Journal of agricultural and food chemistry. 2006 Jan 25;54(2):434-40.

256- Hassen I, Casabianca H, Hosni K. Biological activities of the natural antioxidant oleuropein: Exceeding the expectation–A mini-review. Journal of Functional Foods. 2015 Oct 1;18:926-40.

257- El SN, Karakaya S. Olive tree (Olea europaea) leaves: potential beneficial effects on human health. Nutrition reviews. 2009 Nov 1;67(11):632-8.

258- Ansari M, Kazemipour M, Fathi S. Development of a simple green extraction procedure and HPLC method for determination of oleuropein in olive leaf extract applied to a multi-source comparative study. Journal of the Iranian Chemical Society. 2011 Mar 1;8(1):38-47.

259- Paiva-Martins F, Pinto M. Isolation and characterization of a new hydroxytyrosol derivative from olive (Olea europaea) leaves. Journal of agricultural and food chemistry. 2008 Jul 23;56(14):5582-8.

260- Mohagheghi F, Bigdeli MR, Rasoulian B, Hashemi P, Pour MR. The neuroprotective effect of olive leaf extract is related to improved blood–brain barrier permeability and brain edema in rat with experimental focal cerebral ischemia. Phytomedicine. 2011 Jan 15;18(2-3):170-5.

261- Bazoti FN, Bergquist J, Markides KE, Tsarbopoulos A. Noncovalent interaction between amyloid-β-peptide (1–40) and oleuropein studied by electrospray ionization mass spectrometry. Journal of the American Society for Mass Spectrometry. 2006 Apr 1;17(4):568-75.

262- Schaffer S, Podstawa M, Visioli F, Bogani P, Müller WE, Eckert GP. Hydroxytyrosol-rich olive mill wastewater extract protects brain cells in vitro and ex vivo. Journal of agricultural and food chemistry. 2007 Jun 27;55(13):5043-9.

263- Romani A, Ieri F, Urciuoli S, Noce A, Marrone G, Nediani C, Bernini R. Health effects of phenolic compounds found in extra-virgin olive oil, by-products, and leaf of Olea europaea L. Nutrients. 2019 Aug;11(8):1776.

264- Hansen M, Verity A. Olive Leaf Extract Potent Antibacterial, Antiviral and Antifungal Agent.

265- Singh I, Mok M, Christensen AM, Turner AH, Hawley JA. The effects of polyphenols in olive leaves on platelet function. Nutrition, metabolism and cardiovascular diseases. 2008 Feb 1;18(2):127-32.

266- Visioli F, Bellomo G, Montedoro G, Galli C. Low density lipoprotein oxidation is inhibited in vitro by olive oil constituents. Atherosclerosis. 1995 Sep 1;117(1):25-32.

267- Wongcharoen W, Phrommintikul A. The protective role of curcumin in cardiovascular diseases. International journal of cardiology. 2009 Apr 3;133(2):145-51.

268- Diaz MN, Frei B, Vita JA, Keaney Jr JF. Antioxidants and atherosclerotic heart disease. New England Journal of Medicine. 1997 Aug 7;337(6):408-16.

269- Bruneton J. Pharmacognosy, phytochemistry, medicinal plants. Lavoisier publishing; 1995.

270- Manna C, Migliardi V, Golino P, Scognamiglio A, Galletti P, Chiariello M, Zappia V. Oleuropein prevents oxidative myocardial injury induced by ischemia and reperfusion. The journal of nutritional biochemistry. 2004 Aug 1;15(8):461-6.

271- Federico A, Morgillo F, Tuccillo C, Ciardiello F, Loguercio C. Chronic inflammation and oxidative stress in human carcinogenesis. International journal of cancer. 2007 Dec 1;121(11):2381-6.

272- Jemai H, Bouaziz M, Fki I, El Feki A, Sayadi S. Hypolipidimic and antioxidant activities of oleuropein and its hydrolysis derivative-rich extracts from Chemlali olive leaves. Chemico-Biological Interactions. 2008 Nov 25;176(2-3):88-98.

273- Rahman I, Biswas SK, Kirkham PA. Regulation of inflammation and redox signaling by dietary polyphenols. Biochemical pharmacology. 2006 Nov 30;72(11):1439-52.

274- Poudyal H, Campbell F, Brown L. Olive leaf extract attenuates cardiac, hepatic, and metabolic changes in high carbohydrate–, high fat–fed rats. The journal of nutrition. 2010 May 1;140(5):946-53.

275- Heneka MT, Carson MJ, El Khoury J, Landreth GE, Brosseron F, Feinstein DL, Jacobs AH, Wyss-Coray T, Vitorica J, Ransohoff RM, Herrup K. Neuroinflammation in Alzheimer's disease. The Lancet Neurology. 2015 Apr 1;14(4):388-405.

276- Minter MR, Taylor JM, Crack PJ. The contribution of neuroinflammation to amyloid toxicity in Alzheimer's disease. Journal of neurochemistry. 2016 Feb;136(3):457-74.

277- Atluri VS, Tiwari S, Rodriguez M, Kaushik A, Yndart A, Kolishetti N, Yatham M, Nair M. Inhibition of Amyloid-Beta Production, Associated Neuroinflammation, and Histone Deacetylase 2-Mediated Epigenetic Modifications Prevent Neuropathology in Alzheimer's Disease in vitro Model. Frontiers in Aging Neuroscience. 2019;11.

278- World Alzheimer Report. (2018). The state of art of dementia research: new frontiers. *Alzheimer's disease international*.

279- Prince M, Bryce R, Albanese E, Wimo A, Ribeiro W, Ferri CP. The global prevalence of dementia: a systematic review and metaanalysis. Alzheimer's & dementia. 2013 Jan 1;9(1):63-75.

280- Selkoe DJ. Alzheimer's disease: genes, proteins, and therapy. Physiological reviews. 2001 Apr 1.

281- Selkoe DJ, Schenk D. Alzheimer's disease: molecular understanding predicts amyloid-based therapeutics. Annual review of pharmacology and toxicology. 2003 Apr;43(1):545-84.

282- Lane, C., Hardy, J., & Schott, J. (2018). Alzheimer's disease. European Journal of Neurology, 25(1), 59-70.

283- Brown RC, Davis TP. Calcium modulation of adherens and tight junction function: a potential mechanism for blood-brain barrier disruption after stroke. Stroke. 2002 Jun 1;33(6):1706-11.

284- Bell RD, Zlokovic BV. Neurovascular mechanisms and blood–brain barrier disorder in Alzheimer's disease. Acta neuropathologica. 2009 Jul 1;118(1):103-13.

285- Chen GF, Xu TH, Yan Y, Zhou YR, Jiang Y, Melcher K, Xu HE. Amyloid beta: structure, biology and structure-based therapeutic development. Acta Pharmacologica Sinica. 2017 Sep;38(9):1205-35.

286- Hensley K. Neuroinflammation in Alzheimer's disease: mechanisms, pathologic consequences, and potential for therapeutic manipulation. Journal of Alzheimer's disease. 2010 Jan 1;21(1):1-4.

287- Ohtsuki S, Terasaki T. Contribution of carrier-mediated transport systems to the blood–brain barrier as a supporting and protecting interface for the brain; importance for CNS drug discovery and development. Pharmaceutical research. 2007 Sep 1;24(9):1745-58.

288- van Assema DM, Lubberink M, Bauer M, van der Flier WM, Schuit RC, Windhorst AD, Comans EF, Hoetjes NJ, Tolboom N, Langer O, Müller M. Blood–brain barrier P-glycoprotein function in Alzheimer's disease. Brain. 2012 Jan 1;135(1):181-9.

289- Li Q, Chen L, Liu X, Li X, Cao Y, Bai Y, Qi F. Pterostilbene inhibits amyloid-β-induced neuroinflammation in a microglia cell line by inactivating the NLRP3/caspase-1 inflammasome pathway. Journal of Cellular Biochemistry. 2018 Aug;119(8):7053-62.

290- Tan MS, Yu JT, Jiang T, Zhu XC, Tan L. The NLRP3 inflammasome in Alzheimer's disease. Molecular neurobiology. 2013 Dec 1;48(3):875-82.

291- McGeough MD, Pena CA, Mueller JL, Pociask DA, Broderick L, Hoffman HM, Brydges SD. Cutting edge: IL-6 is a marker of inflammation with no direct role in inflammasome-mediated mouse models. The Journal of Immunology. 2012 Sep 15;189(6):2707-11.

292- Place DE, Kanneganti TD. Recent advances in inflammasome biology. Current opinion in immunology. 2018 Feb 1;50:32-8.

293- Sutterwala FS, Haasken S, Cassel SL. Mechanism of NLRP3 inflammasome activation. Annals of the New York Academy of Sciences. 2014 Jun;1319(1):82.

294- Granic I, Dolga AM, Nijholt IM, van Dijk G, Eisel UL. Inflammation and NF-κB in Alzheimer's disease and diabetes. Journal of Alzheimer's Disease. 2009 Jan 1;16(4):809-21.

295- Bauernfeind FG, Horvath G, Stutz A, Alnemri ES, MacDonald K, Speert D, Fernandes-Alnemri T, Wu J, Monks BG, Fitzgerald KA, Hornung V. Cutting edge: NF-κB activating pattern recognition and cytokine receptors license NLRP3 inflammasome activation by regulating NLRP3 expression. The Journal of Immunology. 2009 Jul 15;183(2):787-91.

296- He P, Zhong Z, Lindholm K, Berning L, Lee W, Lemere C, Staufenbiel M, Li R, Shen Y. Deletion of tumor necrosis factor death receptor inhibits amyloid β generation and prevents learning and memory deficits in Alzheimer's mice. The Journal of cell biology. 2007 Aug 27;178(5):829-41.

297- Lim JE, Kou J, Song M, Pattanayak A, Jin J, Lalonde R, Fukuchi KI. MyD88 deficiency ameliorates β-amyloidosis in an animal model of Alzheimer's disease. The American journal of pathology. 2011 Sep 1;179(3):1095-103.

298- Fung TT, Rexrode KM, Mantzoros CS, Manson JE, Willett WC, Hu FB. Mediterranean diet and incidence and mortality of coronary heart disease and stroke in women. Circulation. 2009 Mar 3;119(8):1093.

299- Estruch, R., Ros, E., Salas-Salvadó, J., Covas, M. I., Corella, D., Arós, F., ... & Lamuela-Raventos, R. M. (2013). Primary prevention of cardiovascular disease with a Mediterranean diet. *New England Journal of Medicine*, *368*(14), 1279-1290.

300- Sofi F, Macchi C, Abbate R, Gensini GF, Casini A. Mediterranean diet and health. Biofactors. 2013 Jul;39(4):335-42.

301- Dussaillant C, Echeverria G, Urquiaga I, Velasco N, Rigotti A. Current evidence on health benefits of the mediterranean diet. Revista medica de Chile. 2016 Aug 1;144(8):1044-52.

302- Scarmeas N, Stern Y, Tang MX, Mayeux R, Luchsinger JA. Mediterranean diet and risk for Alzheimer's disease. Annals of Neurology: Official Journal of the American Neurological Association and the Child Neurology Society. 2006 Jun;59(6):912-21.

303- Féart C, Samieri C, Barberger-Gateau P. Mediterranean diet and cognitive function in older adults. Current opinion in clinical nutrition and metabolic care. 2010 Jan;13(1):14.

304- Pitozzi V, Jacomelli M, Zaid M, Luceri C, Bigagli E, Lodovici M, Ghelardini C, Vivoli E, Norcini M, Gianfriddo M, Esposto S. Effects of dietary extra-virgin olive oil on behaviour and brain biochemical parameters in ageing rats. British Journal of Nutrition. 2010 Jun;103(11):1674-83.

305- Monti MC, Margarucci L, Tosco A, Riccio R, Casapullo A. New insights on the interaction mechanism between tau protein and oleocanthal, an extra-virgin olive-oil bioactive component. Food & function. 2011;2(7):423-8.

306- Mohagheghi F, Bigdeli MR, Rasoulian B, Zeinanloo AA, Khoshbaten A. Dietary virgin olive oil reduces blood brain barrier permeability, brain edema, and brain injury in rats subjected to ischemia-reperfusion. TheScientificWorldJournal. 2010 Jun 29;10.

307- Keys A. Mediterranean diet and public health: personal reflections. The American journal of clinical nutrition. 1995 Jun 1;61(6):1321S-3S.

308- Rigacci S, Guidotti V, Bucciantini M, Nichino D, Relini A, Berti A, Stefani M. Aβ (1-42) aggregates into non-toxic amyloid assemblies in the presence of the natural polyphenol oleuropein aglycon. Current Alzheimer Research. 2011 Dec 1;8(8):841-52.

309- Nardiello P, Pantano D, Lapucci A, Stefani M, Casamenti F. Diet supplementation with hydroxytyrosol ameliorates brain pathology and restores cognitive functions in a mouse model of amyloid-β deposition. Journal of Alzheimer's Disease. 2018 Jan 1;63(3):1161-72.

310- Pitt J, Roth W, Lacor P, Smith III AB, Blankenship M, Velasco P, De Felice F, Breslin P, Klein WL. Alzheimer's-associated Aβ oligomers show altered structure, immunoreactivity and synaptotoxicity with low doses of oleocanthal. Toxicology and applied pharmacology. 2009 Oct 15;240(2):189-97.

311- Batarseh YS, Kaddoumi A. Oleocanthal-rich extra-virgin olive oil enhances donepezil effect by reducing amyloid-β load and related toxicity in a mouse model of Alzheimer's disease. The Journal of nutritional biochemistry. 2018 May 1;55:113-23.

312- Qosa H, Batarseh YS, Mohyeldin MM, El Sayed KA, Keller JN, Kaddoumi A. Oleocanthal enhances amyloid-β clearance from the brains of TgSwDI mice and in vitro across a human blood-brain barrier model. ACS chemical neuroscience. 2015 Nov 18;6(11):1849-59.

313- Qosa H, Mohamed LA, Batarseh YS, Alqahtani S, Ibrahim B, LeVine III H, Keller JN, Kaddoumi A. Extra-virgin olive oil attenuates amyloid-β and tau pathologies in the brains of TgSwDI mice. The Journal of nutritional biochemistry. 2015 Dec 1;26(12):1479-90.

314- Servili M, Selvaggini R, Esposto S, Taticchi A, Montedoro G, Morozzi G. Health and sensory properties of virgin olive oil hydrophilic phenols: agronomic and technological aspects of production that affect their occurrence in the oil. Journal of Chromatography A. 2004 Oct 29;1054(1-2):113-27.

315- Rigacci S, Guidotti V, Bucciantini M, Parri M, Nediani C, Cerbai E, Stefani M, Berti A. Oleuropein aglycon prevents cytotoxic amyloid aggregation of human amylin. The Journal of nutritional biochemistry. 2010 Aug 1;21(8):726-35.

316- Daccache A, Lion C, Sibille N, Gerard M, Slomianny C, Lippens G, Cotelle P. Oleuropein and derivatives from olives as Tau aggregation inhibitors. Neurochemistry international. 2011 May 1;58(6):700-7.

317- Dell'Agli M, Fagnani R, Galli GV, Maschi O, Gilardi F, Bellosta S, Crestani M, Bosisio E, De Fabiani E, Caruso D. Olive oil phenols modulate the expression of metalloproteinase 9 in THP-1 cells by acting on nuclear factor-κB signaling. Journal of agricultural and food chemistry. 2010 Feb 24;58(4):2246-52.

318- Wang L, Geng C, Jiang L, Gong D, Liu D, Yoshimura H, Zhong L. The anti-atherosclerotic effect of olive leaf extract is related to suppressed inflammatory response in rabbits with experimental atherosclerosis. European journal of nutrition. 2008 Aug 1;47(5):235-43.

319- Serra A, Rubió L, Borràs X, Macià A, Romero MP, Motilva MJ. Distribution of olive oil phenolic compounds in rat tissues after administration of a phenolic extract from olive cake. Molecular nutrition & food research. 2012 Mar;56(3):486-96.

320- Grossi C, Rigacci S, Ambrosini S, Dami TE, Luccarini I, Traini C, Failli P, Berti A, Casamenti F, Stefani M. The polyphenol oleuropein aglycone protects TgCRND8 mice against Aß plaque pathology. PloS one. 2013 Aug 8;8(8):e71702.

321- Pantano D, Luccarini I, Nardiello P, Servili M, Stefani M, Casamenti F. Oleuropein aglycone and polyphenols from olive mill waste water ameliorate cognitive deficits and neuropathology. British journal of clinical pharmacology. 2017 Jan 1;83(1):54-62.

322- Abuznait AH, Qosa H, Busnena BA, El Sayed KA, Kaddoumi A. Olive-oil-derived oleocanthal enhances β-amyloid clearance as a potential neuroprotective mechanism against Alzheimer's disease: in vitro and in vivo studies. ACS chemical neuroscience. 2013 Jun 19;4(6):973-82.

323- Al Rihani SB, Darakjian LI, Kaddoumi A. Oleocanthal-Rich Extra-Virgin Olive Oil Restores the Blood–Brain Barrier Function through NLRP3 Inflammasome Inhibition Simultaneously with Autophagy Induction in TgSwDI Mice. ACS chemical neuroscience. 2019 Jun 25;10(8):3543-54.

324. Oakley H, Cole SL, Logan S, Maus E, Shao P, Craft J, Guillozet-Bongaarts A, Ohno M, Disterhoft J, Van Eldik L, Berry R. Intraneuronal β-amyloid aggregates, neurodegeneration, and neuron loss in transgenic mice with five familial Alzheimer's disease mutations: potential factors in amyloid plaque formation. Journal of Neuroscience. 2006 Oct 4;26(40):10129-40.

325. Tuck KL, Hayball PJ. Major phenolic compounds in olive oil: metabolism and health effects. The Journal of nutritional biochemistry. 2002 Nov 1;13(11):636-44.

326. Angel A, Volkman R, Royal TG, Offen D. Caspase-6 Knockout in the 5xFAD Model of Alzheimer's Disease Reveals Favorable Outcome on Memory and Neurological Hallmarks. International journal of molecular sciences. 2020 Jan;21(3):1144.

327. Wang H, Bloom O, Zhang M, Vishnubhakat JM, Ombrellino M, Che J, Frazier A, Yang H, Ivanova S, Borovikova L, Manogue KR. HMG-1 as a late mediator of endotoxin lethality in mice. Science. 1999 Jul 9;285(5425):248-51.

328. Wang Z, Li DD, Liang YY, Wang DS, Cai NS. Activation of astrocytes by advanced glycation end products: cytokines induction and nitric oxide release. Acta Pharmacologica Sinica. 2002 Nov 1;23(11):974-80.

329. Hudson BI, Lippman ME. Targeting RAGE signaling in inflammatory disease. Annual review of medicine. 2018 Jan 29;69:349-64.

330. Park R, Kook SY, Park JC, Mook-Jung I. A β 1–42 reduces P-glycoprotein in the blood–brain barrier through RAGE–NF-κ B signaling. Cell death & disease. 2014 Jun;5(6):e1299.

331. García-Villalba R, Larrosa M, Possemiers S, Tomás-Barberán FA, Espín JC. Bioavailability of phenolics from an oleuropein-rich olive (Olea europaea) leaf extract and its acute effect on plasma antioxidant status: comparison between pre-and postmenopausal women. European journal of nutrition. 2014 Jun 1;53(4):1015-27.

332. Serrano-Pozo A, Mielke ML, Gómez-Isla T, Betensky RA, Growdon JH, Frosch MP, Hyman BT. Reactive glia not only associates with plaques but also parallels tangles in Alzheimer's disease. The American journal of pathology. 2011 Sep 1;179(3):1373-84.

333. Serrano-Pozo A, Frosch MP, Masliah E, Hyman BT. Neuropathological alterations in Alzheimer disease. Cold Spring Harbor perspectives in medicine. 2011 Sep 1;1(1):a006189.

334. Hardman RJ, Kennedy G, Macpherson H, Scholey AB, Pipingas A. Adherence to a Mediterranean-style diet and effects on cognition in adults: a qualitative evaluation and systematic review of longitudinal and prospective trials. Frontiers in nutrition. 2016 Jul 22;3:22.

335. El Riachy M, Priego-Capote F, León L, Rallo L, Luque de Castro MD. Hydrophilic antioxidants of virgin olive oil. Part 1: Hydrophilic phenols: A key factor for virgin olive oil quality. European Journal of Lipid Science and Technology. 2011 Jun;113(6):678-91.

336. Boss A, Bishop KS, Marlow G, Barnett MP, Ferguson LR. Evidence to support the anti-cancer effect of olive leaf extract and future directions. Nutrients. 2016 Aug;8(8):513.

337. Omar SH, Scott CJ, Hamlin AS, Obied HK. Olive biophenols reduces alzheimer's pathology in SH-SY5Y cells and APPswe mice. International Journal of Molecular Sciences. 2019 Jan;20(1):125.

338. Omar SH. Cardioprotective and neuroprotective roles of oleuropein in olive. Saudi Pharmaceutical Journal. 2010 Jul 1;18(3):111-21.

339. Rodríguez-Morató J, Xicota L, Fitó M, Farre M, Dierssen M, De la Torre R. Potential role of olive oil phenolic compounds in the prevention of neurodegenerative diseases. Molecules. 2015 Mar;20(3):4655-80.

340. Freeman LR, Keller JN. Oxidative stress and cerebral endothelial cells: regulation of the blood–brain-barrier and antioxidant based interventions. Biochimica et Biophysica Acta (BBA)-Molecular Basis of Disease. 2012 May 1;1822(5):822-9.

341. Al Ahmad A, Gassmann M, Ogunshola OO. Involvement of oxidative stress in hypoxia-induced blood–brain barrier breakdown. Microvascular research. 2012 Sep 1;84(2):222-5.

342. Miyakawa T. Vascular pathology in Alzheimer's disease. Psychogeriatrics. 2010 Mar;10(1):39-44.

343. Baloyannis, S. J. (2015). Brain capillaries in Alzheimer's disease. *Hellenic journal of nuclear medicine*, *18*, 152-152.

344. Montagne A, Barnes SR, Sweeney MD, Halliday MR, Sagare AP, Zhao Z, Toga AW, Jacobs RE, Liu CY, Amezcua L, Harrington MG. Blood-brain barrier breakdown in the aging human hippocampus. Neuron. 2015 Jan 21;85(2):296-302.

345. Hawkins BT, Davis TP. The blood-brain barrier/neurovascular unit in health and disease. Pharmacological reviews. 2005 Jun 1;57(2):173-85.

346. Hardy JA, Higgins GA. Alzheimer's disease: the amyloid cascade hypothesis. Science. 1992 Apr 10;256(5054):184-6.

347. Bates KA, Verdile G, Li QX, Ames D, Hudson P, Masters CL, Martins RN. Clearance mechanisms of Alzheimer's amyloid-β peptide: implications for therapeutic design and diagnostic tests. Molecular psychiatry. 2009 May;14(5):469-86.

348. Murphy MP, LeVine III H. Alzheimer's disease and the amyloid-β peptide. Journal of Alzheimer's disease. 2010 Jan 1;19(1):311-23.

349. Kuhnke D, Jedlitschky G, Grube M, Krohn M, Jucker M, Mosyagin I, Cascorbi I, Walker LC, Kroemer HK, Warzok RW, Vogelgesang S. MDR1-P-Glycoprotein (ABCB1) Mediates Transport of Alzheimer's Amyloid-β Peptides—Implications for the Mechanisms of Aβ Clearance at the Blood–Brain Barrier. Brain Pathology. 2007 Oct;17(4):347-53.

350. Brenn A, Grube M, Peters M, Fischer A, Jedlitschky G, Kroemer HK, Warzok RW, Vogelgesang S. Beta-amyloid downregulates MDR1-P-glycoprotein (Abcb1) expression at the blood-brain barrier in mice. International journal of Alzheimer's disease. 2011 Jan 1;2011.

351. Sharma HS, Castellani RJ, Smith MA, Sharma A. The blood-brain barrier in Alzheimer's disease: novel therapeutic targets and nanodrug delivery. Int Rev Neurobiol. 2012 Jan 1;102:47-90.

352. Sagare AP, Deane R, Zlokovic BV. Low-density lipoprotein receptor-related protein 1: a physiological Aβ homeostatic mechanism with multiple therapeutic opportunities. Pharmacology & therapeutics. 2012 Oct 1;136(1):94-105.

353. Vogelgesang S, Jedlitschky G, Brenn A, C Walker L. The role of the ATP-binding cassette transporter P-glycoprotein in the transport of β-amyloid across the blood-brain barrier. Current pharmaceutical design. 2011 Sep 1;17(26):2778-86.

354. Hartz AM, Miller DS, Bauer B. Restoring blood-brain barrier P-glycoprotein reduces brain amyloid-β in a mouse model of Alzheimer's disease. Molecular pharmacology. 2010 May 1;77(5):715-23.

355. Kostomoiri M, Fragkouli A, Sagnou M, Skaltsounis LA, Pelecanou M, Tsilibary EC, Tzinia AK. Oleuropein, an anti-oxidant polyphenol constituent of olive promotes α-

secretase cleavage of the amyloid precursor protein (AβPP). Cellular and molecular neurobiology. 2013 Jan 1;33(1):147-54.

356. De Felice FG, Lourenco MV. Brain metabolic stress and neuroinflammation at the basis of cognitive impairment in Alzheimer's disease. Frontiers in aging neuroscience. 2015 May 19;7:94.

357. Jung YJ, Chung WS. Phagocytic roles of glial cells in healthy and diseased brains. Biomolecules & therapeutics. 2018 Jul;26(4):350.

358. Gomez-Nicola D, Boche D. Post-mortem analysis of neuroinflammatory changes in human Alzheimer's disease. Alzheimer's Research & Therapy. 2015 Dec 1;7(1):42.

359. Sullivan SM. GFAP variants in health and disease: stars of the brain… and gut. Journal of Neurochemistry. 2014 Sep;130(6):729-32.

360. Sasaki N, Fukatsu R, Tsuzuki K, Hayashi Y, Yoshida T, Fujii N, Koike T, Wakayama I, Yanagihara R, Garruto R, Amano N. Advanced glycation end products in Alzheimer's disease and other neurodegenerative diseases. The American journal of pathology. 1998 Oct 1;153(4):1149-55.

361. Takeuchi M, Yamagishi S. TAGE (toxic AGEs) hypothesis in various chronic diseases. Medical hypotheses. 2004 Jan 1;63(3):449-52.

362. Galasko D, Bell J, Mancuso JY, Kupiec JW, Sabbagh MN, van Dyck C, Thomas RG, Aisen PS. Clinical trial of an inhibitor of RAGE-Aβ interactions in Alzheimer disease. Neurology. 2014 Apr 29;82(17):1536-42.

363. Takeuchi M, Yamagishi SI. Possible involvement of advanced glycation end-products (AGEs) in the pathogenesis of Alzheimer's disease. Current pharmaceutical design. 2008 Apr 1;14(10):973-8.

364. Krautwald M, Münch G. Advanced glycation end products as biomarkers and gerontotoxins–a basis to explore methylglyoxal-lowering agents for Alzheimer's disease?. Experimental gerontology. 2010 Oct 1;45(10):744-51.

365. Gironès X, Guimerà A, Cruz-Sánchez CZ, Ortega A, Sasaki N, Makita Z, Lafuente JV, Kalaria R, Cruz-Sánchez FF. Nϵ-Carboxymethyllysine in brain aging, diabetes mellitus, and Alzheimer's disease. Free Radical Biology and Medicine. 2004 May 15;36(10):1241-7.

366. Lue LF, Walker DG, Brachova L, Beach TG, Rogers J, Schmidt AM, Stern DM, Du Yan S. Involvement of microglial receptor for advanced glycation endproducts (RAGE) in Alzheimer's disease: identification of a cellular activation mechanism. Experimental neurology. 2001 Sep 1;171(1):29-45.

367. Du Yan S, Chen X, Fu J, Chen M, Zhu H, Roher A, Slattery T, Zhao L, Nagashima M, Morser J, Migheli A. RAGE and amyloid-β peptide neurotoxicity in Alzheimer's disease. Nature. 1996 Aug;382(6593):685-91.

368. Chavakis E, Hain A, Vinci M, Carmona G, Bianchi ME, Vajkoczy P, Zeiher AM, Chavakis T, Dimmeler S. High-mobility group box 1 activates integrin-dependent homing of endothelial progenitor cells. Circulation research. 2007 Feb 2;100(2):204-12.

369. Hofmann MA, Drury S, Fu C, Qu W, Taguchi A, Lu Y, Avila C, Kambham N, Bierhaus A, Nawroth P, Neurath MF. RAGE mediates a novel proinflammatory axis: a central cell surface receptor for S100/calgranulin polypeptides. Cell. 1999 Jun 25;97(7):889-901.

370. Chen J, Song M, Yu S, Gao P, Yu Y, Wang H, Huang L. Advanced glycation endproducts alter functions and promote apoptosis in endothelial progenitor cells through

receptor for advanced glycation endproducts mediate overpression of cell oxidant stress. Molecular and cellular biochemistry. 2010 Feb 1;335(1-2):137-46.

371. Wang X, Sun X, Niu M, Zhang X, Wang J, Zhou C, Xie A. RAGE Silencing Ameliorates Neuroinflammation by Inhibition of p38-NF-κB Signaling Pathway in Mouse Model of Parkinson's Disease. Frontiers in Neuroscience. 2020 Apr 29;14:353.

372. Scaffidi, P., Misteli, T., & Bianchi, M. E. (2002). Release of chromatin protein HMGB1 by necrotic cells triggers inflammation. *Nature*, *418*(6894), 191-195.

373. Bianchi ME, Manfredi AA. High-mobility group box 1 (HMGB1) protein at the crossroads between innate and adaptive immunity. Immunological reviews. 2007 Dec;220(1):35-46.

374. Gao HM, Zhou H, Zhang F, Wilson BC, Kam W, Hong JS. HMGB1 acts on microglia Mac1 to mediate chronic neuroinflammation that drives progressive neurodegeneration. Journal of Neuroscience. 2011 Jan 19;31(3):1081-92.

375. Mosquera JA. Role of the receptor for advanced glycation end products (RAGE) in inflammation. Investigacion clinica. 2010 Jun;51(2):257.

376. Son MO, Lee S, Byun K. Ligands receptor for advanced glycation end products produced by activated microglia are critical in neurodegenerative diseases. Journal of Alzheimers Dis Parkinsonism. 2017;7:318.

377. He Y, Hara H, Núñez G. Mechanism and regulation of NLRP3 inflammasome activation. Trends in biochemical sciences. 2016 Dec 1;41(12):1012-21.

Supplementary Data

Appendix A

Preliminary data for the effect of OLE on Aβ-related pathology and neuroinflammation in female 5xFAD mice

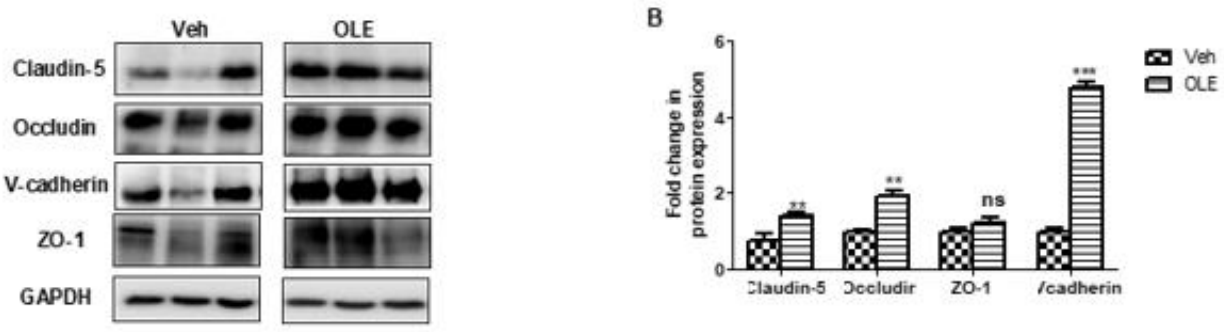

Fig 8.S1: OLE treatment significantly increased the tight junction proteins expression in 5xFAD mice brain homogenate. Representative western blot and densitometry analysis of claudin-5, occludin, ZO-1, and V-cadherin. Results showed significant upregulation in all TJ proteins in females (n=3) except ZO-1 protein. Mice were treated with OLE 366 µg/kg daily for 3 months. Data represented as mean ± SEM, ** $p < 0.01$, *** $p < 0.001$.

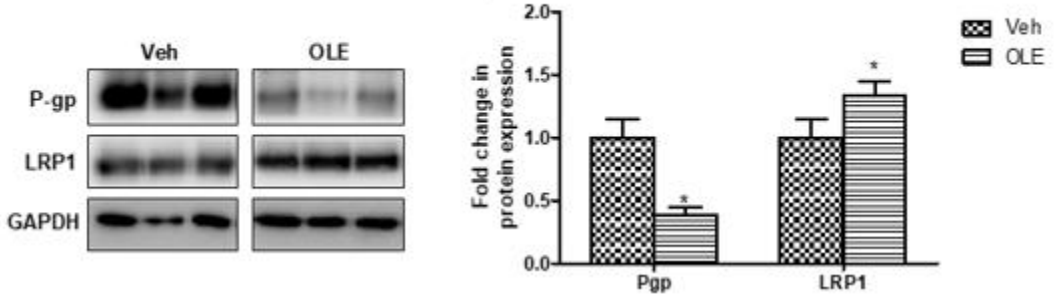

Fig 8.S2: The effect of OLE on Aβ major efflux transporter proteins (P-gp and LRP1). Representative western blot and densitometry analysis of P-gp and LRP. Results showed that OLE treatment significantly reduced the expression of P-gp, while the LRP1 was significantly increased in females (n=3) compared to vehicle-treated 5xFAD mice. Mice were treated with OLE 366 µg/kg daily for 3 months. All proteins were measured from brain homogenate and normalized to GAPDH. Data represented as mean ± SEM. * $p < 0.05$.

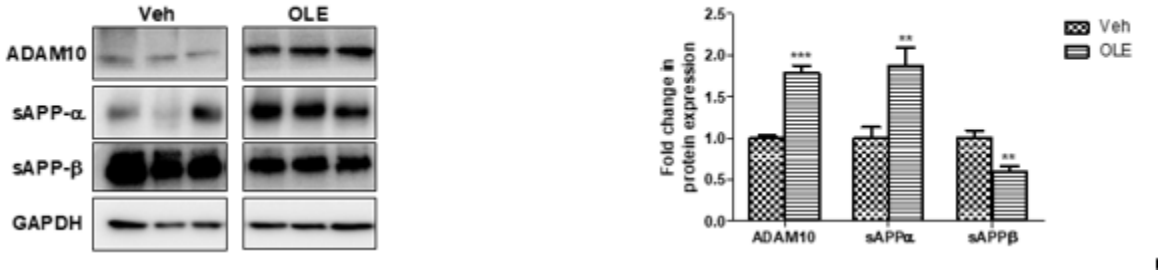

Fig 8.S3: The effect of OLE treatment on the Aβ production through APP processing in 5xFAD brain homogenate. Representative western blot and densitometry analysis of ADAM-10, sAPP-α and sAPP-β in female mice brain demonstrated that level of ADAM-10 was significantly increased in females (n=3) with a significant increase in sAPPα expression and a significant reduction in the expression of sAPPβ. Mice were treated with OLE 366 µg/kg daily for 3 months. All proteins were measured from brain homogenate and normalized to GAPDH. Data represented as mean ± SEM. ** $p < 0.01$ and *** $p < 0.001$.

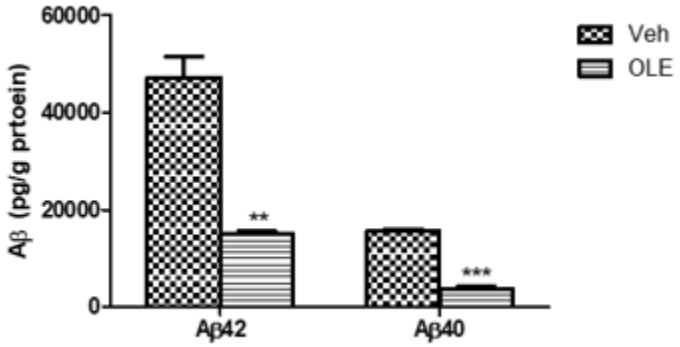

Fig 8.S4: Effect of OLE treatment (366 µg/kg) for 3 months on Aβ burden in 5xFAD mice. ELISA for $A\beta_{40}$ and $A\beta_{42}$ (n=3 females). Results showed OLE treatment significantly reduced the $A\beta_{40}$ and $A\beta_{42}$ in female mice brain homogenate. Data represented as mean ± SEM. ** $p < 0.01$, *** $p < 0.001$.

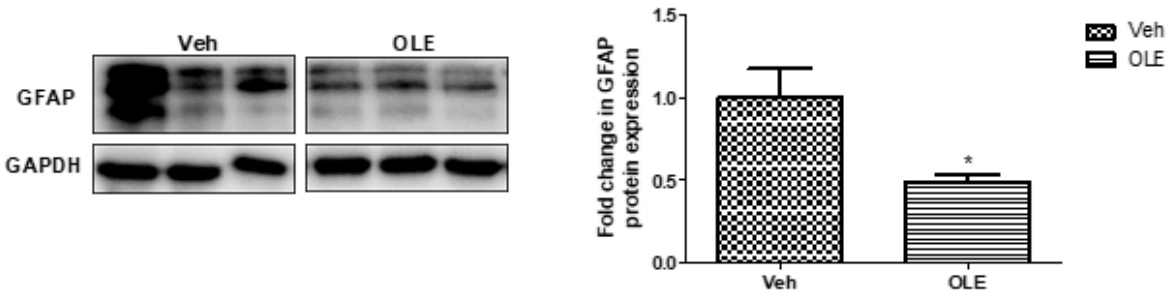

Fig 8.S5: Effect of OLE treatment on astrogliosis. Mice treated with OLE at 366 µg/kg for 3 months. Representative western blot and densitometry analysis of GFAP in females brain homogenate. Results showed a significant reduction in GFAP expression compared to vehicle-treated mice (n=3). Data is presented as mean± SEM for females (n=3) ** $p < 0.01$.

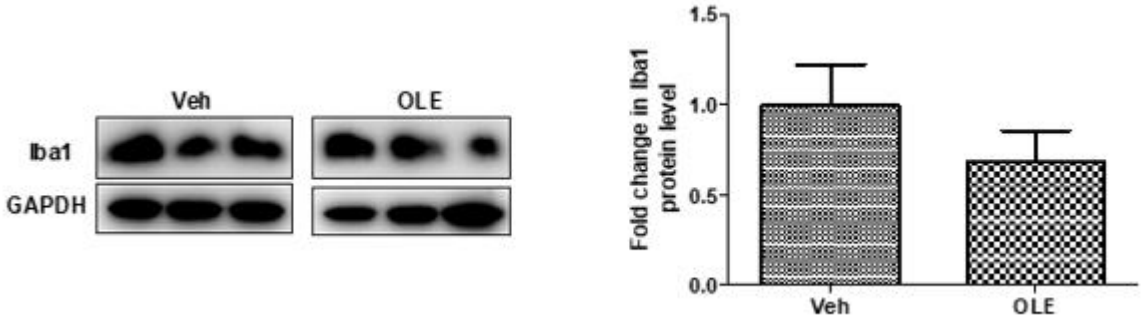

Fig 8.S6: Effect of OLE treatment on microgliosis. Mice treated with OLE at 366 µg/kg for 3 months. Representative western blot and densitometry analysis of Iba-1 in female mice (n=3) brain homogenates. Results showed a reduction in Iba-1 expression compared to vehicle-treated. The difference was not significant. Data represented as mean± SEM.

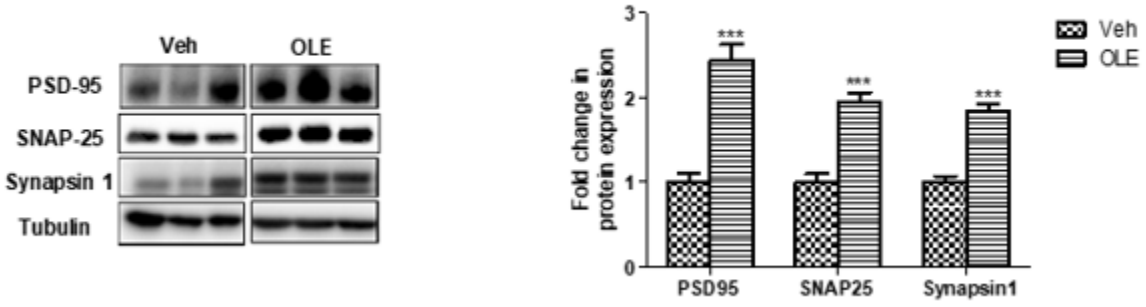

Fig 8.S7: Treatment with OLE (366 µg/kg) for 3 months increased the expression of synaptic markers in 5xFAD mice brains. Representative western blot analysis of synaptic markers, named SNAP-25, Synapsin-1, and PSD-95 in females (n=3). Results showed a significant increase compared to vehicle-treated mice. All proteins were measured from brain homogenate and normalized to Tubulin. Data represented as mean± SEM. *** $p < 0.001$.

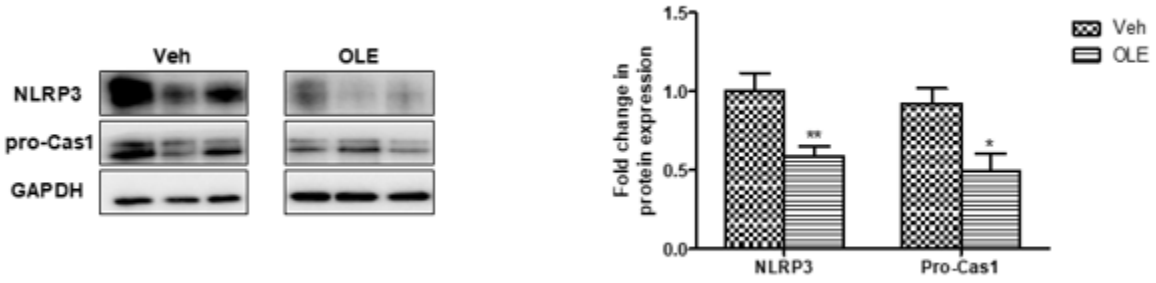

Fig 8.S8: Treatment with OLE (366 µg/kg) for 3 months reduced the neuroinflammation in 5xFAD mice. Representative western blot and densitometry analysis of NLRP3 and pro-caspase 1 in 5xFAD females (n=3). Results showed a significant reduction compared to vehicle-treated mice. All proteins were measured from the brain homogenate and normalized to GAPDH. Data represented as mean± SEM. * $p < 0.05$, ** $p < 0.01$.

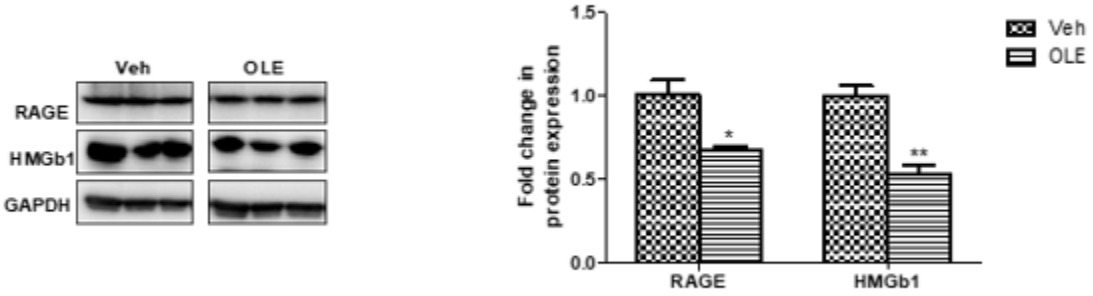

Fig 8.S9: Treatment with OLE (366 µg/kg) for 3 months reduced the neuroinflammation in 5xFAD mice. Representative western blot and densitometry analysis of RAGE and HMGb1 in 5xFAD females (n=3). Results showed a significant reduction compared to vehicle-treated mice. All proteins were measured from the brain homogenate and normalized to GAPDH. Data represented as mean± SEM. * $p < 0.05$, ** $p < 0.01$.

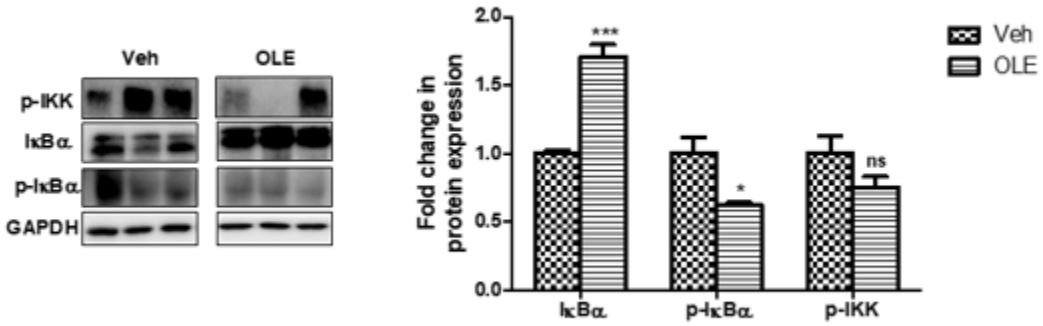

Fig 8.S10: Treatment with OLE (366 µg/kg) for 3 months reduced the neuroinflammation through inactivation of NF-κB signaling pathway in 5xFAD mice brain homogenates. Representative western blot and densitometry analysis of IκBα, p-IκBα (Ser32) and p-IKKβ in 5xFAD females (n=3). Results showed a significant reduction in p-IKKβ and p-IκBα (Ser32), and increase in IκBα compared to vehicle-treated mice. All proteins were measured from brain homogenate and normalized to GAPDH. Data represented as mean± SEM. * $p < 0.05$, ** $p <$ 0. 01 and *** $p < 0.001$.

Appendix B

In addition to my dissertation work, before transferring to Auburn University, I worked on a second research project while at the University of Louisiana Monroe (ULM). Most of the work was performed at ULM except part of the in vitro data. Findings from this project is submitted to Brain Research and currently is under review.

The submitted manuscript is presented below.

Blood-brain barrier disruption increases amyloid-related pathology in TgSwDI mice

Abstract

In Alzheimer's disease (AD), several studies reported the blood-brain barrier (BBB) breakdown with compromised function. P-glycoprotein (P-gp) and breast cancer resistance protein (BCRP) are transport proteins localized at the BBB luminal membrane and play important role in the clearance of amyloid-β (Aβ). The purpose of this study was to investigate the effect of pharmacological inhibition of Aβ efflux transporters on BBB function and Aβ accumulation and related pathology. Recently, we have developed an in vitro high-throughput screening assay to screen for compounds that modulate the integrity of a cell-based BBB model, which identified elacridar as a disruptor of the monolayer integrity. Elacridar, an investigational compound, known for its P-gp and BCRP inhibitory effect and widely used in cancer research. Therefore, it was used as a model compound for further evaluation in a mouse model of AD namely TgSwDI. TgSwDI mouse is also used as a model for cerebral amyloid angiopathy (CAA). Results showed that P-gp and BCRP inhibition by elacridar disrupted the BBB integrity as measured by increased IgG extravasation and reduced expression of tight junction proteins, increased amyloid deposition due to P-gp and BCRP downregulation and receptor for advanced glycation end products (RAGE) upregulation, and increased astrogliosis. Further studies revealed the effect was mediated by activation of NF-κB pathway. In conclusion, results suggest that BBB disruption by inhibiting P-gp and BCRP exacerbates AD pathology in a mouse model of AD, and indicate that therapeutic drugs that inhibit P-gp and BCRP could increase the risk for AD.

1. Introduction

Alzheimer's disease (AD) is a progressive neurodegenerative disorder and most common cause of dementia (Citron, 2010, Wilson et al., 2012). It is considered the sixth leading cause of death and the fifth among Americans above 65 years old. The pathogenesis of AD is complex and to date no effective treatment exists. AD is characterized by the deposition and accumulation of amyloid-β (Aβ) in brain parenchyma and cerebral vessels (Selkoe, 2001, Selkoe and Schenk, 2003). Aβ accumulation in the brain parenchyma forms senile plaques, whereas the extracellular deposition of Aβ in cerebral vessels forms cerebral amyloid angiopathy (CAA) (Jellinger, 2002, Thal et al., 2008). Aβ peptides derived from the proteolytic cleavage of the amyloid precursor protein (APP) to form $A\beta_{40}$ and $A\beta_{42}$. Aβ generated in the brain can be eliminated through transport proteins across the blood-brain barrier (BBB), enzymatic degradation, and perivascular drainage via the vascular basement membrane (Bell and Zlokovic, 2009).

Dysfunction of the BBB could be involved in the pathogenesis of AD and CAA (Jellinger, 2002). While additional studies are necessary to clarify the mechanism of BBB dysfunction, available reports support that disruption of Aβ clearance across the BBB may result in exacerbated Aβ accumulation in the brain (Montagne et al., 2017, Bennett et al., 2018, Sweeney et al., 2018). BBB integrity is strictly controlled by cells and basement membranes in the neurovascular unit in physiological conditions. However, the barrier function is likely compromised during aging and AD (Sweeney et al., 2019).

The BBB is composed of a basement membrane, astrocytes, pericytes and endothelial cells. The endothelial cells are tightly connected at a junctional complex via tight junction (TJs) and adherence junction proteins (Zlokovic, 2008), which limit the transport of solutes from the

blood to brain and vice versa (Ohtsuki and Terasaki, 2007). Aβ transport across the BBB is bidirectional where its transport from brain to blood and vice versa requires carrier- or receptor-mediated transport proteins (van Assema et al., 2012). Efflux transporters P-glycoprotein (P-gp, ABCB1), breast cancer resistant protein (BCRP, ABCG2), and low-density lipoprotein receptor related protein-1 (LRP-1) regulate the traffic across the BBB to the blood, and play key roles in brain Aβ homeostasis (Shibata et al., 2000, van Assema et al., 2012). Whereas, the receptor for advanced glycated end products (RAGE) in the endothelial cells is able to transport Aβ from blood to brain across the BBB (Donahue et al., 2006).

P-gp and BCRP belong to the family of ATP-binding cassette transporters and are highly expressed at the luminal side of BBB endothelium (Demeule et al., 2001). Both proteins function as efflux transporters to limit foreign molecules access to the brain and extrude substances from brain to blood to protect the brain from potentially toxic substances (Schinkel, 1999). In normal aging and AD, P-gp and BCRP are downregulated (Toornvliet et al., 2006). In addition, several lines of evidence have shown that compromised BBB integrity and function is associated with altered proteins expression and cellular secretions, and inflammatory activation (Bowman et al., 2007). Studies reported that reduced expression/function of P-gp and BCRP led to a reduction in the clearance of Aβ and increase in Aβ-related pathology (Lam et al., 2001, Kuhnke et al., 2007, Do et al., 2012, Qosa et al., 2016b), while restoring the function of P-gp at the BBB increased Aβ clearance from the brain (Abuznait and Kaddoumi, 2012, Hartz et al., 2010). These findings suggest that P-gp and BCRP-suited BBB play important role in BBB function and brain homeostasis, and that an alteration in these transporters function thus could alter the BBB function.

Aging is associated with increased risk of chronic diseases necessitating the prescription of multiple medications, which could independently and/or through drug-drug interaction inhibit transporters function and thus affect the BBB. In this work, we sought to study the effect of pharmacological disruption of BBB via P-gp and BCRP inhibition on Aβ pathology in TgSwDI, a mouse model for AD and CAA. For this, the third generation P-gp and BCRP inhibitor elacridar (Dash et al., 2017) was used as a model compound to investigate the effect of both transporters inhibition on BBB function and on Aβ levels in the brains of TgSwDI mice. Elacridar was identified as a BBB disruptor by our recently developed high throughput screening (HTS) assay using a cell-based BBB model (Qosa et al., 2016a).

2. Methodology

2.1. Materials and chemicals

Elacridar and dithiothreitol (DTT) were purchased from Sigma-Aldrich (St. Louis, MO). Dulbecco's modified Eagle's medium (DMEM), sterile phosphate-buffered saline (PBS), and penicillin/streptomycin antibiotics were obtained from Gibco (Grand Island, NY). Fetal bovine serum (FBS) was purchased from Atlanta biologicals (Flowery Branch, GA). Total protein measurement reagents using the bicinchoninic acid (BCA) method were obtained from Pierce (Rockford, IL). Antibodies used were mouse monoclonal antibody against light chain LRP1 (Abcam, Cambridge, MA), mouse monoclonal antibody C-219 against P-gp from BioLegend (San Diego, CA), mouse monoclonal antibody against BCRP (Cell signaling; Boston, MA). Monoclonal antibodies for claudin-5, ZO-1 and HRP-labeled secondary antibodies were purchased from Invitrogen (Carlsbad, CA), goat polyclonal antibodies against actin (C-11) and Matrix Metallopeptidase 9 (MMP9) were purchased from Santa Cruz Biotechnology (Dallas, TX). Antibodies for pre- and post-synaptic proteins SNAP-25 and PSD-95, respectively, were purchased from GeneTex (Irvine, CA), antibodies for IKB-α, p-IKB-α, NF-κB p65 and p-NF-κB p65 were purchased from Cell Signaling. All other reagents and supplies were purchased from VWR (West Chester, PA) and Fisher Scientific (Hampton, NH).

2.2. Cell culture

The immortalized mouse brain endothelial cell line, bEnd3, was obtained from ATCC (Manassas, VA, USA). bEnd3 cells, passage 25–35, were cultured in DMEM supplemented with 10% FBS, penicillin G (100 IU/ml), streptomycin (100 g/ml), 1% w/v nonessential amino

acids, and glutamine 2 mM. Cultures were maintained in a humidified atmosphere (5% CO2/95% air) at 37^{o}C, and media were changed every other day.

2.3. In vitro permeability assay

The permeability assay across bEnd3 cells monolayer was performed as we reported previously (Qosa et al., 2016a, Elfakhri et al., 2018). In brief, cells were seeded on inserts of HTS transwell 96-well plate (Corning, NY, USA), coated with 50 µl of fibronectin solution (30 µg/ml in PBS) as a basement membrane substitute. bEnd3 cells were seeded at a density of 50,000 cells/cm^2 on the apical side, and 200 µl of fresh media were added to the basolateral side. To achieve optimal barrier integrity of bEnd3 cells, cells were incubated at 37°C, 5% CO2 for 5 days (Qosa et al., 2016a). The effect of elacridar on the barrier integrity of bEnd3 cells was evaluated on sixth day of seeding by monitoring transendothelial electrical resistance (TEER) measurements and by Lucifer yellow (LY) assay as described below.

Cells were treated with different concentrations of elacridar starting on day three and four of cell seeding, which correspond to treatment time of 48 and 72 h, respectively. At the end of treatment period (day 6 post-seeding), the integrity of the endothelial barrier was evaluated by measuring monolayer tightness through TEER, and permeability of LY across the monolayer. For LY permeability, 50 µl of LY (100 µM) diluted in transport buffer (141 mM NaCl, 4 mM KCl, 2.8 mM CaCl2, 1 mM MgSO4, 10 mM HEPES, and 10 mM D-glucose, pH 7.4) were added to the apical side, while the media in the basal side (lower chamber) were replaced with 200 µl of warmed transport buffer. One hour later, the concentrations of LY in the apical and basal sides were determined by measuring LY fluorescence intensity at excitation and emission wavelengths of 485 and 528 nm, respectively, by using cytation-5 microplate reader (Biotek,

VT) supported with Gene5 software (Biotek) for data acquisition. To calculate the apparent permeation coefficient (Pc) of LY, the following was used:

$$Pc\ (cm/sec) = (V_b \times C_b) / (C_a \times A \times T)$$

Where, V_b is the volume of the basal side (200 µl), C_b is the concentration of LY (µM) in the basal side, C_a is the concentration of LY (µM) in the apical side, A is the membrane area (0.143 cm^2), and T is the time of transport (3600 sec). LY concentration was calculated against a standard curve prepared by measuring the fluorescence intensity of various concentrations of LY (Qosa et al., 2016a). While for TEER measurements, an automated TEER measurement system with Corning HTS Transwell-96 (REMS-96C) electrodes (World Precision Instrument, USA) was used. To reflect the actual readings of the bEnd3 cell layers, TEER of blank inserts was subtracted from the measured TEER of each experimental insert. Values were expressed as $\Omega \cdot cm^2$.

2.4. Preparation of cytosolic or nuclear extracts from bEnd3 cells

Cytosolic and nuclear extracts were obtained as previously described (Schreiber et al., 1990). bEnd3 cells were plated at a density of 1×10^6 cells in 100 mm dishes and cultured for 24 h; subsequently, the cultures were treated with or without 5 µM elacridar for an additional 4 and 24 h. After each time point, cells were scraped off the plates, collected by centrifugation and washed with PBS. The cell pellet was resuspended in cytosol extraction buffer consists of 10 mM HEPES (pH 7.5), 10 mM KCl, 0.1 mM EDTA, 1 mM DTT, 0.5% Nonidet-40, and 0.5 mM phenylmethylsulfonyl fluoride (PMSF) protease inhibitor; allowed to swell on ice for 20 min with intermittent mixing (Schreiber et al., 1990). Tubes were vortexed to disrupt the cell membrane and homogenate was centrifuged at 12,000 *g* for 10 min at 4°C. The supernatant

(cytosolic extract) was collected and frozen at -80 C° until use. The pellet was further treated for nuclear protein extractions. The nucleus pellet was resuspended in an equal volume of nuclear extraction buffer consists of 20 mM HEPES (pH 7.5), 400 mM NaCl, 1 mM EDTA, 1 mM DTT, and 1 mM PMSF with protease inhibitor. The lysing nucleus was left on ice for 30 min and then centrifuged at 12,000 *g* for 15 min at 4°C. The supernatant (nuclear extract) was removed and stored -80 C° until analysis.

2.5. Animals treatment

All animal experiments and procedures were approved by the Institutional Animal Care and Use Committee of the University of Louisiana at Monroe and according to the National Institutes of Health guide for the care and use of Laboratory animals (NIH Publications No. 8023, revised 1978). Surgical and treatment procedures were consistent with the IACUC policies and procedures. Male TgSwDI mice (Jackson laboratory; Bar Harbor, ME) aged 4 months were used. All mice were housed in plastic containers under the conditions of 12 h light/dark cycle, 22°C, 35% relative humidity, and *ad libitum* access to water and food. This mouse model expresses human APP KM670/671NL (Swedish), APP E693Q (Dutch), APP D694N (Iowa) mutations. TgSwDI mice develop fibrillary amyloid deposits primarily in cerebral microvasculature starting at age 2-3 months and extensively at 12 months of age (Davis et al., 2004). Aβ deposition also occurs in the brain parenchyma of these mice, generally in the form of diffuse plaque-like structures beginning at approximately three months of age in the subiculum, hippocampus and cortex (Davis et al., 2004).

Mice were divided into two groups (n = 5 mice per group), a vehicle-treated group received intraperitoneal injection (i.p.) of the vehicle used to dissolve elacridar composed of

70% water: 16.5% DMSO: 13.5% PEG 400, and treatment group received elacridar (10mg/kg/day, i.p. injection) for 28 days. Elacridar dose and route of administration were selected based on previous reports (Durk et al., 2014). Elacridar is a third generation dual P-gp and BCRP inhibitor (Oostendorp et al., 2009). During the treatment period, animals' body weights were measured weekly; health status and normal behavior were checked daily. Mice body weights were not significantly different between the treatment and control groups and were in the range of 28.5 ± 2.5 to 26 ± 2.4 g. respectively. At the end of treatment, mice were intraperitoneally anesthetized with ketamine and xylazine (125 and 20 mg/kg, respectively), followed by decapitation to collect brain tissues.

2.6. Isolation of brain microvessels

Brain microvessels were isolated as described previously (Elfakhri et al., 2018). Brain hemisphere was homogenized in ice-cold DPBS followed by the addition of one volume of 30% Ficoll 400 (Sigma-Aldrich). Homogenate was centrifuged at 8000×*g* for 10 min and the resulting pellet was suspended in ice-cold DPBS containing 1% BSA and passed over a glass bead column to collect microvessels adhering to the glass beads. Isolated microvessels were used to determine the expression of tight junction proteins ZO-1 and claudin-5, and Aβ transport proteins P-gp, BCRP, RAGE and LRP1 by western blot.

2.7. Western blot for cell lysate, brain homogenate, and microvessels

Total protein for each sample was determined using the BCA protein assay. Protein samples (25 μg) were loaded and resolved on 10% SDS-polyacrylamide gel, then transferred electrophoretically onto PVDF membranes. Membranes were incubated in 1% blocking

solution followed by overnight incubation at 4°C with primary antibodies. Analyzed proteins for cytoplasmic and nuclear fraction lysates from in vitro experiments included IκB-α (1:1000 dilution), NF-κB (p65; 1:1000 dilution), phosphorylated IκB-α (1:1000 dilution), phosphorylated NF-κB (1:1000 dilution) and housekeeping proteins tubulin (cytoplasmic) and histone H3 (nuclear) (1:500 dilution). For brain homogenate and isolated microvessels samples, proteins analyzed were P-gp (1:200 dilution), BCRP (1:200 dilution), LRP1 (1:5000 dilution), synaptic markers (PSD-95 and SNAP-25), RAGE, MMP9, GFAP (1:500 dilution), tight junctions (ZO-1 and Claudin-5), tubulin and actin-β, and GAPDH from Invitrogen. For detection, the membranes were washed free of primary antibodies and incubated with HRP-labeled secondary IgG anti-mouse antibody for P-gp, PSD-95, RAGE, GFAP, MMP9, claudin-5, and GAPDH; anti-rabbit antibody for LRP1, ZO-1, BCRP, and SNAP-25. Similar antibodies to those used to probe NF-κB pathway proteins in cell lysates were also used for homogenate lysates. All secondary antibodies were from Invitrogen.

Protein blots were developed using a chemiluminescence detection kit (Thermo Fisher Scientific). Bands were visualized using ChemiDoc imaging system (Bio Rad; Hercules, CA), and analyzed by Image Lab software v 6.0 (Bio-Rad). The results were expressed as fold change in protein level compared to control group after normalization to the house keeping proteins.

2.8. Immunohistochemical analysis

All cryostat brain slices (16 μm) were methanol-fixed then blocked for 30 min with 10% normal donkey serum in PBS. Double immunostaining of microvessels with Aβ was performed using rabbit polyclonal collagen-IV antibody (Millipore; Temecula, CA) at 1:200 dilution detection followed by IgG-CFL 594 conjugated donkey anti-rabbit (Santa Cruz Biotechnology)

as a secondary antibody. For Aβ detection, Alexa fluor-488 conjugated anti-Aβ antibody (6E10; BioLegend) at 1:200 dilution was used.

To assess IgG extravasation from brain microvessels, brain sections were fixed and blocked, as described above, then probed by dual immunohistochemical staining for collagen-IV and mouse IgG using rabbit anti-collagen-IV, and fluorescein-conjugated donkey anti-IgG to detect IgG (Santa Cruz Biotechnology), both at 1:200 dilution. To evaluate astrogliosis, brain sections were fixed and prepared as above. Double immunostaining was performed using GFAP antibody for astrocytes at 1:100 dilution and Alexa fluor-488 labeled 6E10 for total Aβ at 1:200 dilution. All images were captured using Nikon Eclipse Ti-S inverted fluorescence microscope (Melville, NY). Quantification of total Aβ load in the hippocampus and cortex was performed using ImageJ version 1.44 software (National Institutes of Health, Bethesda, MD) after adjusting for threshold.

2.9. Statistical analysis

All values were expressed as mean ± SEM. Statistical analysis was done with Prism v5.0 software (Graphpad). The statistical significance for all result was assessed by Student t-test compared to control group. A p value of <0.05 was considered statistically significant.

3. Results

3.1. P-gp and BCRP inhibition by elacridar reduced the cell-based BBB model function through activation of NF-κB pathway in bEnd3 cells

To confirm our previous HTS findings for elacridar disruptive effect on the integrity of a cell-based BBB model, in vitro concentration dependent studies were performed using bEnd3 cells. The effect of increasing concentrations of elacridar on the barrier function of the monolayer is shown in Fig. 1. Elacridar treatment for 48 and 72 h resulted in a concentration-dependent reduction in TEER measurements where the monolayer tightness was disrupted by elacridar at the concentration range from 2.5-10 μM with treatment times of 48 and 72 h when compared to vehicle-treated cells (Fig. 1A). The reduction in TEER values was associated with a significant increase in the permeability of LY across the monolayer (Fig. 1B), suggesting a leaky monolayer that is consistent with results observed with TEER measurements. Besides, results from Western blotting showed the inhibitory effect of elacridar on P-gp and claudin-5 expressions (Fig. 1C).

To study the role of NF-κB signaling in the observed outcome of the leaky monolayer, bEnd3 cells were treated with 5 μM elacridar for 4 and 24 h and then analyzed by Western blotting for NF-κB signaling pathway in cytosolic and nuclear fractions. As shown in Fig. 2A, in the cytosolic fraction, elacridar significantly reduced the expression of IκB-α at 24 h post-treatment. This reduction in IκB-α was paralleled with a significant increase of cytosolic p-IκB-α as an indicator of activated degradation of IκB-α in response to elacridar. Elacridar treatment for 4 h did not demonstrate any changes in IκB-α and its phosphorylated form. However, elacridar effect on NF- κB was different where at 4 h treatment NF- κB levels were higher than control, which was reversed following 24 h treatment (Fig. 2A). Furthermore, elacridar

increased the translocation of p-NF-κB in the nuclear fraction following 4 and 24 h of treatment as shown in (Fig. 2B).

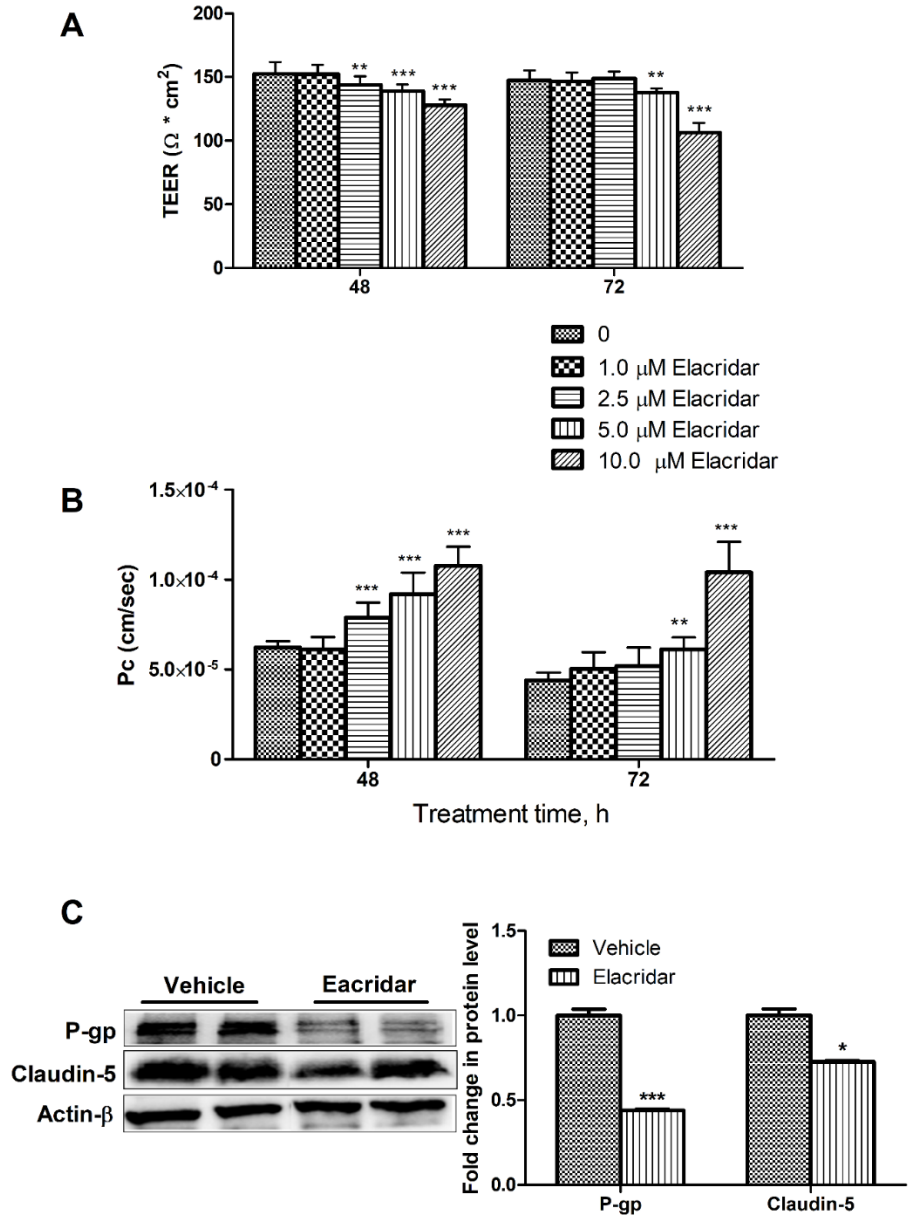

Fig. 1. Effects of elacridar on barrier function of bEnd3 cells. **A.** Exposing bEnd3 cells monolayers to elacridar resulted in reduction of TEER measurements. **B**. Elacridar significantly increased the permeability of LY in a concentration and time dependent manner. Data are presented as mean ± SD of at least 3 independent experiments. * $p \leq 0.05$, ** $p \leq 0.01$, and *** $p \leq 0.001$.

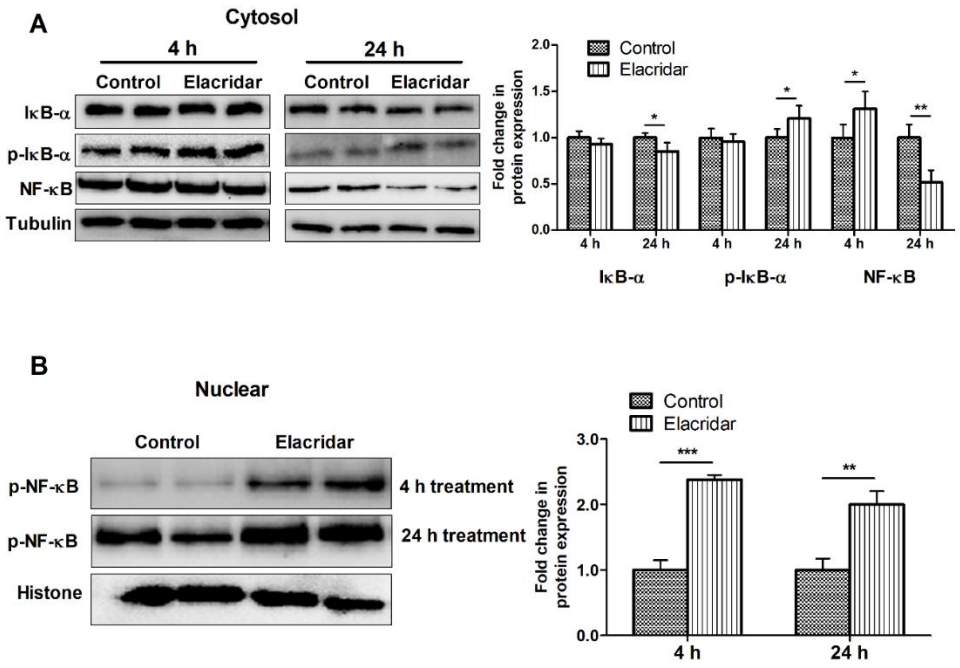

Fig. 2. Treatment with elacridar (5 μM) significantly activated NF-κB pathway in cultured bEnd3 cells in vitro. **(A)** Representative western blot and densitometry analysis of cytosolic fraction of IκB-α, p- IκB-α, and NF-κB at 4 and 24 h post-treatment. **(B)** Representative western blot and densitometry analysis of nuclear fraction of p-NF-κB at 4 and 24 h post-treatment. Data are presented as mean ± SD of 3 independent experiments. * $p< 0.05$, ** $p< 0.01$, *** $p< 0.001$ compared to control.

3.2. Elacridar disrupted the BBB integrity in TgSwDI mice

To investigate the effect of TgSwDI mice treatment with elacridar for 28 days on the BBB integrity, the expression of tight junction proteins ZO-1 and claudin-5 in the isolated microvessels from mice brains were analyzed by Western blot, and levels of IgG extravasation in mice brains by immunostaining. Elacridar treatment significantly reduced the expression of ZO-1 by >75% when compared to vehicle treated mice. In addition, claudin-5, while did not reach a statistically significant level, it showed about 50% reduction in its expression (Fig. 3A). This effect was associated with a significant increase in IgG extravasation in the cortexes and hippocampi of mice brains (Fig. 3B), where IgG leakiness was obvious surrounding the vessels (white arrows). These results suggest that elacridar disrupted the BBB integrity in TgSwDI mice brains.

3.3. Elacridar reduced the expression of Aβ transport proteins in isolated microvessels from TgSwDI mice brains

Figure 4 demonstrates the effect of elacridar on Aβ efflux transporters in isolated microvessels from mice brains as measured by Western blotting. As expected, elacridar significantly downregulated the expression of P-gp by 40% and BCRP by 53% without altering LRP1 levels. On the other hand, elacridar significantly induced RAGE expression approximately by 60% (Fig. 4).

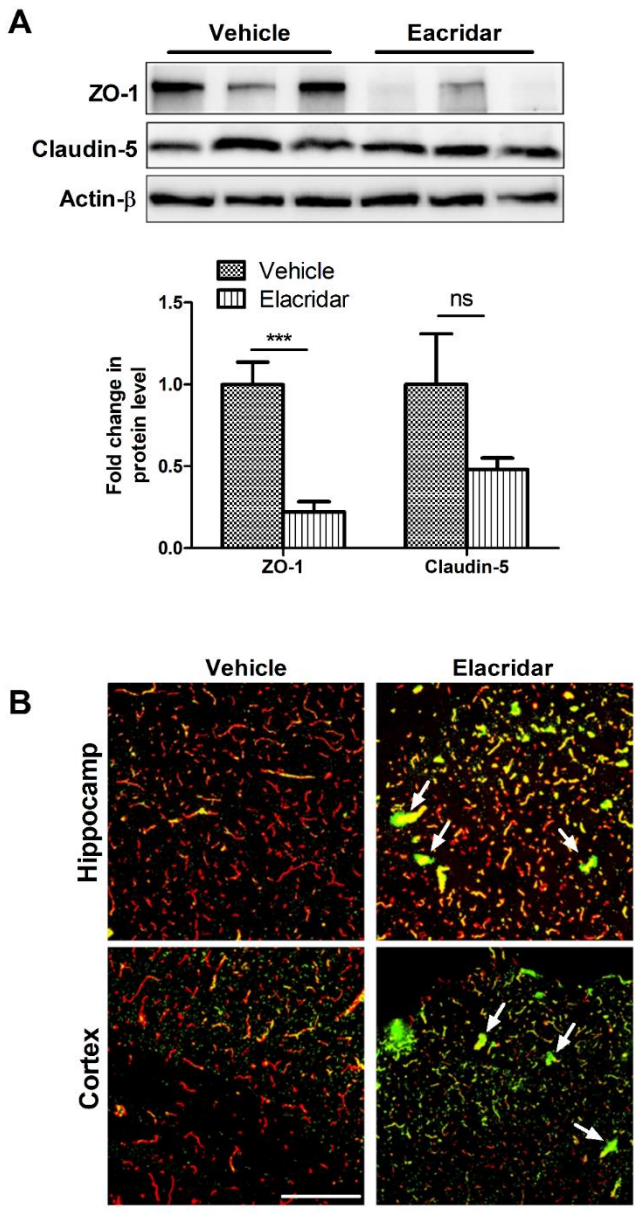

Fig. 3. Treatment with elacridar (10 mg/kg) i.p. for 28 days disrupted BBB integrity in TgSwDI mice. **A.** Representative western blot and densitometry analysis of ZO-1 and claudin-5 in vivo from microvessels isolated from mice brains. Elacridar treatment significantly decreased the expression of tight junction proteins in isolated microvessels from mice brains when compared to vehicle treated group. Data represented as mean ± SEM of n=5 mice per group. ns=not significant; *** $p<0.001$ compared to vehicle. **B.** Representative brain sections stained with anti-mouse IgG antibody to detect IgG extravasation (green) and anti-collagen antibody (red). Elacridar increased IgG extravasation in mice hippocampi and cortexes compared to vehicle treated groups. Scale bar =50 µm.

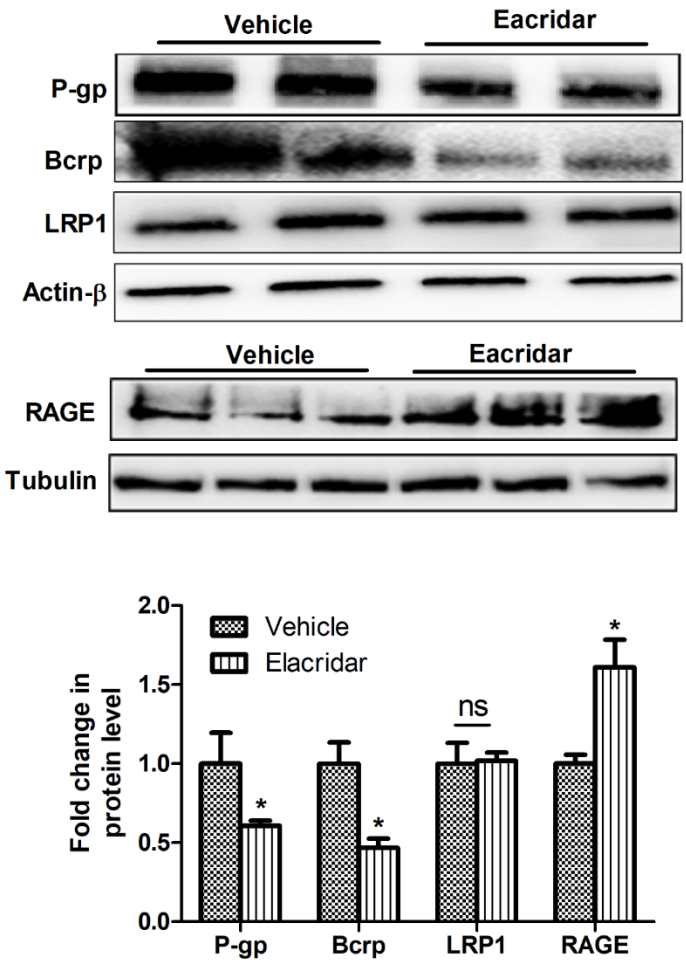

Fig. 4. Treatment with elacridar (10 mg/kg) i.p. for 28 days altered the expression Aβ transport proteins in isolated microvessels from TgSwDI mice brains. Representative western blot and densitometry analysis of P-gp, BCRP, LRP1 and RAGE demonstrated that eladridar reduced the expression of P-gp and BCRP, while increased RAGE. Data represented as mean ± SEM of n=5 mice per group, ns=not significant; * $p<0.05$ compared to vehicle treated mice.

3.4. BBB disruption by elacridar increased Aβ load in TgSwDI mice brains

Compared to vehicle treated mice, elacridar significantly increased total Aβ load in mice brains as determined by immunohistochemical analysis (Fig. 5). Aβ deposition on microvessels, besides parenchyma, was also observed as detected by its co-localization with collagen-IV used as a marker for microvessels. Semi-quantitative analysis of total Aβ showed elacridar caused a significant increase by 146 and 133% in the cortexes and hippocampi of mice brains, respectively, when compared to the vehicle-treated group (Fig. 5A). In addition, elacridar treatment increased Aβ plaques deposition in brain parenchyma and microvessels as determined by Thioflavin S staining (Fig. 5B). These results suggest elacridar further induced CAA, an effect that was associated with the downregulation of Aβ clearance proteins P-gp and BCRP, and upregulation of RAGE.

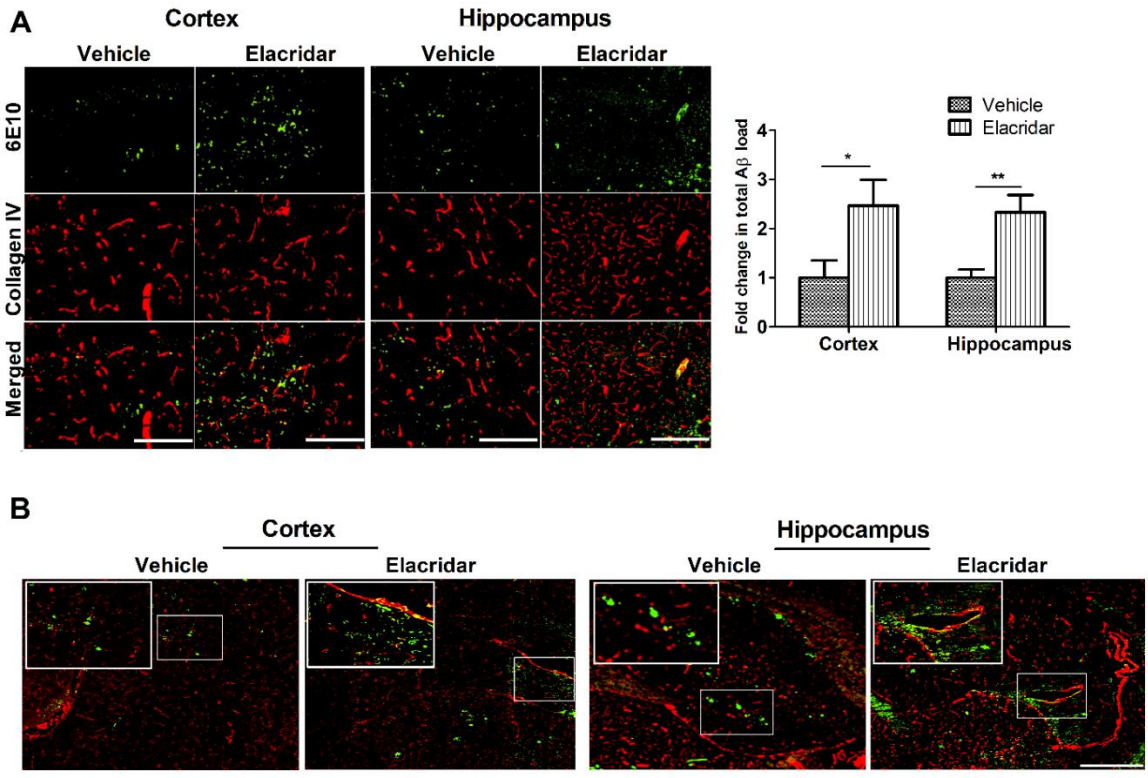

Fig. 5. Elacridar treatment increased brain Aβ burden in the brains of TgSwDI mice. **A.** Representative brain sections from mice cortex and hippocampus regions stained with 6E10 (green) antibody against Aβ to detect total Aβ load and anti-collagen IV (red) to stain microvessels. Semi-quantification analysis of both regions showed significant increase in Aβ burden. Data are presented as mean ± SEM of n=5 mice per group, * $p<0.05$, ** $p<0.01$ compared to vehicle treated group. **B.** Representative brain sections stained with ThioS (green) and anti-collagen IV (red) to stain microvessels in cortex and hippocampus regions. Top white square is a magnification of the small square showing increased Aβ deposit on the microvessels caused by elacridar. Scale bar = 50 μm.

3.5. BBB disruption by elacridar increased astrocytes activation and MMP9 levels

To evaluate the effect of BBB disruption by elacridar on astrogliosis, a feature of Aβ-related pathology, we assessed astrocytes activation and GFAP levels by immunostaining and Western blot. Results demonstrated a significant increase in the number and intensity of cells immunolabeled for the astrocytic marker GFAP that is associated with an increase in cells branching in the hippocampal region of mice brains (Fig. 6A). Consistent with these results, findings from Western blotting demonstrated elacridar significantly increased GFAP levels by 128% compared to vehicle-treated mice (Fig. 6B). In addition, elacridar significantly increased MMP9 levels in mice brains by 3.7-fold (Fig. 6B).

3.6. Elacridar treatment did not alter the expression of synaptic markers

Two synaptic markers were evaluated, the pre-synaptic marker synaptosomal-associated protein-25 (SNAP-25), and the post-synaptic marker postsynaptic density protein-95 (PSD-95). As shown in Fig. 6C, mice treated with elacridar did not alter the expression of either protein, PSD-95 or SNAP-25.

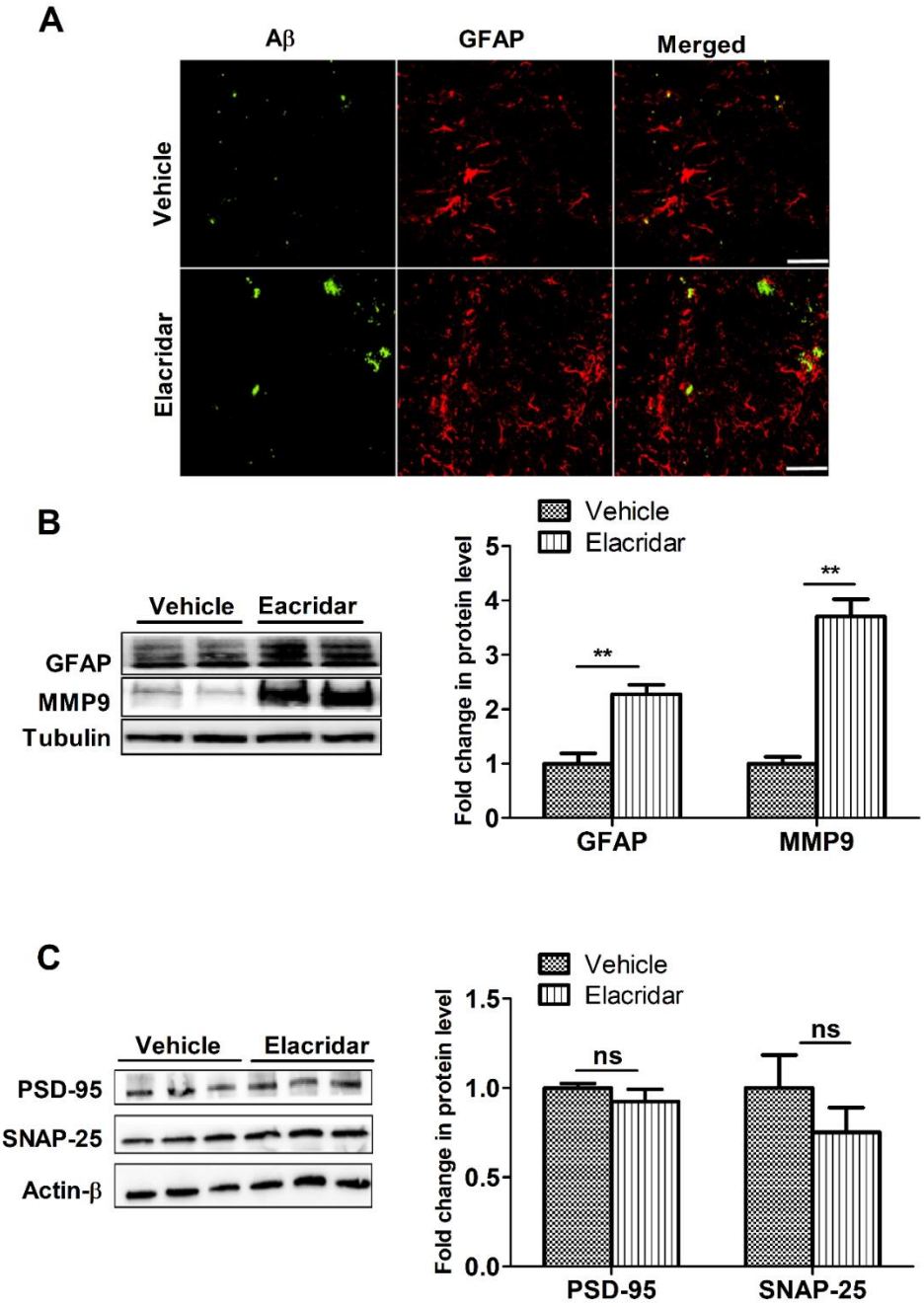

Fig 6: Elacridar treatment (10 mg/kg/day i.p. for 28 days) significantly increased astrogliosis marker GFAP in TgSwDI mice brains. **A.** Representative brain sections from mice hippocampi stained with GFAP antibody (red) to stain activated astrocytes and with 6E10 (green) antibody to detect total Aβ. Scale bar, 50 μm. **B.** Representative Western blot and densitometry analysis of GFAP expressions in mice brain homogenates. Data are presented as mean ± SEM for n=5 mice per group. ns = not significant, ** p<0.01compared to vehicle treated mice.

3.7. BBB disruption by elacridar was associated with induced activation of NF-κB pathway in TgSwDI mice brains

The effect of elacridar on the expression of proteins associated with NF-κB pathway in mice brain homogenates was determined by Western blot. As shown in Fig. 7, the effect of elacridar was accompanied with a significant increase in the expression of activated NF-κB (p-NF-κB), inhibitor of NF-kB kinase (IKK) complex and its phosphorylated form, and p-IkB proteins.

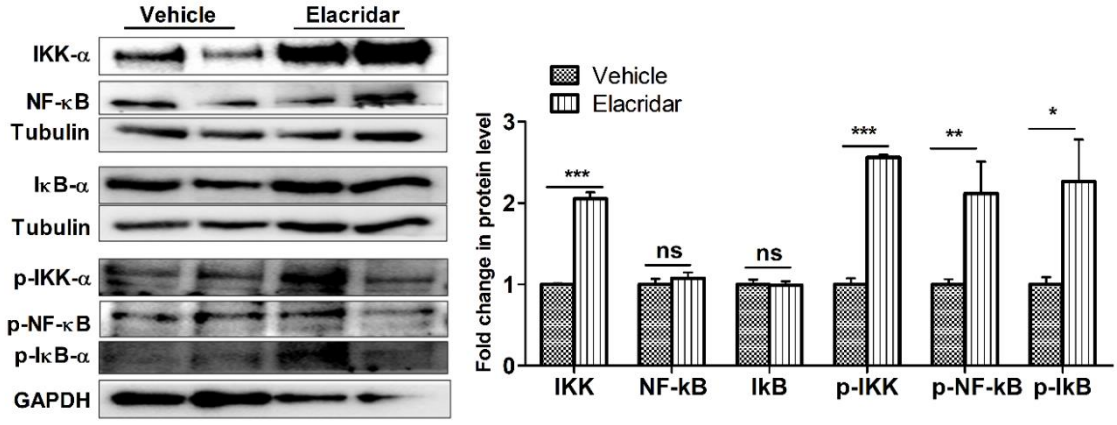

Fig. 7. Representative Western blot and densitometry analysis of PSD-95 and SNAP-25 expressions in mice brain homogenates. TgSwDI mice were treated with elacridar at 10 mg/kg/day each for 28 days. Data are presented as mean ± SEM for n=5 mice per group. ns = not significant, * $p<0.05$, ** $p<0.01$, *** $p<0.001$ compared to vehicle treated group.

4. Discussion

Age is associated with increased risk for dementia. Besides, aging is associated with chronic diseases, which necessitate receiving drugs that might interact adversely with each other and/or with endogenous molecules, which could result in irreversible consequences such as cognitive dysfunction and dementia. For example, it has been reported that prolonged use of proton pump inhibitors may increase incidence of dementia by acting as inhibitors of choline-acetyltransferase (Kumar et al., 2020). Recent findings from our laboratory, using a cell-based BBB model to high throughput screen compounds for their ability to enhance the function of the in vitro model (Qosa et al., 2016a), we identified several of marketed approved drugs and investigational compounds as enhancers of the model function that protected against Aβ toxicity on the monolayer intactness. Besides enhancers, we also were able to identify compounds that disrupted the monolayer function (Qosa et al., 2016a). These results suggest the chronic use of some drugs could alter the barrier function of the BBB, which could potentially affect brain function. To clarify further these results, the objective of this study was to investigate the effect of pharmacological disruption of the BBB on Aβ-related pathology in TgSwDI, a mouse model for CAA and AD. For this purpose, elacridar was used as a model drug that disrupts the BBB function by inhibiting key efflux transport proteins for BBB function and Aβ clearance across the BBB. It has been reported that a single dose of elacridar increases BBB permeability of P-gp substrates via P-gp inhibition (Kallem et al., 2012). In addition, it has been shown that in an AD mouse model, the administration of elacridar blocks 1α,25 dihydroxyvitamin D3-induced reduction of soluble Aβ brain levels by inhibiting P-gp (Durk et al., 2014). However, studies on the effect of BBB disruption by the chronic administration of

elacridar, as a model inhibitor compound of P-gp and BCRP, on BBB function and Aβ-related pathology are limited.

Elacridar daily administration for 28 days in TgSwDI mice disrupted the BBB function, and increased Aβ brain load with marked increase in astrocytes activation. Elacridar is an investigational compound in cancer research used to overcome drugs resistance and enhances the distribution of chemotherapeutic agents into tumors and organs including the brain (Hyafil et al., 1993). Elacridar is a highly specific inhibitor of efflux transporters P-gp and BCRP (Oostendorp et al., 2009). With aging and in AD, the expression of Aβ major transport proteins including P-gp, LRP1 and BCRP is downregulated, an effect that is associated with reduced Aβ clearance (Erdo and Krajcsi, 2019, Toornvliet et al., 2006, Do et al., 2016, Yan et al., 2020, Wijesuriya et al., 2010, Chiu et al., 2015). This observation suggested that restoring Aβ-BBB transporters could protect the brain from Aβ-mediated pathology (Davis et al., 2004, Zlokovic, 2005), as supported by preclinical studies reported the upregulation of P-gp and LRP1 induced Aβ clearance across the BBB, an effect that was associated with reduced Aβ and related pathology (Pan et al., 2020, Mohamed et al., 2016, Qosa et al., 2012, Abuznait et al., 2013, Patel and Shah, 2017, Guo et al., 2016, Mohamed et al., 2015). On the other hand, compounds that inhibit Aβ transport proteins are expected to reduce Aβ clearance and increase its deposition in mice brains and on microvessels. For example, it has been reported that borneol, a monoterpenoid compound derived from *Dryobalanops aromatica Gaertn f.* and *Blumea balsamifera DC* widely used in traditional Chinese medicine, to disrupt the endothelial tight junctions, downregulate P-gp expression and disrupt the BBB in vitro and in vivo (Chen and Wang, 2004, Yu et al., 2011, Yu et al., 2013). Similarly, in the current study, P-gp and BCRP downregulation by elacridar treatment disrupted the BBB function and integrity as

demonstrated by the reduced expression of tight junction proteins ZO-1 and clauidn-5 in isolated brain microvessels. These proteins play important role in maintaining functional BBB and brain homeostasis. Jiao et al. reported that disruption of claudin-5 alone is enough to cause functional changes in the BBB, which could subsequently allow the inconsistent movement of substances and toxin from brain to blood and vice versa (Jiao et al., 2011) . In another study, reduced ZO-1 expression was closely associated with the degree of BBB damage, and thus was considered as a marker of BBB disruption (Wang et al., 2019). In our study, the reduction in tight junction proteins was associated with increased IgG extravasation in mice brain indicating a leaky BBB. This in vivo observation was consistent with results from the in vitro data where elacridar significantly reduced LY permeation across the monolayer as well as TEER values.

Several studies reported role of the BBB in controlling brain Aβ levels (Yoon and Jo, 2012, Qosa et al., 2014, Qosa et al., 2015, Duong et al., 2019). RAGE regulates the influx of peripheral Aβ *into the brain (*Yan et al., 2010)*, while LRP1, P-gp and BCRP clear brain Aβ* from brain to blood and/or by peripheral extrusion of peripheral Aβ by the efflux transporters (Erdo and Krajcsi, 2019, Toornvliet et al., 2006, Do et al., 2016, Yan et al., 2020). Mice treatment with elacridar reduced expression levels of P-gp and BCRP, but not LRP1, and increased expression of RAGE in brain microvessels an effect that could contributed to the significant increase in total Aβ and deposits in mice brains. Furthermore, altered transporters function expressed at the endothelial cells of the BBB increased Aβ deposits on the microvessels as shown by ThioS staining and Aβ immunostaining. Others and we previously reported t*hat P-gp deficiency in mice models of AD suppressed Aβ clearance and increased* brain Aβ deposition (Cirrito et al., 2005, Mohamed et al., 2016). These findings are consistent with those observed in humans that demonstrated cerebrovascular expression of P-gp is

inversely correlated with Aβ plaque numbers in subjects without dementia (Vogelgesang et al., 2002). Moreover, BCRP has been shown to play role in controlling Aβ brain levels by preventing Aβ entry from the blood into the brain across the BBB; in CAA, BCRP expression is upregulated to limit $A\beta_{40}$ access to the brain (Xiong et al., 2009). Thus, the downregulation of these efflux transporters at the BBB may accelerate parenchymal and vascular Aβ accumulation which could contribute to AD pathogenesis.

RAGE, an immunoglobulin superfamily member, functions as a receptor for a series of ligands including Aβ (Yan et al., 2010). RAGE is known to mediate the entry of circulating Aβ into the brain across the BBB (Yan et al., 2010). A significant increase in endothelial RAGE expression was observed in postmortem AD brains compared to controls (Miller et al., 2008). Beside downregulating Aβ efflux transporters, elacridar increased RAGE, which could contributed to the increased levels of brain Aβ.

In response to inflammation, GFAP intensity increases and astrocytes remodels into activated star-like shape (Kassubek et al., 2017). Similarly, our data demonstrated that compared to vehicle treated mice, the downregulation of P-gp and BCRP by elacridar significantly increased GFAP intensity in mice brains as determined by immunostaining and Western blotting. While further studies are required, this observed effect could be a direct effect of elacridar on astrocytes activation and/or indirectly through increased brain levels of Aβ. Yet, based on the in vitro findings showing elacridar to reduce the intactness of the cell-based BBB model, BBB disruption associated with Aβ accumulation could largely contributed to astrocytes activation. In addition, increased Aβ was associated with increased levels of MMP9, which has been linked to BBB breakdown in neurodegenerative diseases, including AD (Duits et al., 2015, Weekman and Wilcock, 2016). For example, Yang et al. showed that endothelial cells treatment

with $A\beta_{42}$ induced the monolayer permeability by disrupting ZO-1 expression through increased MMP9 secretion in vitro (Yang and Rosenberg, 2011), an effect that was also observed in vivo in the brains of 5xFAD mice. Interestingly, however, BBB disruption by elacridar did not alter the expression of synaptic markers suggesting a lag time between BBB disruption and synaptic loss, which could be observed with longer treatment time than 28 days.

To explain the observed effect, we investigated elacridar effect on NF-κB pathway as a potential mechanism for BBB disruption. Data from the in vivo studies showed downregulation of P-gp and BCRP, and upregulation of RAGE accompanied activation of NF-κB pathway in mice brains. To evaluate elacridar specific effect on the endothelial cells, we performed in vitro studies with bEnd3. Findings showed that, as expected, cells treatment with elacridar reduced P-gp expression and claudin-5, which was associated with increased permeability as measured by LY assay, which support in vivo findings demonstrating increased IgG extravasation. Activation of inflammatory NF-κB signaling pathway has been shown to compromise the BBB-endothelium function by reducing P-gp and increasing RAGE expressions (Chen et al., 2018, Yu et al., 2013, Park et al., 2014), and activate inflammatory mediators that facilitate disease progression (Bierhaus et al., 2005, Srikanth et al., 2011).

5. Conclusion

In conclusion, findings from this study suggest that pharmacological downregulation of BBB-suited P-gp and BCRP could disrupt the BBB function and increase Aβ brain accumulation and thus have the potential to increase the risk of AD and CAA.

References

ABUZNAIT, A. H. & KADDOUMI, A. 2012. Role of ABC transporters in the pathogenesis of Alzheimer's disease. *ACS Chem Neurosci,* 3**,** 820-31.

ABUZNAIT, A. H., QOSA, H., BUSNENA, B. A., EL SAYED, K. A. & KADDOUMI, A. 2013. Olive-oil-derived oleocanthal enhances beta-amyloid clearance as a potential neuroprotective mechanism against Alzheimer's disease: in vitro and in vivo studies. *ACS Chem Neurosci,* 4**,** 973-82.

BELL, R. D. & ZLOKOVIC, B. V. 2009. Neurovascular mechanisms and blood-brain barrier disorder in Alzheimer's disease. *Acta Neuropathol,* 118**,** 103-13.

BENNETT, R. E., ROBBINS, A. B., HU, M., CAO, X., BETENSKY, R. A., CLARK, T., DAS, S. & HYMAN, B. T. 2018. Tau induces blood vessel abnormalities and angiogenesis-related gene expression in P301L transgenic mice and human Alzheimer's disease. *Proc Natl Acad Sci U S A,* 115**,** E1289-E1298.

BIERHAUS, A., HUMPERT, P. M., MORCOS, M., WENDT, T., CHAVAKIS, T., ARNOLD, B., STERN, D. M. & NAWROTH, P. P. 2005. Understanding RAGE, the receptor for advanced glycation end products. *J Mol Med (Berl),* 83**,** 876-86.

BOWMAN, G. L., KAYE, J. A., MOORE, M., WAICHUNAS, D., CARLSON, N. E. & QUINN, J. F. 2007. Blood-brain barrier impairment in Alzheimer disease: stability and functional significance. *Neurology,* 68**,** 1809-14.

CHEN, F., GHOSH, A., HU, M., LONG, Y., SUN, H., KONG, L., HONG, H. & TANG, S. 2018. RAGE-NF-kappaB-PPARgamma Signaling is Involved in AGEs-Induced Upregulation of Amyloid-beta Influx Transport in an In Vitro BBB Model. *Neurotox Res,* 33**,** 284-299.

CHEN, Y. M. & WANG, N. S. 2004. [Effect of borneol on the intercellular tight junction and pinocytosis vesicles in vitro blood-brain barrier model]. *Zhongguo Zhong Xi Yi Jie He Za Zhi,* 24**,** 632-4.

CHIU, C., MILLER, M. C., MONAHAN, R., OSGOOD, D. P., STOPA, E. G. & SILVERBERG, G. D. 2015. P-glycoprotein expression and amyloid accumulation in human aging and Alzheimer's disease: preliminary observations. *Neurobiol Aging,* 36**,** 2475-82.

CIRRITO, J. R., DEANE, R., FAGAN, A. M., SPINNER, M. L., PARSADANIAN, M., FINN, M. B., JIANG, H., PRIOR, J. L., SAGARE, A., BALES, K. R., PAUL, S. M., ZLOKOVIC, B. V., PIWNICA-WORMS, D. & HOLTZMAN, D. M. 2005. P-glycoprotein deficiency at the blood-brain barrier increases amyloid-beta deposition in an Alzheimer disease mouse model. *J Clin Invest,* 115**,** 3285-90.

CITRON, M. 2010. Alzheimer's disease: strategies for disease modification. *Nat Rev Drug Discov,* 9**,** 387-98.

DAVIS, J., XU, F., DEANE, R., ROMANOV, G., PREVITI, M. L., ZEIGLER, K., ZLOKOVIC, B. V. & VAN NOSTRAND, W. E. 2004. Early-onset and robust cerebral microvascular accumulation of amyloid beta-protein in transgenic mice expressing low levels of a vasculotropic Dutch/Iowa mutant form of amyloid beta-protein precursor. *J Biol Chem,* 279**,** 20296-306.

DEMEULE, M., LABELLE, M., REGINA, A., BERTHELET, F. & BELIVEAU, R. 2001. Isolation of endothelial cells from brain, lung, and kidney: expression of the multidrug resistance P-glycoprotein isoforms. *Biochem Biophys Res Commun,* 281**,** 827-34.

DO, T. M., DODACKI, A., ALATA, W., CALON, F., NICOLIC, S., SCHERRMANN, J. M., FARINOTTI, R. & BOURASSET, F. 2016. Age-Dependent Regulation of the Blood-Brain Barrier Influx/Efflux Equilibrium of Amyloid-beta Peptide in a Mouse Model of Alzheimer's Disease (3xTg-AD). *J Alzheimers Dis,* 49**,** 287-300.

DO, T. M., NOEL-HUDSON, M. S., RIBES, S., BESENGEZ, C., SMIRNOVA, M., CISTERNINO, S., BUYSE, M., CALON, F., CHIMINI, G., CHACUN, H., SCHERRMANN, J. M., FARINOTTI, R. & BOURASSET, F. 2012. ABCG2- and ABCG4-mediated efflux of amyloid-beta peptide 1-40 at the mouse blood-brain barrier. *J Alzheimers Dis,* 30**,** 155-66.

DONAHUE, J. E., FLAHERTY, S. L., JOHANSON, C. E., DUNCAN, J. A., 3RD, SILVERBERG, G. D., MILLER, M. C., TAVARES, R., YANG, W., WU, Q., SABO, E., HOVANESIAN, V. & STOPA, E. G. 2006. RAGE, LRP-1, and amyloid-beta protein in Alzheimer's disease. *Acta Neuropathol,* 112**,** 405-15.

DUITS, F. H., HERNANDEZ-GUILLAMON, M., MONTANER, J., GOOS, J. D., MONTANOLA, A., WATTJES, M. P., BARKHOF, F., SCHELTENS, P., TEUNISSEN, C. E. & VAN DER FLIER, W. M. 2015. Matrix Metalloproteinases in Alzheimer's Disease and Concurrent Cerebral Microbleeds. *J Alzheimers Dis,* 48**,** 711-20.

DUONG, Q. V., KINTZING, M. L., KINTZING, W. E., ABDALLAH, I. M., BRANNEN, A. D. & KADDOUMI, A. 2019. Plasma Rich in Growth Factors (PRGF) Disrupt the Blood-Brain Barrier Integrity and Elevate Amyloid Pathology in the Brains of 5XFAD Mice. *Int J Mol Sci,* 20.

DURK, M. R., HAN, K., CHOW, E. C., AHRENS, R., HENDERSON, J. T., FRASER, P. E. & PANG, K. S. 2014. 1alpha,25-Dihydroxyvitamin D3 reduces cerebral amyloid-beta accumulation and improves cognition in mouse models of Alzheimer's disease. *J Neurosci,* 34**,** 7091-101.

ELFAKHRI, K. H., DUONG, Q. V., LANGLEY, C., DEPAULA, A., MOUSA, Y. M., LEBEOUF, T., CAIN, C. & KADDOUMI, A. 2018. Characterization of Hit Compounds Identified from High-throughput Screening for their Effect on Blood-brain Barrier Integrity and Amyloid-beta Clearance: In Vitro and In Vivo Studies. *Neuroscience,* 379**,** 269-280.

ERDO, F. & KRAJCSI, P. 2019. Age-Related Functional and Expressional Changes in Efflux Pathways at the Blood-Brain Barrier. *Front Aging Neurosci,* 11**,** 196.

GUO, Y. X., HE, L. Y., ZHANG, M., WANG, F., LIU, F. & PENG, W. X. 2016. 1,25-Dihydroxyvitamin D3 regulates expression of LRP1 and RAGE in vitro and in vivo, enhancing Abeta1-40 brain-to-blood efflux and peripheral uptake transport. *Neuroscience,* 322**,** 28-38.

HARTZ, A. M., MILLER, D. S. & BAUER, B. 2010. Restoring blood-brain barrier P-glycoprotein reduces brain amyloid-beta in a mouse model of Alzheimer's disease. *Mol Pharmacol,* 77**,** 715-23.

HYAFIL, F., VERGELY, C., DU VIGNAUD, P. & GRAND-PERRET, T. 1993. In vitro and in vivo reversal of multidrug resistance by GF120918, an acridonecarboxamide derivative. *Cancer Res,* 53**,** 4595-602.

JELLINGER, K. A. 2002. Alzheimer disease and cerebrovascular pathology: an update. *J Neural Transm (Vienna),* 109**,** 813-36.

JIAO, H., WANG, Z., LIU, Y., WANG, P. & XUE, Y. 2011. Specific role of tight junction proteins claudin-5, occludin, and ZO-1 of the blood-brain barrier in a focal cerebral ischemic insult. *J Mol Neurosci,* 44**,** 130-9.

KASSUBEK, R., GORGES, M., SCHOCKE, M., HAGENSTON, V. A. M., HUSS, A., LUDOLPH, A. C., KASSUBEK, J. & TUMANI, H. 2017. GFAP in early multiple sclerosis: A biomarker for inflammation. *Neurosci Lett,* 657**,** 166-170.

KUHNKE, D., JEDLITSCHKY, G., GRUBE, M., KROHN, M., JUCKER, M., MOSYAGIN, I., CASCORBI, I., WALKER, L. C., KROEMER, H. K., WARZOK, R. W. & VOGELGESANG, S. 2007. MDR1-P-Glycoprotein (ABCB1) Mediates Transport of Alzheimer's amyloid-beta peptides--implications for the mechanisms of Abeta clearance at the blood-brain barrier. *Brain Pathol,* 17**,** 347-53.

KUMAR, R., KUMAR, A., NORDBERG, A., LANGSTROM, B. & DARREH-SHORI, T. 2020. Proton pump inhibitors act with unprecedented potencies as inhibitors of the acetylcholine biosynthesizing enzyme-A plausible missing link for their association with incidence of dementia. *Alzheimers Dement*.

LAM, F. C., LIU, R., LU, P., SHAPIRO, A. B., RENOIR, J. M., SHAROM, F. J. & REINER, P. B. 2001. beta-Amyloid efflux mediated by p-glycoprotein. *J Neurochem,* 76**,** 1121-8.

MILLER, M. C., TAVARES, R., JOHANSON, C. E., HOVANESIAN, V., DONAHUE, J. E., GONZALEZ, L., SILVERBERG, G. D. & STOPA, E. G. 2008. Hippocampal RAGE immunoreactivity in early and advanced Alzheimer's disease. *Brain Res,* 1230**,** 273-80.

MOHAMED, L. A., KELLER, J. N. & KADDOUMI, A. 2016. Role of P-glycoprotein in mediating rivastigmine effect on amyloid-beta brain load and related pathology in Alzheimer's disease mouse model. *Biochim Biophys Acta,* 1862**,** 778-787.

MOHAMED, L. A., QOSA, H. & KADDOUMI, A. 2015. Age-Related Decline in Brain and Hepatic Clearance of Amyloid-Beta is Rectified by the Cholinesterase Inhibitors Donepezil and Rivastigmine in Rats. *ACS Chem Neurosci,* 6**,** 725-36.

OHTSUKI, S. & TERASAKI, T. 2007. Contribution of carrier-mediated transport systems to the blood-brain barrier as a supporting and protecting interface for the brain; importance for CNS drug discovery and development. *Pharm Res,* 24**,** 1745-58.

OOSTENDORP, R. L., BUCKLE, T., BEIJNEN, J. H., VAN TELLINGEN, O. & SCHELLENS, J. H. 2009. The effect of P-gp (Mdr1a/1b), BCRP (Bcrp1) and P-gp/BCRP inhibitors on the in vivo absorption, distribution, metabolism and excretion of imatinib. *Invest New Drugs,* 27**,** 31-40.

PAN, J., HE, R., HUO, Q., SHI, Y. & ZHAO, L. 2020. Brain Microvascular Endothelial Cell Derived Exosomes Potently Ameliorate Cognitive Dysfunction by Enhancing the Clearance of Abeta Through Up-Regulation of P-gp in Mouse Model of AD. *Neurochem Res*.

PARK, R., KOOK, S. Y., PARK, J. C. & MOOK-JUNG, I. 2014. Abeta1-42 reduces P-glycoprotein in the blood-brain barrier through RAGE-NF-kappaB signaling. *Cell Death Dis,* 5**,** e1299.

PATEL, P. & SHAH, J. 2017. Role of Vitamin D in Amyloid clearance via LRP-1 upregulation in Alzheimer's disease: A potential therapeutic target? *J Chem Neuroanat,* 85**,** 36-42.

QOSA, H., ABUASAL, B. S., ROMERO, I. A., WEKSLER, B., COURAUD, P. O., KELLER, J. N. & KADDOUMI, A. 2014. Differences in amyloid-beta clearance across mouse and human blood-brain barrier models: kinetic analysis and mechanistic modeling. *Neuropharmacology,* 79**,** 668-78.

QOSA, H., ABUZNAIT, A. H., HILL, R. A. & KADDOUMI, A. 2012. Enhanced brain amyloid-beta clearance by rifampicin and caffeine as a possible protective mechanism against Alzheimer's disease. *J Alzheimers Dis,* 31**,** 151-65.

QOSA, H., BATARSEH, Y. S., MOHYELDIN, M. M., EL SAYED, K. A., KELLER, J. N. & KADDOUMI, A. 2015. Oleocanthal enhances amyloid-beta clearance from the brains of TgSwDI mice and in vitro across a human blood-brain barrier model. *ACS Chem Neurosci,* 6**,** 1849-59.

QOSA, H., MOHAMED, L. A., AL RIHANI, S. B., BATARSEH, Y. S., DUONG, Q. V., KELLER, J. N. & KADDOUMI, A. 2016a. High-Throughput Screening for Identification of Blood-Brain Barrier Integrity Enhancers: A Drug Repurposing Opportunity to Rectify Vascular Amyloid Toxicity. *J Alzheimers Dis,* 53**,** 1499-516.

QOSA, H., MOHAMED, L. A., ALQAHTANI, S., ABUASAL, B. S., HILL, R. A. & KADDOUMI, A. 2016b. Transporters as Drug Targets in Neurological Diseases. *Clin Pharmacol Ther,* 100**,** 441-453.

SCHINKEL, A. H. 1999. P-Glycoprotein, a gatekeeper in the blood-brain barrier. *Adv Drug Deliv Rev,* 36**,** 179-194.

SCHREIBER, E., HARSHMAN, K., KEMLER, I., MALIPIERO, U., SCHAFFNER, W. & FONTANA, A. 1990. Astrocytes and glioblastoma cells express novel octamer-DNA

binding proteins distinct from the ubiquitous Oct-1 and B cell type Oct-2 proteins. *Nucleic Acids Res,* 18**,** 5495-503.

SELKOE, D. J. 2001. Alzheimer's disease: genes, proteins, and therapy. *Physiol Rev,* 81**,** 741-66.

SELKOE, D. J. & SCHENK, D. 2003. Alzheimer's disease: molecular understanding predicts amyloid-based therapeutics. *Annu Rev Pharmacol Toxicol,* 43**,** 545-84.

SHIBATA, M., YAMADA, S., KUMAR, S. R., CALERO, M., BADING, J., FRANGIONE, B., HOLTZMAN, D. M., MILLER, C. A., STRICKLAND, D. K., GHISO, J. & ZLOKOVIC, B. V. 2000. Clearance of Alzheimer's amyloid-ss(1-40) peptide from brain by LDL receptor-related protein-1 at the blood-brain barrier. *J Clin Invest,* 106**,** 1489-99.

SRIKANTH, V., MACZUREK, A., PHAN, T., STEELE, M., WESTCOTT, B., JUSKIW, D. & MUNCH, G. 2011. Advanced glycation endproducts and their receptor RAGE in Alzheimer's disease. *Neurobiol Aging,* 32**,** 763-77.

SWEENEY, M. D., ZHAO, Z., MONTAGNE, A., NELSON, A. R. & ZLOKOVIC, B. V. 2019. Blood-Brain Barrier: From Physiology to Disease and Back. *Physiol Rev,* 99**,** 21-78.

TOORNVLIET, R., VAN BERCKEL, B. N., LUURTSEMA, G., LUBBERINK, M., GELDOF, A. A., BOSCH, T. M., OERLEMANS, R., LAMMERTSMA, A. A. & FRANSSEN, E. J. 2006. Effect of age on functional P-glycoprotein in the blood-brain barrier measured by use of (R)-[(11)C]verapamil and positron emission tomography. *Clin Pharmacol Ther,* 79**,** 540-8.

VAN ASSEMA, D. M., LUBBERINK, M., BAUER, M., VAN DER FLIER, W. M., SCHUIT, R. C., WINDHORST, A. D., COMANS, E. F., HOETJES, N. J., TOLBOOM, N., LANGER, O., MULLER, M., SCHELTENS, P., LAMMERTSMA, A. A. & VAN BERCKEL, B. N. 2012. Blood-brain barrier P-glycoprotein function in Alzheimer's disease. *Brain,* 135**,** 181-9.

VOGELGESANG, S., CASCORBI, I., SCHROEDER, E., PAHNKE, J., KROEMER, H. K., SIEGMUND, W., KUNERT-KEIL, C., WALKER, L. C. & WARZOK, R. W. 2002. Deposition of Alzheimer's beta-amyloid is inversely correlated with P-glycoprotein expression in the brains of elderly non-demented humans. *Pharmacogenetics,* 12**,** 535-41.

WANG, H., LI, T., ZHAO, L., SUN, M., JIAN, Y., LIU, J., ZHANG, Y., LI, Y., DANG, M. & ZHANG, G. 2019. Dynamic Effects of Ioversol on the Permeability of the Blood-Brain Barrier and the Expression of ZO-1/Occludin in Rats. *J Mol Neurosci,* 68**,** 295-303.

WEEKMAN, E. M. & WILCOCK, D. M. 2016. Matrix Metalloproteinase in Blood-Brain Barrier Breakdown in Dementia. *J Alzheimers Dis,* 49**,** 893-903.

WIJESURIYA, H. C., BULLOCK, J. Y., FAULL, R. L., HLADKY, S. B. & BARRAND, M. A. 2010. ABC efflux transporters in brain vasculature of Alzheimer's subjects. *Brain Res,* 1358**,** 228-38.

WILSON, R. S., SEGAWA, E., BOYLE, P. A., ANAGNOS, S. E., HIZEL, L. P. & BENNETT, D. A. 2012. The natural history of cognitive decline in Alzheimer's disease. *Psychol Aging,* 27**,** 1008-17.

XIONG, H., CALLAGHAN, D., JONES, A., BAI, J., RASQUINHA, I., SMITH, C., PEI, K., WALKER, D., LUE, L. F., STANIMIROVIC, D. & ZHANG, W. 2009. ABCG2 is upregulated in Alzheimer's brain with cerebral amyloid angiopathy and may act as a gatekeeper at the blood-brain barrier for Abeta(1-40) peptides. *J Neurosci,* 29**,** 5463-75.

YAN, L., XIE, Y., SATYANARAYANAN, S. K., ZENG, H., LIU, Q., HUANG, M., MA, Y., WAN, J. B., YAO, X., SU, K. P. & SU, H. 2020. Omega-3 polyunsaturated fatty acids promote brain-to-blood clearance of beta-Amyloid in a mouse model with Alzheimer's disease. *Brain Behav Immun,* 85**,** 35-45.

YAN, S. F., RAMASAMY, R. & SCHMIDT, A. M. 2010. The RAGE axis: a fundamental mechanism signaling danger to the vulnerable vasculature. *Circ Res,* 106**,** 842-53.

YANG, Y. & ROSENBERG, G. A. 2011. MMP-mediated disruption of claudin-5 in the blood-brain barrier of rat brain after cerebral ischemia. *Methods Mol Biol,* 762**,** 333-45.

YOON, S. S. & JO, S. A. 2012. Mechanisms of Amyloid-beta Peptide Clearance: Potential Therapeutic Targets for Alzheimer's Disease. *Biomol Ther (Seoul),* 20**,** 245-55.

YU, B., LU, G. H., SUN, Y., LIN, X. & FANG, T. H. 2011. [Effect of electroacupuncture combined with intragastric administration of borneol on the permeability of blood-brain barrier in the mouse]. *Zhen Ci Yan Jiu,* 36**,** 335-40.

YU, B., RUAN, M., DONG, X., YU, Y. & CHENG, H. 2013. The mechanism of the opening of the blood-brain barrier by borneol: a pharmacodynamics and pharmacokinetics combination study. *J Ethnopharmacol,* 150**,** 1096-108.

ZLOKOVIC, B. V. 2005. Neurovascular mechanisms of Alzheimer's neurodegeneration. *Trends Neurosci,* 28**,** 202-8.

ZLOKOVIC, B. V. 2008. The blood-brain barrier in health and chronic neurodegenerative disorders. *Neuron,* 57**,** 178-201.